Title	The Role of Group 3-5 Cyclopentadienylmetal Complexes in Oranic and polymer Synthesis
Author(s)	山本, 仁
Citation	大阪大学, 1990, 博士論文
Version Type	VoR
URL	https://hdl.handle.net/11094/2570
rights	
Note	

THE ROLE OF GROUP 3-5 CYCLOPENTADIENYLMETAL

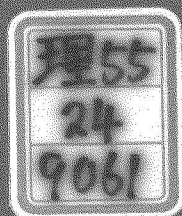# COMPLEXES IN ORGANIC AND POLYMER SYNTHESIS

A Doctoral Thesis

by

HITOSHI YAMAMOTO

Submitted to

the Faculty of Science, Osaka University

February, 1990

THE ROLE OF GROUP 3-5 CYCLOPENTADIENYLMETAL

COMPLEXES IN ORGANIC AND POLYMER SYNTHESIS

A Doctoral Thesis

by

HITOSHI YAMAMOTO

Submitted to

the Faculty of Science, Osaka University

February, 1990

APPROVALS

February, 1990

This thesis is approved as to

style and content by

中村 晃
_____
Akira NAKAMURA

Member-in-chief

安田 源   高橋 成年
_____   _____
Hajime YASUDA   Shigetoshi TAKAHASHI

Member   Member

Acknowledgement

Contents

Chapter 1

General Introduction

The chemistry of compounds containing carbon-metal bonds has a special place in modern chemistry for their unique reactivity and potential ability as catalyst and precursor of functional materials. During past two decades, a wide range of such organometallic compounds have exerted their great utilities in both fundamental and industrial syntheses: they are now recognized as superb reagents in organic synthesis to realize highly regio- and stereoselective formation of C-C, C-H, C-O, C-N, and C-X bonds, and further other carbon-metal bonds. Specially designed the transition metal organometallic compounds are frequently used as catalyst with unusually high activity and high selectivity in oxidation, reduction, carbonylation, isomerization, oligomerization, and polymerization processes. More recently, organometallic compounds and organometallic polymer have found their unique utility also in the field of functional materials involving electrical conductors, thin metallic films, magnetic compounds, and metal-carbon composites.

Such a tremendous prosperity of recent organometallic chemistry is indebted especially to the utilization of cyclopentadienyl ligand and its derivatives. Although vast majority of cyclopentadienyl-metal compounds is traced to the discovery of ferrocene,[2] the organometallic chemistry of early transition metals, especially electron-deficient compounds, has attracted much attention due to their high reactivity towards a variety of

unsaturated compounds.[3]

η^5-Cyclopentadienyl (Cp) complexes are already known for all d-block and most f-block elements.[4] Mononuclear Cp transition metal complexes can be classified into three categories, i.e. 1) MCp_2 type "Sandwich" complex referred to as "metallocene" which have symmetric geometry with nearly parallel Cp rings. 2) MCp_2L_x type "bent metallocenes", very common complexes for electron deficient early transition metals, in which the number x of unidentate ligands L (H, R, X, CO, etc.) varies between zero to three. 3) $MCpL_y$ type "open-sandwich" compounds in which the number of y of unidentate ligands L varies from one to four.
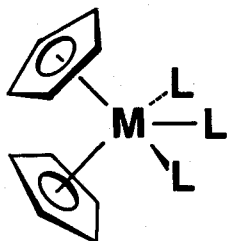
1) metallocene   **2) bent metallocene**   **3) open-sandwich**
"sandwich"
Co, Ni, Fe etc.   **Sc, Ti, Nb etc.**   **Ti, Ta, Fe, Ni etc.**
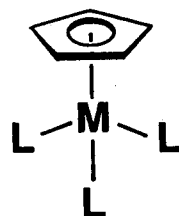
Sandwich compounds having formally more than 18 electrons usually demonstrate a distortion from the symmetric structure. For example, Ni(II)-carborane complex exhibits a slip distortion which has been described as pseudo-π-allylic bonding.[5] These distortions arise from the slip of Cp ligand into a η^3-allyl mode so that the 18e structure is maintained when another ligand enters the coordination sphere.[6]

Actually, the η^3-C_5H_5 coordination was observed in a few complexes,[7] e.g. $W(\eta^5$-$C_5H_5)(\eta^3$-$C_5H_5)(CO)_2$ is a typical example

containing the η^3-C_5H_5 ligand, the 1,3-substituents of which is bent away from the metal by 20° as confirmed by the X-ray analysis.[8]

We must pay attention about such an alternation of η^5- to η^3- or η^1-C_5H_5 coordination of Cp group irrespective of its X-ray structure, when we consider the reaction mechanism for oxidative addition, migratory insertion,[9] and reductive elimination in the stoichiometric and catalytic reactions.[10]

On the other hand, we can replace the simple cyclopentadienyl ligand with more bulky alkyl or trimethylsilyl substituted cyclopentadienyl group, which is in many cases very effective to realize the desired selective reactions. In fact, highly regio- and stereoselective catalytic isomerization,[11] oligomerization,[12] and polymerization[13] of unsaturated hydrocarbons have been achieved by utilizing steric and electronic effect of the substituted cyclopentadienyl groups.

Although, the coordination of the bulky Cp groups to the early transition metals ordinarily results in significant decrease in reactivity as compared with non-substituted Cp or alkyl groups, introduction of such a bulky Cp ligand is quite effective to improve the thermal stability and ability of regio- and stereoselection of the complex.

Olefin, diene, η^3-allyl, and alkyne complexes of early transition metals are thought to play prominent roles in Ziegler-Natta type polymerization processes. In 1964 Cossee and Arlman proposed the direct four-center insertion mechanism on the basis of crystal field theory and surface structure studies of titanium component (Scheme 1).

Scheme 1

$$CpTiCl_2 + R\text{-Al} \longrightarrow$$
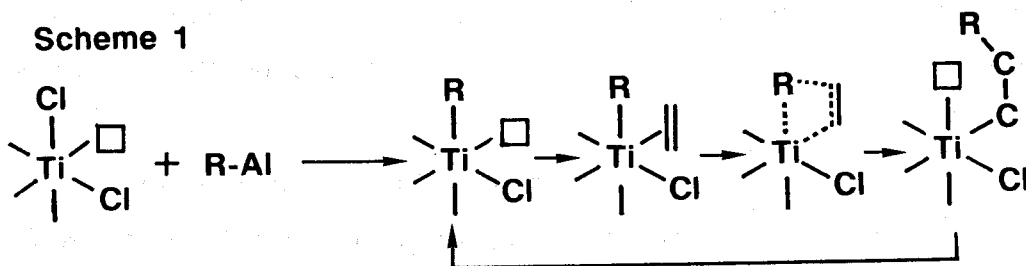
Almost the same mechanism is considered for alkyne polymeri-
zation. However, few examples are reported about the migratory
insertion of <u>coordinated</u> olefin or alkyne molecule into metal-
alkyl or metal-hydride.

For diene polymerization, essentially the same mechanism has
been accepted. In this case, more complicated situation is pre-
dicted, since 1,3-diene contains two double bond units which can
interact with catalyst species independently or collectively.
Representative coordination modes of the diene are shown below.
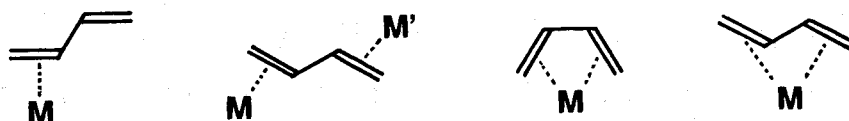
These species are thought to play crucial roles in determining
stereochemistry of the double bonds in a resulted polymer chain.
Although the mechanism of the propagation step has still been
unclear, the stereochemical control of configurations for 1,4-
polymers has been interpreted by the following two mechanism.

1) The obtained polymer structure varies depending upon the
relative stability of syn- and anti-η^3-allyl intermediates which
respectively lead to trans- and cis-1,4-polymer, respectively.

Scheme 2

cis-1,4-polymer ⟵ [M with P] ⇌ [M with P] ⟶ trans-1,4-polymer

2) The mode of diene coordination to the metal center ref-
lects the stereochemistry of resulted polymer, i.e. the s-cis and
s-trans coordination of diene to the metal cause the formation of
cis-1,4- and trans-1,4-polymers, respectively.

Scheme 3

[M diene complex] ⟶ M∼∼∼P ⟶ cis-1,4-polymer

[M diene] or [M diene] ⟶ M∼∼∼P ⟶ trans-1,4-polymer
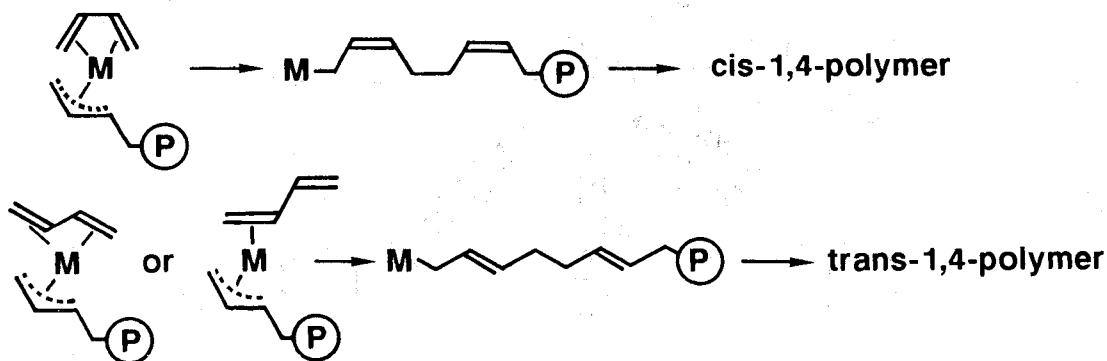
These proposed mechanisms are still obscure, because of the
lack of systematic studies on olefin, diene, η^3-allyl, and alkyne
complexes of early transition metals. Therefore, isolation, full
characterization, and structure investigation of such complexes
of early transition metals are of importance to gain further
insight into the mechanism of Ziegler-Natta type polymerization.

Typical example of well studied chemistry is seen in the
novel synthesis and versatile reactions of $ZrCp_2$(diene) reported
by Yasuda and Nakamura[14) (Scheme 1), i.e. $ZrCp_2$(isoprene) comp-
lex reacts with diverse electrophiles such as ketones, aldehydes,

isonitrile, CO_2, CO, etc. in addition to variety of alkenes, dienes, and alkynes. In these systems, the reactions proceed with high regio- and stereoselectivity and all of the resulted complexes could be isolated and characterized crystallographically and spectroscopically.

Scheme 4
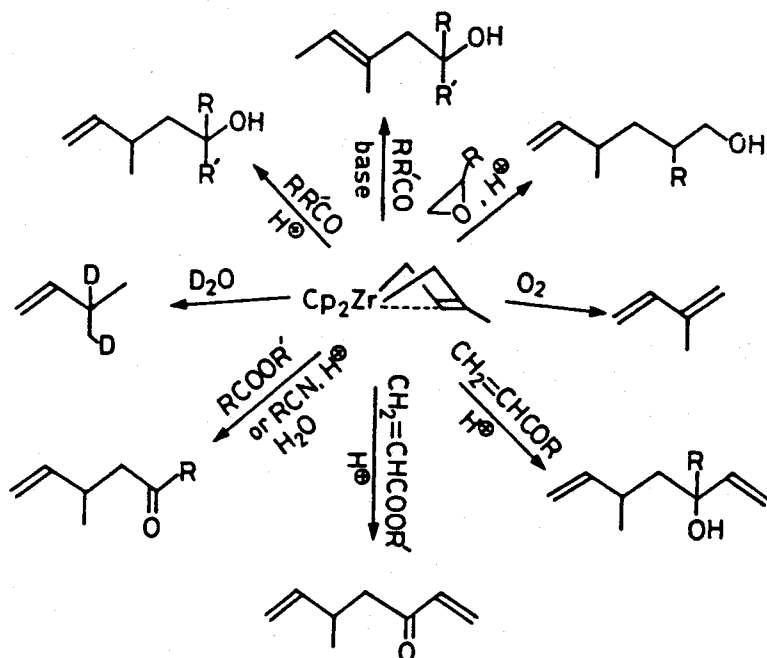
The unique structural and reactivity characteristics observed in the chemistry of bis(cyclopentadienyl)zirconium complexes prompted the author to investigate further on the chemistry of group 4 titanium-diene, titanium-allyl complexes, group 5 niobium-alkene, niobium-alkyne complexes, and also group 3 lanthanide complexes to find their essential roles in organic and polymer syntheses.

Outline of Each Chapter

Chapter 2 describes the novel synthesis of titanium-diene complexes. A series of titanium-diene complexes of type, $TiCp^*X$-(diene) ($Cp^*=C_5Me_5$, $X=Cl$, Br, I) have first been isolated here as pure crystals. The spectral and the crystallographic studies revealed the novel prone and supine structures. The diene ligand in titanium-diene complexes was found to always prefer the s-cis geometry, although the s-trans geometry has been reported for diene complexes of Zr, Hf, Nb, and Mo.

Chapter 3 describes the catalytic activity of the above noted titanium-diene complexes for highly selective linear dimerization of isoprene after reduction of the complexes to Ti(III) species. The low-valent titanium-diene complexes, $TiCp^*$(diene) ($Cp^*=C_5Me_5$), obtained by abstraction of halide using Grignard reagents or Mg metal can induce catalytic the linear dimerization of isoprene with extremely high selectivity (>99%) to produce a tail-to-head bonded isoprene dimer. The active species is estimated to be $TiCp^*$(diene) on the basis of EPR studies. In situ generation of the low-valent titanium-diene species by the reaction of $TiCp^*Cl_3$ with RMgX in the presence of isoprene shows better catalytic activity in comparison with the species prepared from $TiCp^*X$(diene) and RMgX.

Chapter 4 focuses on the structure analyses of a series of titanium-allyl complexes. The complexes were prepared from the reaction of $TiCp_2Cl_2$ with allylic magnesium compounds or by hydrotitanation of conjugated dienes. The X-ray analyses have applied to the resulted titanium-allyl complexes to establish the molecular structure of $TiCp_2(\eta^3\text{-allyl})$ where allyl ligand is 1,3-dimethylallyl, 2-methylallyl, and simple allyl. Steric effect of

the allyl substituents on the whole geometry is discussed.

Chapter 5 is concerned with the facile synthesis of novel mono-alkyl bridged ytterbium-aluminum heterobimetallic complexes and describes its stereochemistry and unique catalysis. The reaction of $YbCp^*_2(THF)$ with trialkylaluminum yields a novel heterobimetallic complexes with formula $YbCp^*_2(\mu\text{-}R)AlR_2(THF)$. The X-ray studies of the $Al(C_2H_5)_3$ complex revealed the unique mono-ethyl-bridged structure. This complex shows good catalysis for a new series of block copolymerization of ethylene and methyl methacrylate in mild conditions.

Chapter 6 describes the catalytic activity of the divalent lanthanide complexes for highly syndiotactic living polymerization of methyl methacrylate. Divalent lanthanide complexes of the type $LnCp^*_2L_x$ (Ln=Yb, Sm; L=donor molecules; x=1 or 2) exhibit superb catalytic action for polymerization of methyl methacrylate. These catalyst systems involve following marked features, i.e. 1) highly syndiotactic poly(MMA) were formed at low temperature in quantitative yield, 2) polydispersity of the resulted polymers are exceedingly narrow ($M_w/M_n < 1.10$), 3) polymerization occurs very rapidly in a living fashion leading to high molecular weight poly(MMA) with narrow polydispersity. Any other catalyst systems have not yet satisfied the whole items 1)-3) noted above.

Chapter 7 gives an account of the novel syntheses of alkyne complexes of niobocene together with their structural features. The alkyne complexes of niobocene of the type, $NbCp_2(R)(alkyne)$, were successfully prepared by the reaction of $NbCp_2(H)(ethylene)$ with various alkynes. The spectral and the crystallographic studies on these complexes revealed that they prefer the exo

geometry. The X-ray analysis of $NbCp_2(C_2H_5)$(2-butyne) elucidated the existence of agostic interaction between one of protons in $Nb-CH_2$ group and niobium atom.

References

1) See for example, (a) Collman, J. P.; Hegedus, L. S.; Norton, J. R.; Finke, R. G. Principles and Applications of Organotransition Metal Chemistry; University Science Books: Mill Valley, 1987. (b) Wilkinson, G.; Stone, F. G. A.; Abel, E. W., Eds. Comprehensive Organometallic Chemistry; Pergamon: London, 1982.

2) (a) Kealy, T. J.; Pauson, P. L. Nature, **1951**, 168, 1039. (b) Miler, S. A.; Tebboth, J. A.; Tremaine, J. F. J. Chem. Soc. **1952**, 632.

3) (a) Cardin, D. J.; Lappert, M. F.; Raston, C. L. Chemistry of Organo-zirconium and -hafnium Compounds; Ellis Horwood Limited: 1986. (b) Reetz, M. T. Organotitanium Reagents in Organic Synthesis; Springer-Verlag; Berlin, Heidelberg, 1986.

4) (a) Marks, T. J. Prog. Inorg. Chem. **1978**, 24, 51. (b) Marks, T. J. Prog. Inorg. Chem. **1979**, 25, 223.

5) (a) Wing, R. M. J. Am. Chem. Soc. **1967**, 89, 5599. (b) Wing, R. M. J. Am. Chem. Soc. **1968**, 90, 4228.

6) Rerek, M. E.; Basolo, F. J. J. Am. Chem. Soc. **1984**, 106, 5908; and references sited therein.

7) Huttner, G.; Briwtzinger, H. H.; Bell, L. G.; Friedrich, P.; Benjenke, V.; Neugevauer, D. J. Organomet. Chem. **1978**, 145, 329.

8) (a) Merola, J. S.; Kacmarick, R. T.; Van Egen, D. J. Am. Chem. Soc. **1986**, 108, 329. (b) Kowala, C.; Wunderlich, J. A. Acta Crystallogr., Sect. B **1976**, B32, 820.

9) (a) Fettes, D. J.; Narayanaswamy, R.; Rest, A. J. J. Chem. Soc., Dalton Trans. **1981**, 2311. (b) Hart-Davis, A. J.; Mawby, R. J. J. Chem. Soc. (A) **1969**, 2403.

10) (a) Caddy, P.; Green, M.; O'Brien, E.; Smart, L. E.; Woodward, P. Angew. Chem., Int. Ed. Engl. **1977**, <u>16</u>, 648. (b) Caddy, P.; Green, M.; O'Brien, E.; Smart, L. E.; Woodward, P. J. Chem. soc., Dalton, Trans. **1980**, 962.

11) Akita, M.; Yasuda, H.; Nagasuna, K. Nakamura, A. Bull. Chem. Soc. Jpn. **1983**, <u>56</u>, 554.

12) Akita, M.; Yasuda, H.; Nakamura, A. Bull. Chem. Soc. Jpn. **1984**, <u>57</u>, 480.

13) (a) Ewen, J. A. J. Am. Chem. Soc. **1984**, <u>106</u>, 6355. (b) Ewen, J. A.; Jones, R. L.; Razavi, A. J. Am. Chem. Soc. **1988**, <u>110</u>, 6256.

14) (a) Yasuda, H.; Nakamura, A. Angew. Chem., Int. Ed. Engl. **1987**, <u>26</u>, 723. (b) Yasuda, H.; Tatsumi, K.; Nakamura, A. Acc. Chem. Res. **1985**, <u>18</u>, 120. (c) Yasuda, H. Okamoto, T.; atsuoka, Y.; Nakamura, A.; Kai, Y.; Kanehisa, N.; Kasai, N. Organometallics **1989**, <u>8</u>, 1139. (d) Akita, M.; Matsuoka, Y.; Yasuda, H.; Nakamura, A. J. Organomet. Chem. **1987**, <u>327</u>, 193.

Chapter 2

Novel Synthesis and Structures of Titanium-Diene Complexes

Introduction

It is well known that the organo-early-transition metal compounds play a prominent role in the Ziegler-Natta type polymerization. Although the accelerated development has seen in the chemistry of polymerization and oligomerization of olefins and acetylenes, the corresponding studies on the chemistry of diene polymerization and oligomerization has been left behind in the last decade, because of the lack of suitable strategy and experimental method.

Recently the diene complex chemistries of zirconium, hafnium,[1] tantalum,[2] and niobium[3] developed by Yasuda and Nakamura, together with Erker, Teuben,[4a] and other workers[5,6] should make a beginning of the chemistry concerning the highly controlled catalytic conversion of conjugated dienes by homogeneous catalyst systems. However, more detailed studies are required especially on the chemistry of titanium-diene complexes since numerous titanium compounds are well known to display an exceedingly high catalytic activity in the oligomerization,[7] polymerization,[8] isomerization,[9] and hydrogenation[10] of conjugated dienes as compared with other early-transition metal compounds. In these reactions, the coordination of dienes to metal is postulated to play an indispensable role,[11] and the great tendency of Ti(IV) species to be readily reduced to Ti(III) spe-

cies[12] has been considered as a dominant factor to bring about the pronounced catalytic activity. In these points of view, the synthesis and full characterization of titanium-diene complexes are the most important and fundamental subject for the chemistry of catalytic diene conversion.

In general, the thermal stability of the complex increases but catalytic activity decreases as increase of the number of the coordinated cyclopentadienyl group to early transition metal species. therefore, mono(cyclopentadienyl)metal-diene complex or
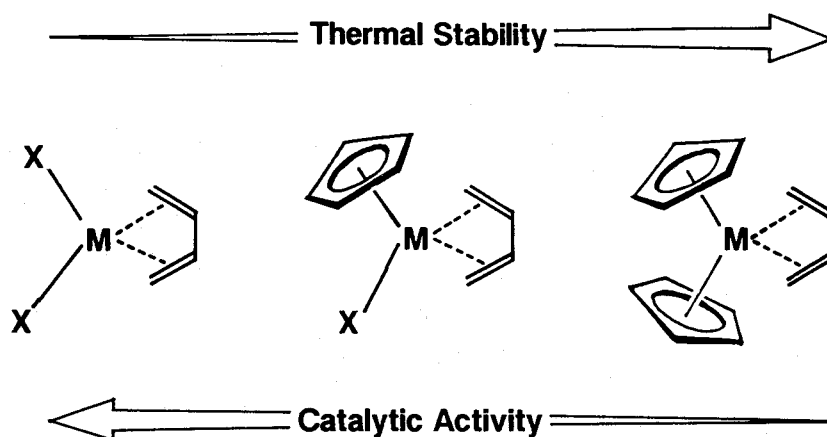
its derivatives are expected to possess moderate thermal stability with good reactivity suited for detailed studies. For this reason, synthesis of a series of titanium-diene complexes of type $TiXCp^*(diene)$ ($Cp^*=C_5Me_5$, X=Cl, Br, I) were examined here. This type of diamagnetic d^0 complexes appears to be suitable precursor for generation of the coordinatively unsaturated low-valent titanium-diene species by reductive abstraction of the halide with appropriate reducing agents.

This chapter describes the synthesis of a series of novel titanium-diene complexes and the first structural analyses of titanium-diene complexes, $TiClCp^*(diene)$, possessing either prone (endo) or supine (exo) conformation.

1. Synthesis of Titanium-Diene Complexes.

Electron-deficient titanium-diene complexes of formula $TiXCp^*$-(diene) ($Cp^* = C_5Me_5$; X = Cl, Br, I), have successfully been prepared upon treatment of TiX_3Cp^* with 0.8-0.9 equivalent of (2-butene-1,4-diyl)magnesium or its higher homologues in THF at low temperature (-78°C for 1 h and then -45°C for 2 h) under an argon atmosphere (eq. 1). Purification of the resulting product by re-

$$TiCp^*Cl_3$$

prone(endo)   supine(exo)

(1)

1a: X=Cl, $R^{1\sim4}$ =H
1b: X=Br, $R^{1\sim4}$ =H
1c: X=I, $R^{1\sim4}$ =H
2a: X=Cl, R^1 =R^4 =Ph, $R^{2,3}$ =H
2b: X=Br, R^1 =R^4 =Ph, $R^{2,3}$ =H
6a: X=Cl, $R^{1\sim3}$ =H, R^4 =CH$_3$
6b: X=Br, $R^{1\sim3}$ =H, R^4 =CH$_3$

3a: X=Cl, $R^{1,2,4}$=H, R^3 =CH$_3$
3b: X=Br, $R^{1,2,4}$=H, R^3 =CH$_3$
4: X=Cl, $R^{1,4}$ =H, $R^{2,3}$=CH$_3$
5: X=Cl, $R^{1,4}$ =H, $R^{2,3}$=Ph
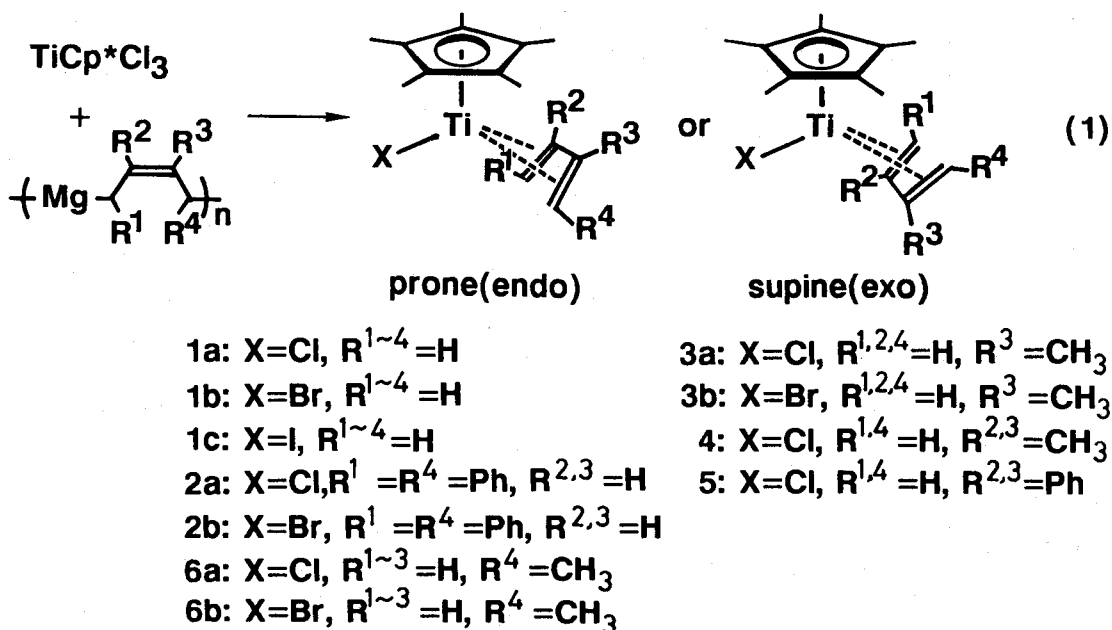
crystallization from oxygen-free hexane and/or sublimation in vacuo (10^{-4} Torr) gives $TiClCp^*$(butadiene) (1a), $TiClCp^*$(1,4-diphenylbutadiene) (2a), $TiClCp^*$(isoprene) (3a), $TiClCp^*$(2,3-dimethylbutadiene) (4), and $TiClCp^*$(2,3-diphenylbutadiene) (5) as highly air-sensitive blue crystals in 40-60% yields. All of these 14e complexes are monomeric as confirmed by the exact EIMS and are soluble in all common hydrocarbon solvents. In analogous procedure, titanium-diene complexes ligated by other halides (Br, I), i.e. $TiBrCp^*$(butadiene) (1b), $TiICp^*$(butadiene) (1c),

TiBrCp*(1,4-diphenylbutadiene) (**2b**), TiBrCp*(isoprene) (**3b**), could be prepared by using TiBr$_3$Cp* or TiI$_3$Cp* as starting materials.

The utility of the magnesium-diene adduct as a synthon of the diene dianion has widely been accepted in the synthesis of diene complexes of transition metals as Zr,[1a-f] Hf,[1g-i] Ta,[2] Nb,[3] Th,[13] Fe,[14] Mn,[15] etc. The propensity of the Ti(IV) species to readily decompose to Ti(III) species under mild conditions has made it difficult to isolate pure Ti(IV)-diene complexes except for the 2,3-dimethylbutadiene complex (**4**) reported recently by Teuben et al.[4a]

Complexes **1-5** along with TiXCp*(1,3-pentadiene) (**6**) are also available in 35-45% yield from an alternative route as shown in eq. 2, i.e. the complexation of a diene to an elusive monomeric TiXCp* species generated in situ on treating TiX$_3$Cp* with 2 equivalents of RMgX (R=i-Pr, t-Bu, Et; X=Cl, Br) or BuLi. Reduction

TiCp*X$_3$

+

2 RMgX

R=Et, i-Pr, t-Bu

$\xrightarrow{\text{-65~0°C}}$

R^1, R^2, R^3, R^4 (diene)

1a, 1b, 2a, 2b, 6a, or 6b } prone

3a, 3b, 4, or 5 } supine

(2)
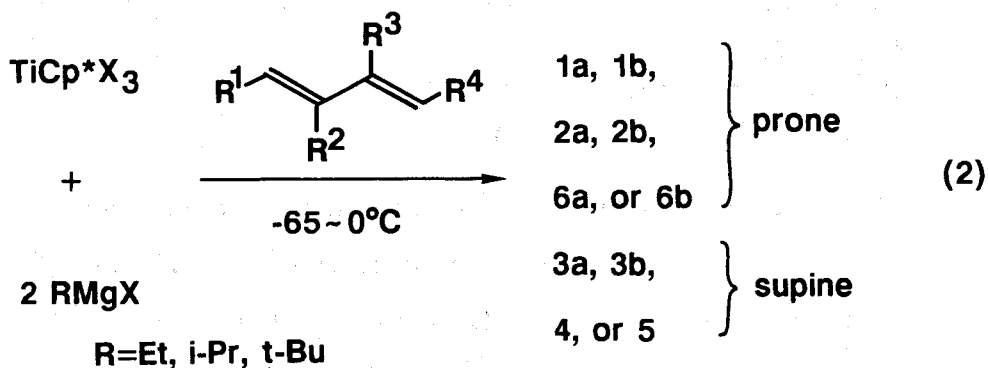
with zinc powder in place of Grignard reagents is unsuitable because it gives TiCl$_2$Cp* as a sole product. Although this type of reaction process (eq. 2) is exploited commonly in synthesizing a series of diene,[1] alkyne,[16] and alkene[16c] complexes of MCp$_2$

(M = Zr, Hf), very slow addition of the reducing agent at low temperature is required for the titanium–diene complexes. Rapid addition causes the formation of an inseparable mixture. The preparation method shown in eq. 1 is superior to the alternative process shown in eq. 2 with respect to high yielding of complexes 1-5. However, the latter method (eq. 2) has a remarkable advantage especially in the synthesis of (pentadiene)titanium and its derivatives, the preparation of which has been inaccessible from the former route due to the lack of suitable methods of generating the pentadiene dianion species.

The ligand exchange reaction also provides an effective route for preparation of the titanium–diene complexes. For example, the mixing of 1a or 3a with 1 equivalent of (E,E)-1,4-diphenylbutadiene (a diene with strong π-acidity) in hexane at 60°C gradually precipitates the sufficiently pure (1,4-diphenylbutadiene)titanium complex (2a) in 50-60% yield (eq. 3). All of the

$$\textbf{3a} \quad \xrightarrow[\text{60 °C, hexane}]{\text{Ph} \diagup\diagdown\diagup\diagdown \text{Ph}} \quad \textbf{2a} \qquad (3)$$

$$\text{(supine)} \qquad\qquad\qquad \text{(prone)}$$
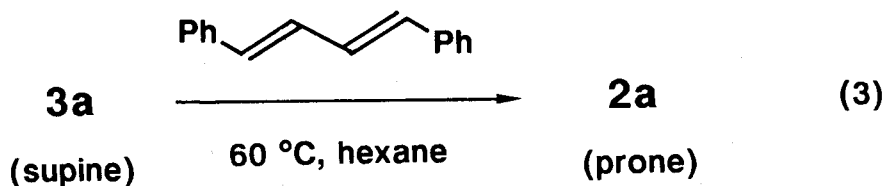
above titanium–diene complexes easily release the coordinated diene quantitatively on exposure to dry air and give 1-butene derivatives on hydrolysis. The corresponding zirconium and hafnium complexes $MClCp^*$(diene) (M = Zr, Hf; diene = isoprene, 2,3-dimethylbutadiene) have already been prepared recently, either by reduction of $TiCl_3Cp^*$ with Na/Hg in the presence of free diene or by the ligand exchange reaction between MCp^*(1-methallyl)(diene) and MCl_3Cp^*.[4a] In sharp contrast to the behavior of Zr and Hf analogues, the titanium–diene complexes exhibit no ability to

form stable complexes upon treatment with pyridine, PMe_3, and THF.

The reactivity of the titanium-diene complexes (typified by 3) toward electrophiles (3-pentanone, ethyl acetate, CO_2, etc.) was found to be essentially the same as that reported for $ZrCp_2$-(isoprene).[1a,c] As typical example of such reactions, the carbometalation of 3-pentanone with $TiClCp^*$(butadiene) (1a), $TiClCp^*$(isoprene) (3a), and $TiClCp^*$(2,3-dimethylbutadiene) (4) are illastrated in eq. 4, 5, and 6. The most striking feature is the exceptionally high regioselectivity (>95%) in the reaction with $TiClCp^*$(isoprene). The reaction proceeds irreversibly at the sterically more congested 1-position. Subsequent hydrolysis of the product of ketone insertion furnishes 3-ethyl-5-methyl-5-heptene-3-ol selectively (>90%). Thus, the present titanium-diene complexes react with nucleophiles in more mild conditions (20 °C, 15 min) than that of the reaction with zirconium-diene complexes (60 °C, 2 h).

$$1a \; + \quad \text{(structure)} \quad \xrightarrow{H^+} \quad \text{(structure)} \qquad (4)$$

$$3a \; + \quad \text{(structure)} \quad \xrightarrow{H^+} \quad \text{(structure)} \qquad (5)$$

$$4 \; + \quad \text{(structure)} \quad \xrightarrow{H^+} \quad \text{(structure)} \qquad (6)$$
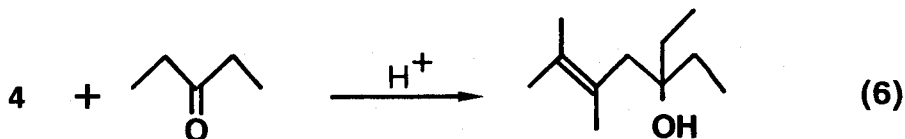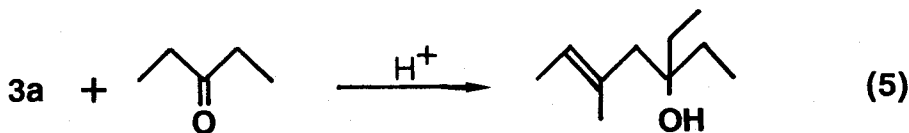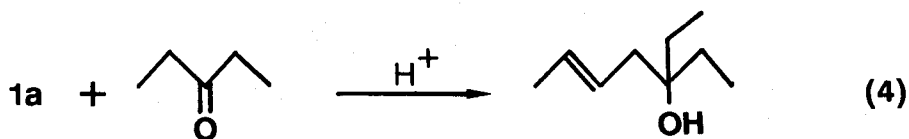
2. NMR Studies. (a) ^{1}H NMR Studies on the Mode of Diene Orientation.

A series of above noted titanium-diene complexes can be classified into two groups based upon their ^{1}H NMR spectral patterns. One is the complex possessing a supine (exo) diene ligand, and the other is the complex exhibiting a prone (endo) diene.[17] Since the chemical shift values and coupling constants

$$R^3 \quad R^1 \quad R^5 \quad M \text{-------} \quad R^2 \quad R^6 \quad R^4$$

R=H, CH$_3$, Ph

7
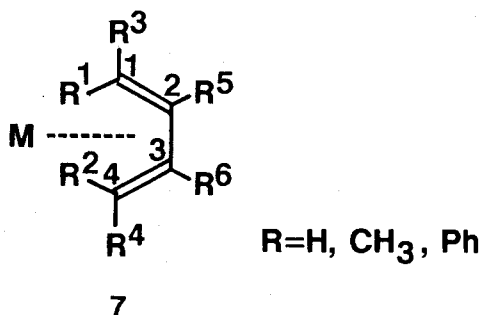
for the isoprene, 2,3-dimethylbutadiene, and 2,3-diphenylbutadiene complexes (3, 4, and 5, respectively) are comparable to those for the crystallographically well-established complexes TaCl$_2$Cp(butadiene)[2] and HfClCp*(2,3-dimethylbutadiene)[4] of supine conformation (Table 1), one can readily assign complexes 3-5 as having the supine structure. The anti protons (H[1] and H[2]) resonate at 1.09-1.60 ppm, syn protons (H[3] and H[4]) at 2.81-3.21 ppm, and inner proton (H[5]) at 5.66 ppm in these cases. Both of anti- and syn-proton signals for the titanium complexes show a significant downfield shift as compared with the corresponding signals for HfClCp*(diene) (ca. 1.3 and 0.5 ppm). Thus, the sp^2 (π-bonding) character is enhanced on the terminal carbons of the titanium complexes. The relatively small geminal coupling constants, $^2J_{HH}$ of 6-7 Hz (Table 1), for titanium complexes also support the above trend (cf. $^2J_{HH}$ for zirconium-diene complexes,

8-10 Hz; $^2J_{HH}$ for hafnium-diene complexes, 11-12 Hz).[1] The magnitude of these values for **3-5** are, however, much larger than those for late-transition metal diene complexes (1.4-4.5 Hz).[18] The X-ray analysis of **5** (vide infra) finally provided an exact experimental scaffolding for the predicted "supine" conformation. The preference of the supine geometry for complexes **3-5** may primarily due to the severe steric repulsion between methyl groups on the auxiliary Cp^* ligand and the substituent(s) on the C(2) and/or C(3) carbons of the coordinated dienes.

Of particular interest is the unusual ^1H NMR chemical shift values observed for the butadiene, 1,4-diphenylbutadiene, and pentadiene complexes (**1**, **2**, and **6**, respectively) as listed in Table I. The signal assignment based on the decoupling and simulation of the 500 MHz spectra reveals that the anti protons (H^1 and H^2) at diene termini resonate at a substantially lower field (3.82-7.18 ppm), while inner protons (H^5 and H^6) resonate at a higher field (3.37-4.22 ppm) as compared with the corresponding (s-cis-diene)metal complexes like $Fe(CO)_3$(butadiene),[18b] $ZrCp_2$-(butadiene),[1] $HfCp_2$(diene),[1d] etc. (Figure 1). This unique spectral pattern may originate from the novel prone orientation of the coordinated dienes. The possibility that the complexes assume the s-trans-diene coordination can be ruled out from the magnitude of the coupling constant, $J_{H^5H^6}$ (9.5-10.1 Hz). The shielding effect from the η^5-Cp^* ligand on the internal protons (H^5 and H^6) may cause the abnormal large upfield shift of these protons signals. On the other hand, the deshielding effect due to the vacant antibonding orbitals of the $TiCp^*$ bond results in the significant downfield shift of the terminal protons (H^1 and H^2).

$^3J_{56}$= 9.5Hz

cf. $^3J_{56}$=15.0Hz
in Zr-s-trans-C_4H_6
$^3J_{56}$=8.0Hz
in Zr-s-cis-C_4H_6

H3,4

H5,6

H1,2

at 500MHz

observed

simulated

δ(ppm)

3.0

4.0

at 100MHz

H3,4

H1,2
H5,6
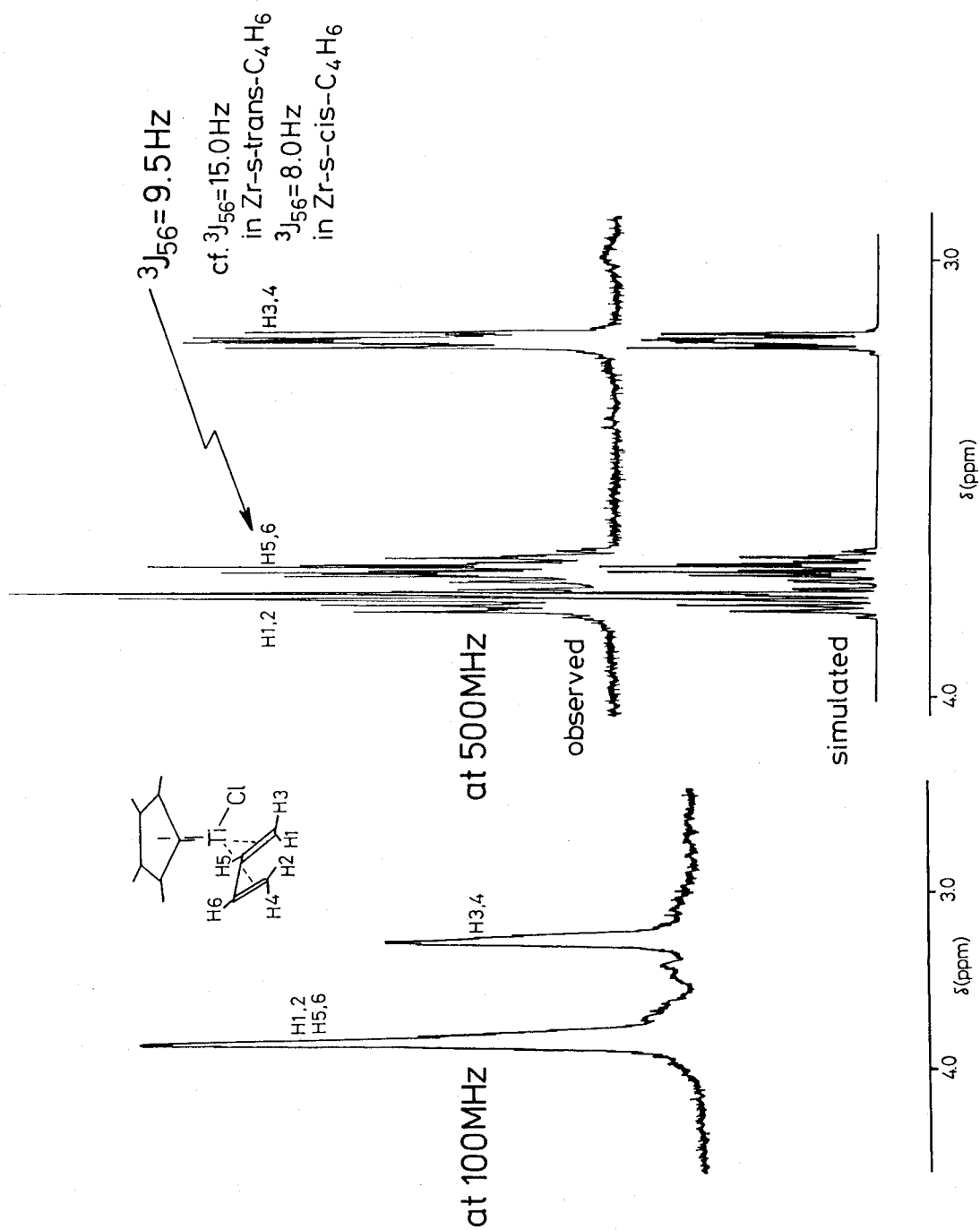
δ(ppm)

3.0

4.0

H6 H5 Ti—Cl
H4 H2 H1
H3

Figure 1. 500MHz 1H-NMR spectrum of **1a**

It should be noted that dienes in complexes **1, 2,** and **6** always adopt the s-cis coordination irrespective of the synthetic routes shown in eq. 1-3. No geometrical interconversion (s-cis ↔ s-trans) was observed for these complexes from -90 to 80 °C where thermal decomposition begins, whereas the geometry of Zr-Cp$_2$(butadiene)[1d] is known to vary from s-trans to s-cis and that of MoCp(NO)(butadiene)[19] from s-cis to s-trans by raising the temperature in the same range. This fact also contrasts to the observation that ZrCp*$_2$(butadiene) and ZrCp$_2$(1,4-diphenylbuta-diene) kinetically favor the s-trans-diene coordination.[1a,c]

Pursuing the essential factor for the preference of the non-fluxional s-cis coordination, the replacement of the Cl ligand in **1a** with other halides, Br and I, have been examined to evaluate the electronic and steric effects of the anionic ligands. However, replacement of the ligand was found ineffective in bringing about the geometrical change, although chemical shift values of the anti protons vary systematically; i.e., the value increases with a decrease of electronegativity of the halide ligands. Similar chemical shift change is also manifested in TiXCp*(1,4-diphenylbutadiene) **(2a,b)** and TiXCp*(isoprene) **(3a,b)**.

To further elucidate the electronic and steric effects of auxiliary ligand X, TiCp*$_2$(isoprene) **(8)** and TiCp*$_2$(2,3-dimethyl-butadiene) **(9)** were prepared following the reaction shown in eq. 4. Complexes **8** and **9** thus obtained again prefer the s-cis-diene coordination as judged from the ^{1}H NMR chemical shifts, i.e. 0.06 (t, H^1), -1.00 (d, H^2), 1.82 (t, H^3), 1.75 (d, H^4), 5.76 (t, H^5) ppm for **8**; 0.86 (d, H^1 and H^2), 1.72 (d, H^3 and H^4) ppm for **9**. The anti protons showed a significant upfield shift due to the

Table I. ¹H NMR Parameters for Supine and Prone TiCp*X(diene) Complexes[a]

complexes	chem shift values (δ, ppm)			coupling constants, Hz								
	ν_1 / ν_2	ν_3 / ν_4	ν_5 / ν_6	$J_{1,2}$	$J_{1,3}$ ($J_{2,4}$)	$J_{1,4}$ ($J_{2,3}$)	$J_{1,5}$ ($J_{2,6}$)	$J_{1,6}$ ($J_{2,5}$)	$J_{3,4}$	$J_{3,5}$ ($J_{4,6}$)	$J_{3,6}$ ($J_{4,5}$)	$J_{5,6}$
Prone Titanium–Diene Complexes												
1a	3.82	3.16	3.71	0.5	−7.0	−0.6	14.5	−1.5	1.0	10.0	1.2	9.5
1b	4.17	3.03	3.63	0.5	−7.0	−0.6	14.5	−1.5	1.0	10.0	1.2	9.5
1c	4.76	2.94	3.71	0.5	−6.9	−0.6	14.4	−1.5	1.0	10.2	1.2	9.4
2a	6.73		4.22	0.1			15.0	−1.2				10.0
2b	7.18		4.06	0.1			15.0	−1.3				9.8
6a	3.89 / 4.68	3.07	3.37 / 3.55	0.2	−6.2	−0.2	14.5 / 14.2	−1.3 / −1.2		9.7	0.2	9.8
6b	4.22 / 5.23	2.92	3.22 / 3.43	0.2	−6.0	−0.2	14.6 / 14.2	−1.3 / −1.2		9.7	0.2	9.7
Supine Titanium–Diene Complexes												
3a	1.23 / 1.10	2.96 / 2.80	5.68	0.1	−9.9 / −8.5	0.0	10.7	0.0	0.0	10.2	−0.1	
3b	1.20 / 1.05	2.82 / 2.67	5.88	0.1	−10.1 / −8.6	0.1 / 0.1	10.8	0.0	0.0	10.3	−0.1	
4	1.42	2.75		0.2	−9.0	1.8			0.5			
5	1.60	3.21		0.3	−9.2	1.7			0.3			
Related Complexes												
Zr(C₄H₆)[b]	−0.69	3.45	4.78	0.6	−10.0	0.2			0.2	9.5	−1.5	8.0
Zr(C₅H₈)[c]	0.87 / 0.75	0.87 / 0.75	5.74		−5.0 / −5.0		4.8			4.8		
Hf(C₆H₁₀)[d]	0.01	2.14			−11.0			−0.8			−0.8	
Fe(C₄H₆)[e]	−0.03	1.46	4.89	−0.3	−2.4	−0.1	9.3	−1.1	0.1	6.9	−1.1	4.7

[a] Data were collected at 500 MHz in C_6D_6 at 30 °C and analyzed by computer simulation. Numbering system is given in text as 7 where R^6 = CH₃ for isoprene and R^4 = CH₃ for pentadiene. [b] ZrCp₂(C₄H₆) given in ref 1c. [c] ZrCp*₂(isoprene) reported in ref 1c. [d] HfClCp*(2,3-dimethylbutadiene) reported in ref 4a. [e] Fe(CO)₃(C₄H₆) reported in ref 18.

strong deshielding effect by Cp* ligands in these case. A

$$\textbf{TiCp}_2^* \textbf{Cl}_2$$
$$+$$
$$\text{R}^5 \text{ R}^6$$
$$+ \text{Mg} \diagdown \Big)_n$$

$$\xrightarrow[\textbf{THF}]{-78\sim-30\ ^\circ\text{C}}$$

H³H¹ H² H⁴ ... Ti ... R⁵ R⁶   (7)

8: R^5=H, R^6=CH₃
9: R^5=R^6=CH₃
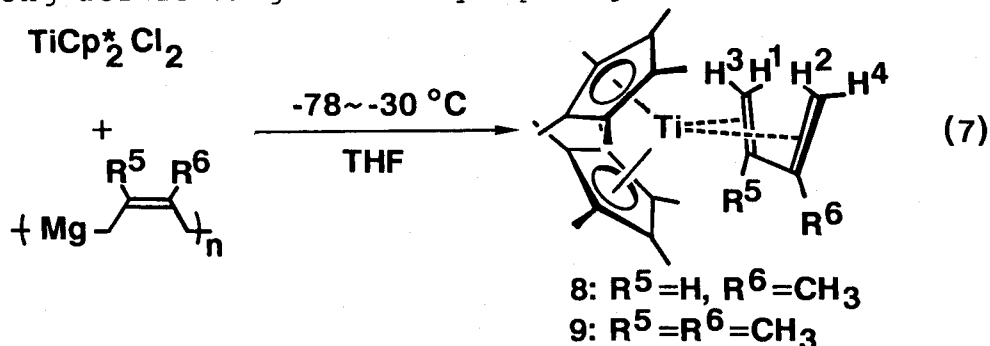
further attempt to isolate pure TiXCp(diene) complexes (X = Cl, Br, I, Cp) bearing a less bulky Cp ligand has been frustrated by the instability of the product even at 0 °C.

In conclusion, the above results indicate that titanium-diene complexes always prefer the s-cis coordination regardless the substituent(s) on the diene ligand. We can therefore postulate that the relative shortness of Ti-C bonds as compared with the Zr-C and Hf-C bonds are crucial for the s-cis-diene coordination.

(b) ^{13}C NMR Studies.

The ^{13}C-^{13}C coupling constant provides the most direct and unambiguous evidence about the topology of the C-C bonded molecular framework. Typical value is 35 Hz for the C-C single bonds and 70 Hz for the C-C double bonds.[20] The indirect scalar ^{13}C-^{13}C coupling for the terminal carbons in ML_2(diene) (M = Zr, Hf; L = Cp, tBuCp) is reported recently to fall into a range of 34-38 Hz and those for η^4-diene coordinated complexes of Mo, Fe, and Co are 42-46 Hz.[21] The magnitude of the corresponding ^{13}C-^{13}C coupling constants for the prone titanium-diene complexes (**1a** and **6a**) obtained from the INEPT-INADEQUATE experiment[22] are found to resemble those for (η^4-diene)iron complexes while those for the

Table II. ^{13}C–^{13}C Coupling Constants (Hz) for Ligated Dienes in Titanium–Diene and Related Complexes[a]

complexes	$J_{C(1)-C(2)}$	$J_{C(2)-C(3)}$	$J_{C(3)-C(4)}$
$TiClCp^*(C_4H_6)$ (**1a**, prone)	43.5	—	43.5
$TiClCp^*(C_5H_8)$ (**6a**, prone)	42.9	45.0	45.1
$TiClCp^*(C_5H_8)$ (**3a**, supine)	39.1	51.3	39.0
$ZrCp_2(C_5H_8)$[b]	37.5	57.3	38.0
$Fe(CO)(C_5H_8)_2$[b]	46.7	46.5	43.6

[a] Measured at 125.65 MHz in C_6D_6 at 35 °C by using INEPT–INADEQUATE pulse sequences. [b] See ref 21. Numbering system is given in **7** in the text.

supine titanium–diene complex (**3a**) exhibit similar values to those of zirconium derivatives (Table II). These results indicate that the (η^4-diene)metal character is more pronounced for the prone titanium–diene isomer as compared with the supine isomer.

The ^{13}C–^1H coupling constant also offers information on the degree of C–H hybridization of carbons in the coordinated dienes. On the basis of the Newton's semiempirical rule,[23] it is possible to calculate the s% of carbon atoms on the dienes and hence the hybridization approximated by n=(100-s)/s for carbon sp^n. The value of n (averaged) for the carbons at diene termini reaches to 2.8-2.9 (132-128 Hz) when the molecule has highly fluxional metallacyclo-3-pentene structure (**10**) as found for $HfCp^*_2$(butadiene) and $ZrCp^*_2$(isoprene),[1c] while the value is in a range of 2.1-2.3 (165-154 Hz) in the case of the conventional η^4-diene complex (**11**) like $Fe(CO)_3$(diene),[24] $Rh(\eta^5-C_9H_7)$-(diene),[25] etc. The n value for the present titanium–diene complexes **1**, **3**, **4**, and **5** falls into the range of 2.2-2.4,
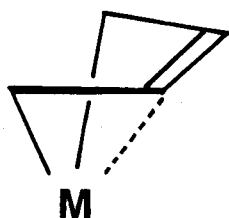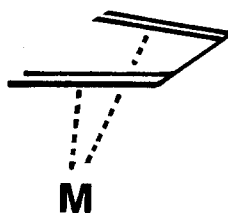
10   **11**

indicating the presence of a pronounced participation of the limiting structure **11** in these complexes as compared with zirconium-diene complexes (Table III). Thus, the n value for the terminal carbons increases in the order Ti<Zr<Hf. However this value varies only slightly with respect to the inner carbons (n=2.2-2.4) even when the metals is replaced with late transition metals.

The alkyl or aryl substitution on C(1) and /or C(4) position of the coordinated diene causes an increased sp^3 character (decrease of ^{13}C-^1H coupling constant) as observed in the complexes of 1,4-diphenylbutadiene (**2**) and pentadiene (**6**). For example, **6a** and **6b** show the J_{CH}(av.) of 153.2-155.4 Hz for C(1) and 137.3-144.0 Hz for C(4). Hence the pentadiene complex may be represented by a σ,π^3-allyl structure (**6'**) rather than **6**. Although
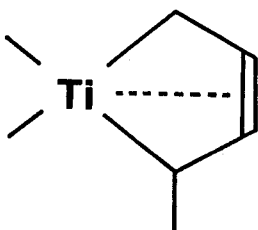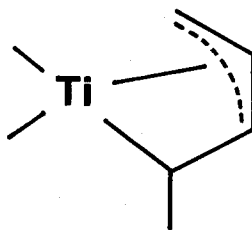
6   **6'**

Table III. ¹³C NMR Parameters for Supine and Prone Titanium–Diene Complexes[a]

complexes	chemical shift values (δ, ppm) (¹³C–¹H coupling constant, Hz)	
	ν₁, ν₄	ν₂, ν₃
TiClCp*(BD) (1a)	77.6 (154.1)	116.0 (164.8)
TiBrCp*(BD) (1b)	79.7 (157.5)	116.0 (156.9)
TiICp*(BD) (1c)	81.9 (153.2)	114.3 (157.5)
TiClCp*(1,4-DP) (2a)	97.8 (137.9)	107.3 (161.1)
TiBrCp*(1,4-DP) (2b)	99.6 (137.9)	107.3 (161.1)
TiClCp*(PD) (6a)	77.2 (144.0), 90.6 (137.3) (163.6)	111.4 (163.6), 118.2 (158.7)
TiBrCp*(PD) (6b)	79.4 (153.2), 92.8 (144.0)	116.1 (161.1), 118.1 (163.6)
TiICp*(IP) (3a)	78.1 (149.4), 77.5 (148.9)	128.5 (159.3), 140.8 (s)
TiBrCp*(IP) (3b)	80.1 (155.1), 79.5 (154.4)	115.4 (158.7), 141.0 (s)
TiClCp*(2,3-DM) (4)	82.6 (142.9) (157.1)	136.1 (s)
TiClCp*(2,3-DP) (5)	84.8 (141.3)	138.3 (s)
ZrCp₂(BP)[b]	48.4 (145)	110.9 (154)
ZrCp*₂(IP)[b]	46.5 (157.5), 51.87 (157.5) (128.2) (128.2)	109.5 (153.8), 121.5 (s)
HfClCp*(2,3-DM)[c]	67.7 (149) (131)	128.6 (s)
Fe(CO)₃(BD)[d]		

[a] Data were collected at 25.1 MHz in C₆D₆ at 30 °C. Numbering scheme follows that given in 7 (R⁶ = CH₃ for IP and R⁴ = CH₃ for PD). Abbreviations: BD, butadiene; 1,4-DP, 1,4-diphenylbutadiene; PD, 1,3-pentadiene; IP, isoprene; 2,3-DM, 2,3-dimethylbutadiene. [b] See ref 1c. [c] See ref 4. [d] See ref 24.

such a distortion has been recognized in the X-ray structure of HfClCp*(2,3-dimethylbutadiene),[4a] ZrCp$_2$(1,4-diphenylbuta-diene),[1g] etc., the present results suggest the presence of σ,π^3-allyl structure in solution.

The ^{13}C chemical shift values for the terminal carbons of titanium–diene complexes (77.6–99.7 ppm) differs greatly from the corresponding value for a series of zirconium- and hafnium-diene complexes of the type MCp$_2$(diene) (46.5–55.7 ppm) and from the values observed in the diene complexes of Co, Fe, and W (31.3–44.2 ppm).[21] The larger value may primarily be due to the electron-withdrawing effect of the halide. Actually replacement of the Cl ligand by Br or I generally results in the downfield shift of the terminal carbon signals. Noteworthy is that there exists only a slight chemical shift difference in the ^{13}C resonance of the terminal carbons between prone and supine dienes, whereas a marked ^{1}H chemical shift difference exists between these isomers (vide supra). The chemical shift values for inner carbons of the prone titanium–diene complexes (107–118 ppm) are smaller than those (128–136 ppm) for zirconium- and hafnium-diene complexes with formula MClCp*(diene),[4] while the values for conventional η^4-diene complexes of Fe,[18,26] Ru,[18] Rh,[27] etc. are much smaller (77–87 ppm). This fact suggests the presence of some metallacyclo-3-pentene character in 1–6.

3. Molecular Structure of Titanium–Diene Complexes. (a) X-ray Analysis of TiCp*Cl(butadiene) (1a).

As a typical example of the complexes of the type TiXCp*-(diene), TiClCp*(C$_4$H$_6$) (1a) was subjected to the crystallographic analysis. The molecular structure is shown in Figure 2 by ORTEP

drawings with numbering scheme. Selected bond distances and angles are listed in Table IV and v, respectively. Crystallographic data are summarized in the Experimental section (Table 12). The titanium atom may be described as having a pseudotetrahedral geometry if the Cp* group is considered to occupy one coordination site and the butadiene ligand is assumed to bind via the two terminal carbons. The most intriguing structural feature lies in the prone orientation of the s-cis-butadiene ligand. Thus, the present work provides the first X-ray structure of the titanium-diene complex and of the complex possessing the "prone" conformation. The dihedral angle between the planes of the Cp* and the diene consisting of C(1), C(2), C(3), and C(4) is 20.2°. The molecular structures of analogous monodiene complexes reported so far all exhibit the supine conformation, although the prone structure has been proposed for $[MoCp(CO)_2]^+$ based on the NMR studies.[28] The terminal C-C bonds C(1)-C(2) (1.416 Å) and C(3)-C(4) (1.418 Å) show nearly the same length as the inner C(2)-C(3) bond (1.400 Å) indicating the presence of a rather weak metallacyclo-3-pentene character (see **10**) in this molecule.

Another remarkable feature is seen in the mean distance of terminal C-C bonds (1.417 Å), which is the shortest among the corresponding bonds involved in the early-transition metal-diene complexes; i.e. the terminal C-C bond distance varies in the ranges 1.420-1.473 Å for zirconium-diene complexes, 1.429-1.478 Å for hafnium derivatives, and 1.456-1.500 Å for tantalum complexes. The observed value compares closely to the C-C bond lengths in $MoCpCl_2(C_4H_6)$,[29] $IrCl(C_4H_6)_2$,[30] and $Mo(PMe_3)(C_4H_6)_2$[31] (1.410-1.412 Å) of conventional η^4-diene-metal structure, but these values exceed over those of $RhCl(C_4H_6)_2$[32] and
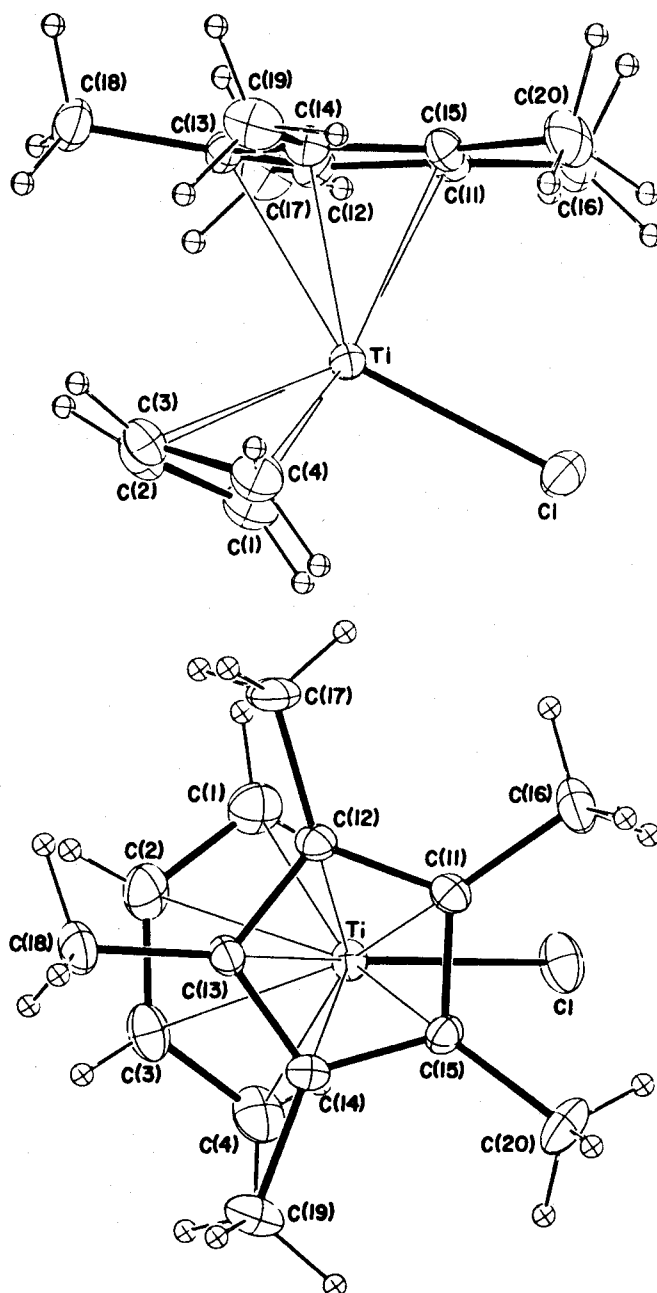
Figure 2.　Molecular Structuer of **1a**

$Mn(CO)(C_4H_6)_2^{15)}$ (1.385-1.387 Å) with typical η^4-diene coordination.

Although the present X-ray result may be suggestive of 14e η^4-metallacyclo-3-pentene structure, which emphasizes the σ-bonding at the diene termini and π-bonding at the inner carbon atoms, the 14e σ^2-bonded η^4-diene-titanium limit still participates substantially in **1a** as deduced from the relatively short terminal C-C bond distances as well as the ^1H and ^{13}C NMR spectral data.

(b) **X-ray Analysis of TiClCp*(1,4-diphenylbutadiene) (2a).** From the crystallographic data, the molecular structure of **2a** was found to have crystallographic mirror symmetry. Its whole geometry resembles very well that of **1a** as shown in Figure 3. The diene ligand binds to metal again in prone fashion. The dihedral angle between the Cp* ring and the diene plane is 18.1°, a value similar to the angle for **1a** and that (18.5°) observed for the prone-diene in $TaCp^*(2,3$-dimethylbutadiene)$_2$ (see Table VIII) but smaller than the corresponding angle (35°) for $TaCp(2,3$-dimethylbutadiene)$_2$.[2)] The terminal C(1)-C(2) and C(3)-C(4) bonds (1.416 Å) of **2a** have nearly the same length as the inner C(2)-C(3) bond (1.390 Å) as well as the respective bonds in the butadiene analogue **1a** (Table IV). The Ti-C(1) and Ti-C(4) bonds (2.233 Å) are slightly shorter (by 0.06 Å) than the Ti-C(2) and Ti-C(3) bonds as found also in complex **1a**. As consequence, the bent angle between the planes defined by C(1)-Ti-C(4) and C(1)-C(2)-C(3)-C(4) becomes 105° for **2a**, a value similar to that (104.3°) for **1a** (Table VIII). The magnitude of these angles is intermediate between 95 and 125° observed for diene complexes of Zr, Hf, and Ta and between 71 and 83° for the middle- and late-transition-metal-diene complexes, indicating a substantial participation of
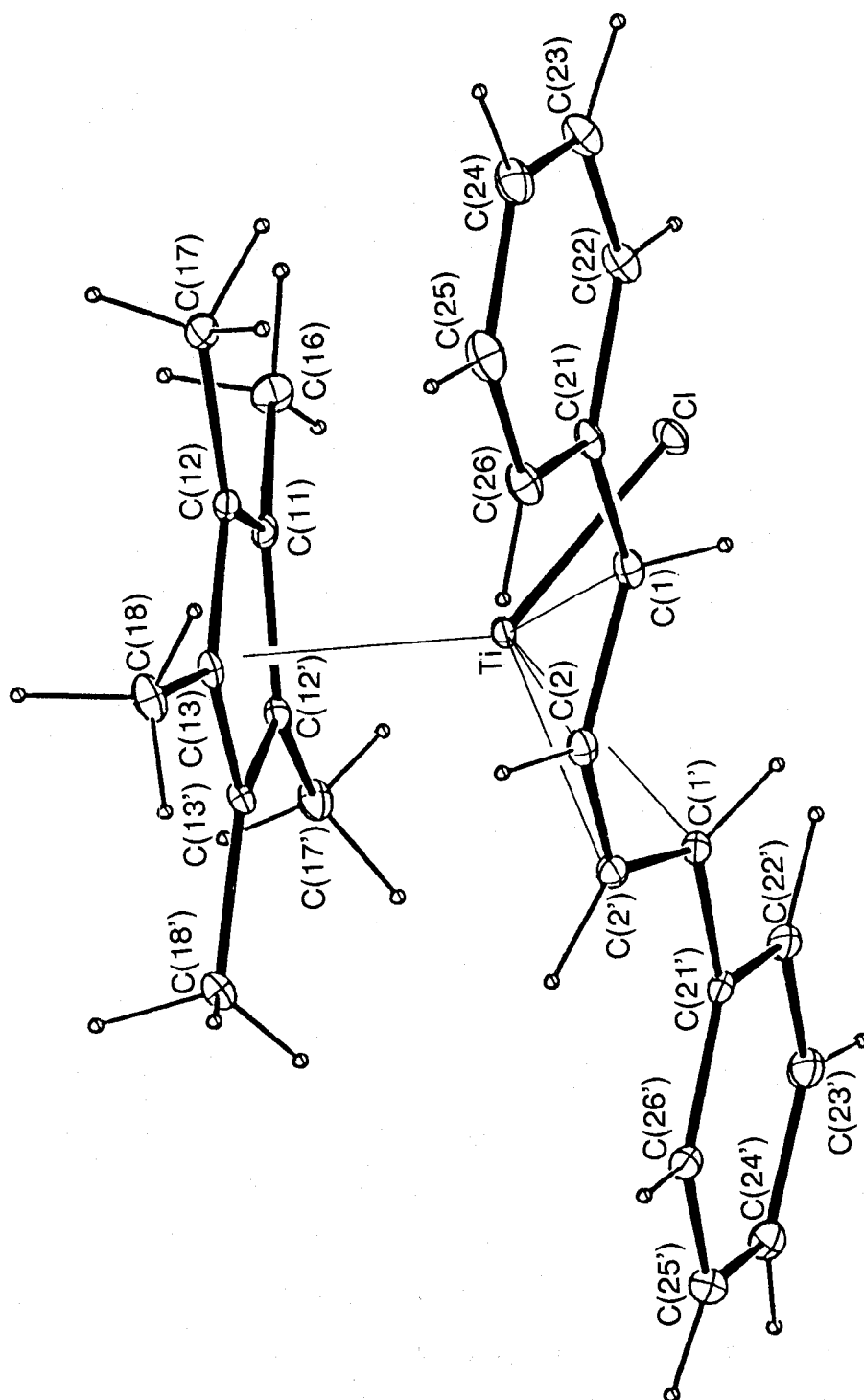
Figure 6. Molecular Structure of **2a**.

the bent metallacyclo-3-pentene limit in these prone titanium-diene complexes.

Other structural characteristics of **1a** and **2a** emerge in the bite angle (β) defined by C(1)-Ti-C(4). The values for **1a** (88.3°) and **2a** (87.7°) are the largest among the angles reported so far for the s-cis-diene metal complexes, i.e. 5.5-13.2° larger than the values reported for zirconium- and hafnium-diene complexes, 10.4-16.9° larger than those for tantalum-diene complexes,[5] and 5-16° larger than those for late-transition metal-diene complexes containing Fe,[33] Mo,[31] Mn,[15] etc. The marked expansion of the bite angle may occur for the sake of lengthened nonbonded C(1)-C(4) distance as the result of relatively short M-C(1) and M-C(4) bond distances. Actually the nonbonded C(1)-C(4) distances in **1a** (3.041 Å) and **2a** (3.093 Å) are remarkably larger than the corresponding distance in 16e and 18e diene complexes of other metals represented by $TaCl_2Cp(C_4H_6)$ (2.694 Å, $\beta=73.3°$)[2] and $Fe(CO)_3(C_4H_6)$ (2.83 Å, $\beta=82.6°$).[33] Since the titanium atom has relatively small atomic radius, the M-C(terminal) bond distances (the mean distance of M-C(1) and M-C(4)) in **1a** (2.184 Å) and **2a** (2.233 Å) become much shorter than those of the other group 4A and 5A early-transition metal-diene complexes, which range from 2.251 Å in $TaCp^*(C_6H_{10})(C_4H_6)$ to 2.317 Å in $Hf(DMPE)(C_4H_6)_2$.[6] The Ti-C(1) and Ti-C(4) bond lengths are nearly equal to those in $TiCp^*_2$(ethylene) (2.160 Å)[34] and $TiCp^*(CO)(PhC{\equiv}CPh)$ (average 2.169 Å).[35]

The methyl groups at Cp^* rings in **1a**, and **2a**, and **5** are all bent out slightly (3.7-4.2°) away from the metal (see Table VI for averaged value). Among them, C(18) atom in **1a** shows the largest deviation (9.6°) while the bent angle (θ) for C(18) in **2a**

Table IV. Selected Interatomic Distance (Å) for Titanium–Diene Complexes TiCp*Cl(CHR^{1}CR^{2}CR^{2}CHR^1) (1a, 2a, and 5) with Estimated Standard Deviations in Parentheses

	1a ($R^1 = R^2 = H$)	2a ($R^1 = C_9H_5$, $R^2 = H$)	5 ($R^1 = H$, $R^2 = C_6H_5$)
Ti–Cl	2.372 (2)	2.312 (2)	2.297 (2)
Ti–C(1)	2.178 (10)	2.233 (6)	2.150 (6)
Ti–C(2)	2.288 (9)	2.293 (5)	2.405 (6)
Ti–C(3) [Ti–C(2′)]	2.281 (9)	2.293 (5)	2.387 (6)
Ti–C(4) [Ti–C(1′)]	2.189 (10)	2.233 (6)	2.123 (6)
Ti–C(11)	2.346 (6)	2.324 (7)	2.369 (6)
Ti–C(12)	2.342 (6)	2.330 (5)	2.375 (6)
Ti–C(13)	2.373 (6)	2.377 (5)	2.395 (7)
Ti–C(14) [Ti–C(13′)]	2.341 (6)	2.377 (5)	2.384 (6)
Ti–C(15) [Ti–C(12′)]	2.343 (6)	2.330 (5)	2.369 (6)
C(1)–C(2)	1.416 (14)	1.416 (7)	1.466 (8)
C(2)–C(3) [C(2)–C(2′)]	1.400 (13)	1.390 (13)	1.368 (8)
C(3)–C(4) [C(1′)–C(2′)]	1.418 (14)	1.416 (7)	1.464 (9)
C(1)–C(21)		1.464 (7)	
C(2)–C(21)			1.508 (8)
C(3)–C(31)			1.511 (9)

Table V. Selected Bond Angles (deg) for Non-Hydrogen Atoms in TiClCp*(CHR¹CR²CR²CHR¹) (1a, 2a, and 5) with Estimated Standard Deviations (Parentheses)

	1a ($R^1 = R^2 = H$)	2a ($R^1 = C_6H_5$, $R^2 = H$)	5 ($R^1 = H$, $R^2 = C_6H_5$)
Cl–Ti–C(1)	96.6 (2)	94.8 (2)	117.6 (2)
Cl–Ti–C(4) [Cl–Ti–C(1′)]	95.3 (2)	94.8 (2)	112.8 (2)
C(1)–Ti–C(4) [C(1)–Ti–C(1′)]	88.3 (3)	87.7 (2)	83.9 (2)
Ti–C(1)–C(2)	75.8 (5)	74.1 (3)	81.0 (3)
C(1)–C(2)–C(3) [C(1)–C(2)–C(2′)]	124.7 (9)	127.0 (5)	120.4 (5)
C(2)–C(3)–C(4)	126.1 (9)	127.0 (5)	120.7 (5)
Ti–C(4)–C(3) [Ti–C(1′)–C(2′)]	75.1 (5)	74.1 (3)	81.2 (4)
C(1)–C(21)–C(22)		119.1 (5)	
C(1)–C(21)–C(26)		123.2 (5)	
C(2)–C(21)–C(22)			122.1 (5)
C(3)–C(31)–C(32)			121.8 (6)
C(2)–C(21)–C(26)			118.4 (5)
C(3)–C(31)–C(36)			117.9 (6)

is reduced to 5.9° due to the sterically more favorable arrangement of the methyl group in its Cp* ligand.

A roughly linear correlation is observed between the difference in Ti-C bond distances defined by $\Delta d=[d(Ti-C(1))+d(Ti-C(4))]/2-[d(Ti-C(2))+d(Ti-C(3))]/2$ and the n value of the sp^n hybridization for terminal carbons C(1) and C(4) as observed in their contour plots (Figure 4). A good correlation was also found between the difference in C-C bond distances, $\Delta l=[l(C(1)-C(2))+l(C(3)-C(4))]/2-l(C(2)-C(3))$ and the n value (Figure 5). These results clearly show the pronounced participation of structure 11 for the first-row titanium complexes as compared with the second- and third-row group 4A metal complexes.

(c) X-ray Analysis of TiClCp*(2,3-diphenylbutadiene) (5). The molecular structure of 5 is shown in Figure 4. Selected bond distances and angles are listed in Tables IV and V, respectively. Remarkable is that complex 5 adopts the supine conformation in sharp contrast to the prone structure found in foregoing titanium-diene complexes 1a and 2a. Consequently, the C(1)-C(2)-C(3)-C(4) diene plane and the Cp* ring make a larger dihedral angle of 74.6°, an entirely different value from the 18.1-20.2° value observed for 1a and 2a. This value corresponds to that of the supine oriented diene in $TaCl_2Cp(C_4H_6)$ (71.9°) and that in $TaCp*(2,3-dimethylbutadiene)_2$ (78.6°) but is smaller than the angle (108.1°) observed for supine HfClCp*(2,3-dimethylbutadiene).[4a] Both C(1)-C(2) (1.466 Å) and C(3)-C(4) (1.464 Å) bonds are much longer than the inner C(2)-C(3) bond (1.368 Å), and the bent angle (θ) between the C(1)-Ti-C(4) and C(1)-C(2)-C(3)-C(4) planes is 106.8°. The respective values observed for 5 compare very closely with those of other 2,3-disubstituted diene
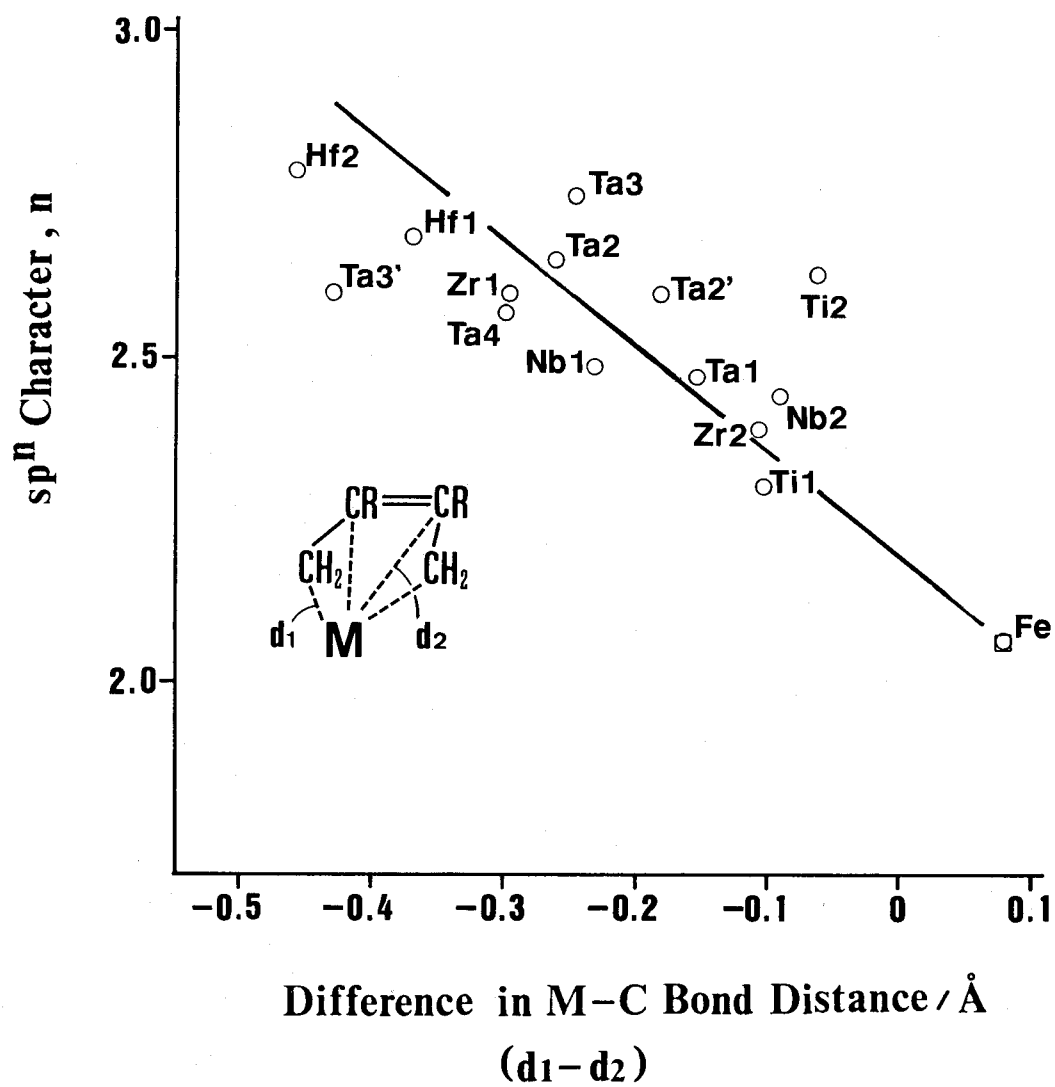
Figure 4. Correlation between $(d_1 - d_2)$ vs. n
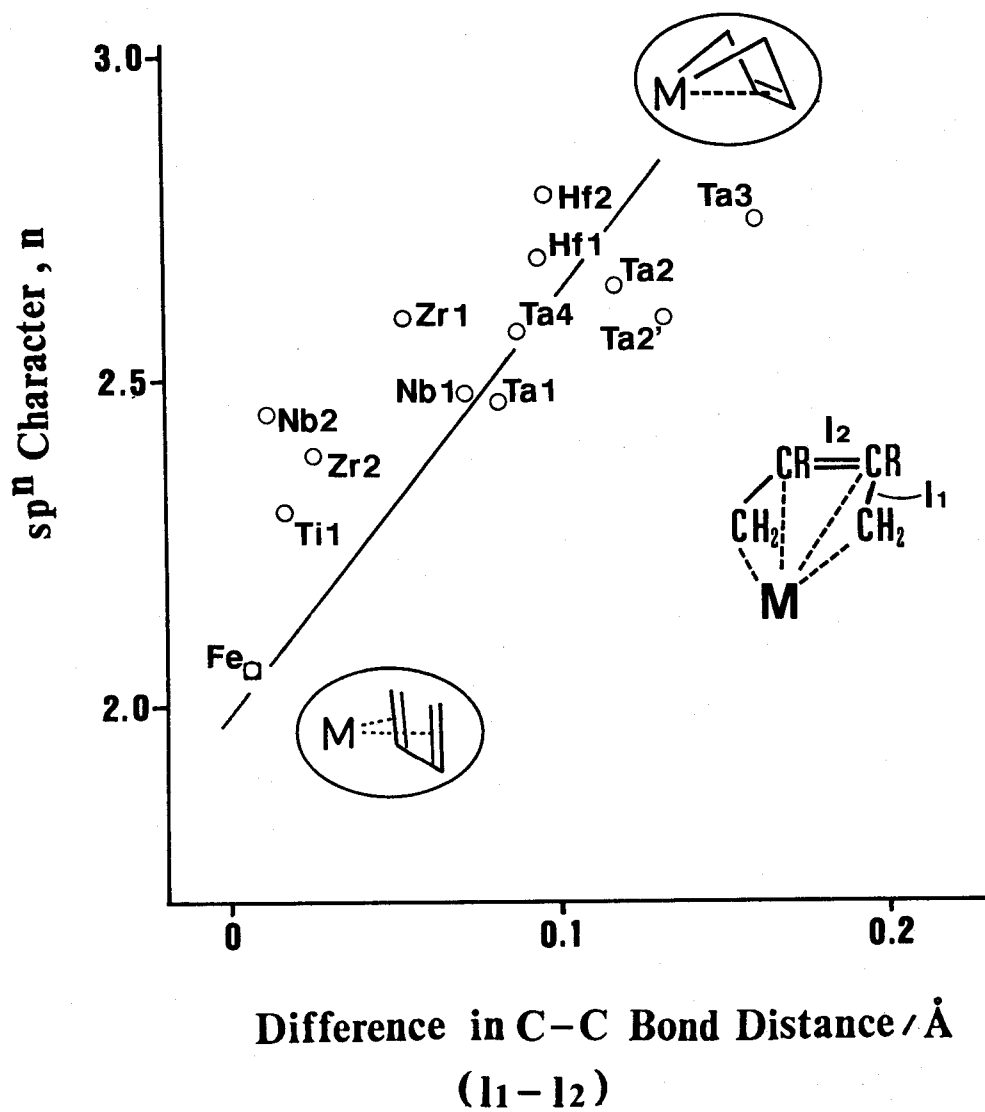
Figure 5. Correlation between (l_1-l_2) vs. n

complexes of group 4A metals, which assume the bent metallacyclo-3-pentene structure, i.e. $ZrCp_2$(2,3-dimethylbutadiene) ($\theta=112.8°$, C–C(terminal)=1.450Å), $ZrCp_2$(2,3-diphenylbutadiene) ($\theta=119.6°$, C–C(terminal)=1.473 Å),[1f] and $HfClCp^*$(2,3-dimethylbutadiene) ($\theta=104.5°$, C–C(terminal)=1.431 Å).[4a] Thus, it is evident from the C–C bond alternation, the relatively large dihedral angle , and the Ti–C distances that the complex 5 exhibits a distinct metallacycle structure. The resulting Ti–C(2) and Ti–C(3) bond distances (average 2.396 Å) are a little smaller than the sum of the ionic radius of Ti^{4+} (0.75 Å) and the van der Waals radius of the carbon atom (1.7 Å). Therefore we can presume the presence of a bonding interaction between the titanium and the inner carbons of the coordinated diene.

A direct information on the sp^n hybridization of terminal carbons in the ligated dienes could be obtained from the angle (α) between the normal of the C(1)–C(2)–C(3)–C(4) plane and the normal of the H(1)–C(1)–H(2) plane or that of H(3)–C(4)–H(4) plane. At a rough estimate, the angle is expected to increase with an increase of the sp^3 character on the CH_2 or CHR group.

12
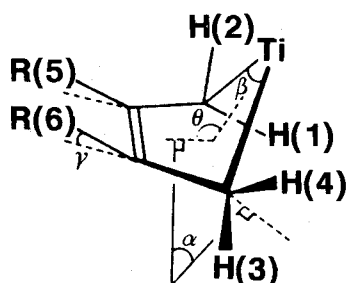
The α values observed for **1a** (32.3 and 38.0°), **2a** (28.8°), and **5** (38.5 and 44.3°) deviate largely from the values (6.3 and 8.6°) observed for late-transition metal complexes like $Fe(CO)_3$(1,4-
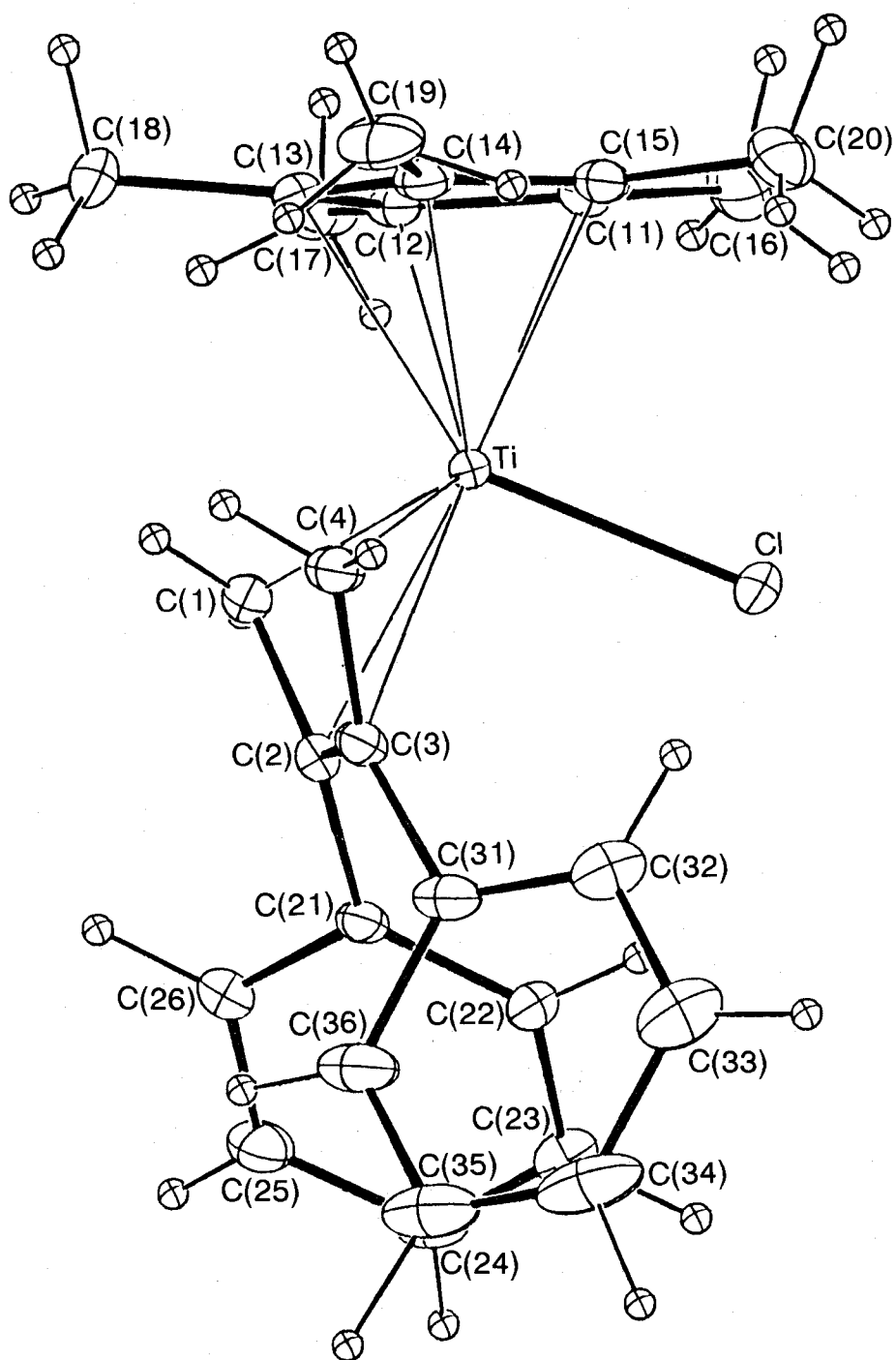
Figure 6. Molecurar Structure of **5.**

Table VI. Coordination Geometry of Ti Atoms in Titanium–Diene Complexes
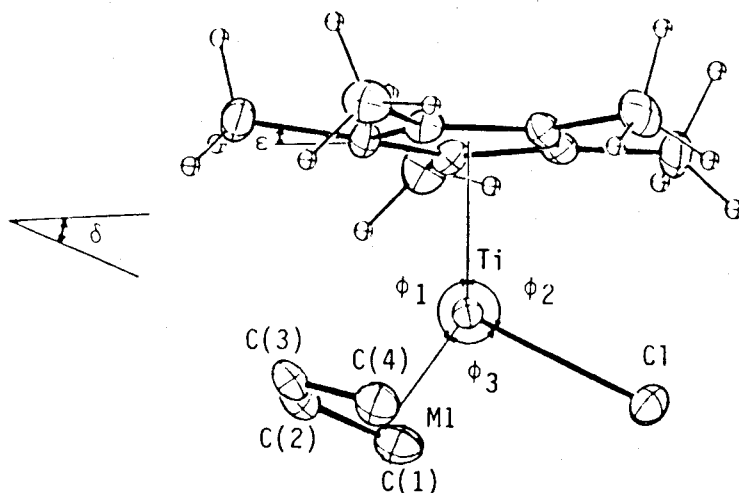
	1a	2a	5
Ti–CCP,[a] Å	2.017	2.223	2.049
Ti–M1,[b] Å	1.568	1.610	1.589
C(1)···C(4), Å	3.041	3.093	2.856
δ,[c] deg	20.2	18.1	74.6
β,[d] deg	88.3	87.7	83.9
θ,[e] deg	105.0	104.3	106.8
ϕ_1,[f] deg	144.4	143.7	121.5
ϕ_2, deg	117.4	119.7	113.5
ϕ_3, deg	98.3	96.6	124.9
ϵ,[g] deg	4.1	3.7	4.2

[a] CCP: centroid of cyclopentadienyl ligand. [b] M1: midpoints of C(1) and C(4). [c] δ: dihedral angle between Cp* ring and the diene plane. [d] β: bite angle, C(1)–Ti–C(4). [e] θ: bent angle between the planes of C(1)–Ti–C(4) and C(1)–C(2)–C(3)–C(4). [f] ϕ_{1-3}: angles formed by the bonds between CCP, M1, and Cl (see below). [g] ϵ: bent angle CCP–C–CH_3.

diphenylbutadiene)[36a) in support of the significant sp³-carbon character.

The H(5) and H(6) atoms in **1a** and the C(5) and C(6) atoms in **2a** are bent away from C(1)-C(4) diene plane toward the metal, presumably due to the electronic effect of the ring current on Cp* group. Similar distortion has been observed in cases of Zr-Cp_2(diene).[36b) The angles γ for **1a** (12.1 and 15.8°) and **2a** (12.2°) are larger but those for **5** (4.6 and 7.3°) are comparable to those (4.4 and 8.0°) observed for $Fe(CO)_3$(1,4-diphenylbutadiene).

Experimental Section

General Remarks. All manipulations were performed by using standard Schlenk tube technique under argon atmosphere. Ethereal and hydrocarbon solvents were distilled from Na/K alloy and thoroughly degassed by trap-to-trap distillation before use. NMR spectra were recorded on a JEOL GX-500 (500.0 MHz for ¹H and 125.65 MHz for ¹³C nuclei) and a Varian XL-100 spectrometers with a spin-simulation system. Mass spectra (EIMS) were recorded on a EOL DX-300 (high resolution, 30 eV) and a JEOL 01-SG instrument (low resolution, 70 eV) with fluorokerocenes as internal standards. Pentamethylcyclopentadiene was prepared by the known method.[37) Melting points were uncorrected.

Preparation of $(C_5Me_5)TiCl_3$. The precursor $C_5Me_5SiMe_5$ was prepared conveniently by using the following procedure. Pentamethylcyclopentadine (33.4 g, 210 mmol) was dropwise added to a THF suspension (150 mL) of potassium hydride (8.4 g, 210 mmol) at 25 °C. Reaction completed by refluxing the mixture for 2 h. To the resulting suspension of C_5Me_5K was dropwise added trimethyl-silylchloride (32 mL, 250 mmol) at 0 °C. After the mixture was

stirred at room temperature for 2 h, n-hexane was added to separate the salt. The mixture was filtered and distilled to give $C_5Me_5SiMe_3$ in 65-75% yield; bp 51 °C (2 Torr). Then freshly distilled $TiCl_4$ (9.5 g, 50 mmol) was added to a hexane solution (150 mL) of $C_5Me_5SiMe_3$ (10.4 g, 50 mmol) heated to 60 °C with stirring (similar procedure has been reported by Royo et al.[38] after the completion of this work). The color of the solution turned to deep red, and a red crystalline solid precipitated immediately after the mixing. The precipitate was separated by filtration and washed with hexane (40 mL). Recrystallization from hexane/THF gave $(C_5Me_5)TiCl_3$ in 75% yield (10.8 g); mp 227 °C. Anal. Calcd for $C_{10}H_{15}TiCl_3$: C, 41.47; H, 5.22. Found: C, 41.49; H, 5.24.

$(C_5Me_5)TiBr_3$ was prepared in essentially the same procedure as described for $(C_5Me_5)TiCl_3$; mp 245 °C. Anal. Calcd for $C_{10}H_{15}TiBr_3$: C, 28.39; H, 3.58. Found: C, 28.53; H, 3.64.

Preparation of $(C_5Me_5)TiI_3$. Triethylamine (4.1 g, 40 mmol) was added dropwise to the stirred solution of $(C_5Me_5)TiCl_3$ (2.9 g, 10 mmol) in methanol (50 mL) at 0 °C. The color of the solution changed from red to yellow during this procedure. The solution was stirred for 2 h at 0 °C and then evaporated to dryness, and the product was extracted with 40 mL of hexane. Contaminated insoluble products were thoroughly removed by filtration or centrifugation under argon atmosphere. Dropwise addition of acetyl iodide (5.1 g, 40 mmol) at 0 °C to the resultant pale yellow clear solution resulted in the precipitation of $(C_5Me_5)TiI_3$ as red-brown solid immediately after mixing. The mixture was stirred for 1 h at room temperature, filtered, and dried in vacuo. Purification of the product by recrystallization from

hexane/THF gives $(C_5Me_5)TiI_3$ in 30% yield (1.7 g) as red-purple crystals, mp 277 °C. Anal. Calcd for $C_{10}H_{15}TiI_3$: C, 21.29; H, 2.68. Found: C, 20.98; H, 2.64.

Preparation of Titanium-Diene Complexes 1-6. Method A. Preparation Using (Enediyl)magnesium. A suspension of (2-butene-1,4-diyl)magnesium[39] (1.8 mmol) in THF (3 mL) was dropwise added over 15-min period to $(C_5Me_5)TiCl_3$ (0.58 g, 2 mmol) dissolved in thoroughly dried and degassed THF (30 mL) at -78 °C with magnetic stirring. The mixture was kept at -45 °C for 2 h with stirring and then allowed to warm to room temperature. The solution was stirred for 2 h and then evaporated to dryness. Extraction of the product from the residue into strictly degassed hexane (30 mL), separation of the salt by centrifugation with specially designed two-necked glass tube, followed by concentration of the solution to 8 mL, and cooling to -20 °C led to the precipitation of $(C_5Me_5)TiCl(C_4H_6)$ (**1a**) as dark blue crystals in 52% yield (0.24 g): mp 126 °C dec; EIMS (30 eV), m/z (relative intensity) 272.0780 (M^+, 36.0; calcd for $(C_5Me_5)Ti^{35}Cl(C_4H_6)$, 272.0810), 274.0780 ($M^+$, species with ^{37}Cl, calcd 274.0780), 218 (($C_5Me_5)Ti$-^{35}Cl, 100.0), 220 (($C_5Me_5)Ti^{37}Cl$, 39.0).

In essentially the same manner, $(C_5Me_5)TiBr(C_4H_6)$ (**1b**), $(C_5Me_5)TiI(C_4H_6)$ (**1c**), $(C_5Me_5)TiCl(PhCHCHCHCHPh)$ (**2a**), $(C_5Me_5)Ti$-$Br(PhCHCHCHCHPh)$ (**2b**), $(C_5Me_5)TiCl(C_5H_8)$ (**3a**), $(C_5Me_5)TiBr(C_5H_8)$ (**3b**), $(C_5Me_5)TiCl(C_6H_{10})$ (**4**), and $(C_5Me_5)TiCl(CH_2CHPhCHPhCH_2)$ (**5**) were prepared and isolated as blue crystals in 40-60% yields. Elemental analyses gave insufficient results except for **2a**, **4**, and 5 due to the extremely high sensitivity of the complexes to air and moisture (single crystals decompose in 5 s and the complexes in solution instantly on exposure to air).

1b: mp 150 °C dec, EIMS, m/z (relative intensity) 318.0285 (M^+, 13.2, calcd for $(C_5Me_5)Ti^{81}Br(C_4H_6)$ 318.0285), 316.0277 (M^+, 15.7, calcd for the species with ^{79}Br 316.0275), 263.9735 (M^+-C_4H_6, 90.2, calcd for $(C_5Me_5)Ti^{81}Br$ 263.9815), 261.9739 (M^+-C_4H_6, 100.0, calcd for $(C_5Me_5)Ti^{79}Br$ 261.9835).

1c: EIMS, m/z (relative intensity) 364 (M^+, 38.2), 310 (M^+-C_4H_6, 100.0).

2a: mp 220 °C dec; EIMS (relative intensity) m/z 426 (M^+, 27.3, species with ^{37}Cl), 424 (M^+, 60.1, species with ^{35}Cl), 389 (M^+-Cl, 13.6), 220 (M^+-$C_{16}H_{14}$, 37.9, species with ^{37}Cl), 218 (M^+-$C_{16}H_{14}$, 100.0, species with ^{35}Cl), 206($C_{16}H_{14}$, 90.4). Anal. Calcd for $C_{26}H_{29}TiCl$: C, 73.50; H, 6.88. Found: C, 73.23; H, 6.89.

2b: mp 181 °C dec; EIMS, m/z (relative intensity) 470 (M^+, 39.5, species with ^{81}Br), 468 (M^+, 40.0, species with ^{79}Br), 264 (M^+-$C_{16}H_{14}$, 99.0, species with ^{81}Br), 262 (M^+-$C_{16}H_{14}$, 100.0, species with ^{79}Br).

3a: mp 67 °C dec; EIMS, m/z (relative intensity) 288 (M^+, 6.8, species with ^{37}Cl), 286 (M^+, 15.8, species with ^{35}Cl), 220 (M^+-C_5H_8, 38.0, species with ^{37}Cl), 218 (M^+-C_5H_8, 100.0, species with ^{35}Cl).

3b: mp 82 °C dec; EIMS, m/z (relative intensity) 332 (M^+, 12.4, species with ^{81}Br), 330 (M^+, 13.6, species with ^{79}Br), 264 (M^+-C_5H_8, 77.0, species with ^{81}Br), 262 (M^+-C_5H_8, 100.0, species with ^{79}Br).

4: mp 134 °C dec; EIMS, m/z (relative intensity) 302.1029 (M^+, 4.9, calcd for the species with ^{37}Cl 302.1091), 300.1171 (M^+, 7.2, calcd for the species with ^{35}Cl 300.1124), 265 (M^+-Cl, 1.5), 220 (M^+-C_6H_{10}, 43.8, species with ^{37}Cl), 218 (M^+-C_6H_{10},

100.0, species with ^{35}Cl). Anal. Calcd for $C_{16}H_{25}TiCl$: C, 63.90; H, 8.38. Found: C, 63.54; H, 8.26.

5: mp 152 °C dec; EIMS m/z (relative intensity) 426 (M$^+$, 22.0, species with ^{37}Cl), 424 (M$^+$, 48.0, species with ^{35}Cl), 220 (M$^+$-$C_4H_4Ph_2$, 50.2, species with ^{37}Cl), 218 (M$^+$-$C_4H_4Ph_2$, 100.0, species with ^{35}Cl), 206 ($C_4H_4Ph_2$, 90.0). Anal. Calcd for $C_{26}H_{29}TiCl$: C, 73.51; H, 6.88. Found: C, 73.51; H, 6.96.

Method B. Preparation with RMgX as a Reducing Agent. Typical procedure is as follows. To a THF solution (40 mL) of $(C_5Me_5)TiCl_3$ (0.7 g, 2.5 mmol) was added a THF solution of 1,3-butadiene (0.14 g, 2.5 mmol). An ethereal solution of iPrMgCl (2.5 M, 1.6 mL, 4 mmol) was dropwise added to the mixture with vigorous stirring at -65 °C. The color of the solution turned to blue-green during the reaction. After stirring the mixture for 1 h at this temperature, the solution was allowed to warm to room temperature and stirring was continued for 2 h to complete the reaction. Then, the mixture was evaporated to dryness, and the product was extracted with two portions of oxygen-free hexane (30 mL). Concentration of the extract to 8 mL followed by cooling to -20 °C gave $(C_5Me_5)TiCl(C_4H_6)$ (**1a**) as blue crystals in 37% yield (0.21 g) in optimized conditions. The preparation method B is applicable for the synthesis of **1b**, **1c**, **2a**, **2b**, **3a**, **3b**, **5**, **6a**, and **6b**, although the optimized yields are relatively lower (25-37%) as compared with those obtained by method A.

6a: mp 87 °C dec; EIMS, m/z (relative intensity) 288 (M$^+$, 7.0, species with ^{37}Cl), 286 (M$^+$, 16.2, species with ^{35}Cl), 220 (M$^+$-C_5H_8, 38.3, species with ^{37}Cl), 218 (M$^+$-C_5H_8, 100.0, species with ^{35}Cl).

6b: mp 117 °C dec; EIMS, m/z (relative intensity) 332.0424

(M^+, 17.3, calcd for species with ^{81}Br 332.0441), 330.0464 (M^+, 18.5, calcd for species with ^{79}Br 330.0464), 264 ($M^+-C_5H_8$, 89.1, species with ^{81}Br), 262 ($M^+-C_5H_8$, 100.0, species with ^{79}Br).

Preparation of $Ti(C_5Me_5)_2$(diene) (8 and 9). $(C_5Me_5)_2Ti$-(isoprene) and $(C_5M_5)_2Ti$(2,3-dimethyl-1,3-butadiene) were prepared in essentially the same way as described for 1-6, utilizing method A. The reaction of $(C_5Me_5)_2TiCl_2$ (2 mmol) with (2-methyl-2-butene-1,4-diyl)magnesium or (2,3-dimethyl-2-butene-1,4-diyl)magneium (1.8 mmol) in THF (40 mL) gave a mixture of $(C_5Me_5)_2TiCl$ and the desired diene complex (ca. 1:1) as a purple powder. Repeated crystallization of the product from hexane/THF gave 8 and 9 as highly air-sensitive red crystals in 15% and 23% yields, respectively (purity is ca. 90% as estimated from the EIMS spectra).

Measurement of $^{13}C-^{13}C$ Coupling Constants. $^{13}C-^{13}C$ spin-spin coupling constants for titanium-diene complexes with natural abundance was measured by using INEPT-INADEQUATE pulse sequences. The pulse sequences used are $90°(x)-\tau_1-180°(x)-\tau_1-90°(y)-\tau_2-180°(x)-\tau_2$ for ^1H nuclei and $180°(x)-\tau_1-90°(y)-\tau_2-180°(y)-\tau_1+\tau_2-180°(a)-\tau_3-90°(x)-\Delta-90°(\theta)$ for ^{13}C nuclei, where $\tau_1=1/4J(CH)=1.67$ ms, $\tau_2=1/6J(CH)=1.11$ ms, $\tau_3=1/4J(CC)-\tau_2=3.89$ ms, and $\Delta=1.6$ ms. The radio-frequency pulse phase (a) and (θ) were cycled through four settings, $+x$, $+y$, $-x$, and $-y$. Spectra were recorded at 125.65 MHz by using sweep width of 16025.6 Hz, 32 K data points with 32 K zero filling, and a relaxation delay of 4.6 s for the INADEQUATE sequence. Under these conditions any $^2J(C-C)$ and $^3J(C-C)$ was not observed.

Structure Determination of 1a, 2a, and 5. A single crystal of **1a, 2a,** and **5** sealed in a thin-walled glass capirally was

mounted on a Rigaku automated four-circle diffractometer.
Relevant crystal and data statistics are summarized in Table VII.
The unit-cell parameters at 20 °C were determined by a least-
squares fit to 2θ values of 25 strong higher reflections for all
the complexes (**1a, 2a**, and**5**). Every sample showed no significant
intensity decay during the data collection. The crystal struc-
ture were solved in every case by the heavy-atom method and
refined by the full-matrix least squares method as implemented in
the X-RAY SYSTEM[40] by the use of observed reflections
[$|F_O| > 3\sigma(F_O)$]. In the subsequent refinement the function $\Sigma\omega(|F_O| -$
$|F_C|)^2$ was minimized, where $|F_O|$ and $|F_C|$ are the observed and
calculated structure factors amplitudes, respectively. The
agreement indices are defined as $R(F)=\Sigma||F_O|-|F_C||/\Sigma|F_O|$ and
$Rw(F)=[\Sigma\omega(|F_O|-|F_C|)^2/\Sigma(|F_O|)^2]^{1/2}$ where $\omega^{-1}=\sigma^2(F_O)+g(F_O)^2$
(g=0.03). After the anisotropic refinement of non-hydrogen
atoms, all hydrogen atoms were located in the difference Fourier
maps with the help of the geometrical calculations and were
refined isotropically. The ORTEP drawings were obtained using
Johnson's program.[41]

All calculations were carried out on an ACOS-850 computer at
the Crystallographic Research Center, Institute for Protein
Research, Osaka University.

Table VII. Crystallographic and Experimental Data for **1a**, **2a**, and **5**.

compd	1a	2a	5
formula	$C_{14}H_{21}ClTi$	$C_{26}H_{29}ClTi$	$C_{26}H_{29}ClTi$
fw	272.6	424.9	424.9
system	monoclinic	orthorhombic	monoclinic
space group	$P2_1/c$	$Pnma$	$C2/c$
a, Å	6.999 (1)	8.260 (1)	22.049 (3)
b, Å	14.625 (3)	16.395 (3)	8.107 (2)
c, Å	13.842 (2)	16.308 (3)	26.869 (4)
β, deg	95.61 (4)		110.11 (1)
V, Å^3	1410.0 (4)	2208.7 (7)	4510.4 (14)
Z	4	4	8
D_{calcd}, g cm^{-3}	1.284	1.278	1.251
$F(000)$, e	576	896	1792
μ(Mo Kα), cm^{-1}	7.9	5.3	5.3
cryst size, mm	0.25 × 0.25 × 0.25	0.50 × 0.30 × 0.25	0.40 × 0.35 × 0.25
T, °C	20	20	20
2θ limits, deg	$4 < 2\theta < 60$	$4 < 2\theta < 60$	$4 < 2\theta < 55$
scan type	θ–2θ	θ–2θ	θ–2θ
scan speed, deg min^{-1} in 2θ	4.0	4.0	4.0
scan width, deg in 2θ	$2.0 + 0.70 \tan\theta$	$2.0 + 0.70 \tan\theta$	$2.0 + 0.70 \tan\theta$
bkgd counting, s	5	5	5
data collected	$\pm h, +k, +l$	$+h, +k, +l$	$\pm h, +k, +l$
unique data	4106	2745	5169
reflctns obsd	2367	1700	3578
no. of params refined	229	192	370
$R(F)$	0.083	0.057	0.076
$R_w(F)$	0.087	0.057	0.077

References

(1) (a) Yasuda, H.; Nakamura, A.; Angew. Chem., Int. Ed. Engl. **1987**, _26_, 723. (b) Yasuda, H.; Tatsumi, K.; Nakamura, A. Acc. Chem. Res. **1985**, _18_, 120. (c) Kai, Y.; Kanehisa, N.; Miki, K.; Kasai, N.; Akita, M.; Yasuda, H.; Nahamura, A. Bull. Chem. Soc. Jpn. **1983**, _56_, 3735. (d) Erker, G.; Kruger, C.; Muller, G. Adv. Organomet. Chem. **1985**, _24_, 1. (e) Erker, G.; Wicher, J.; Engel, K.; Resenfeldt, F.; Dietrich, W; Kruger, C. J. Am. Chem. Soc. **1980**, _102_, 6344. (f) Erker, G.; Engel, K.; Kruger, C.; Chiang, A. P. Chem. Ber. **1982**, _115_, 3311. (g) Yasuda, H.; Kajihara, Y.; Mashima, K.; Lee, K.; Nakamura, A. Chem. Lett. **1981**, 519. (h) Kruger, C.; Muller, G.; Erker, G.; Dorf, U.; Engel, K. organometallics **1985**, _4_, 215. (i) Fryzuk, M. D.; Haddad, T. S.; Rettig, S. J. Organometallics **1988**, _7_, 1224.

(2) Yasuda, H.; Tatsumi, K.; Okamoto, T.; Mashima, K.; Lee, K.; Nakamura, A.; Kai, Y.; Kanehisa, N.; Kasai, N. J. Am. Chem. Soc. **1985**, _107_, 2410.

(3) (a) For a preliminary report, see: Kai, Y.; Kanehisa, N.; Kasai, N.; Yasuda, H.; Nakamura, A. Proceedings of 5th International Symposium on Homogeneous Catalysis, Kobe, 1986, Abstract A-6. (b) Okamoto, T.; Yasuda, H.; Nakamura, A.; Kai, Y.; Kanehisa, N.; Kasai, N. J. Am. Chem. Soc. **1988**, _110_, 5008.

(4) (a) Blenkers, J.; Hessen, B.; van Bolhuis, F.; Wagner, A. J.; Teuben, J. H. Organometallics **1987**, _6_, 459. (b) Chen, J.; Kai, Y.; Kasai, N.; Yamamoto, H.; Yasuda, H.; Nakamura, A. Chem. Lett. **1987**, 1545.

(5) (a) Zwijnenberg, H.; van Oven, H. O.; Groenenboom, C. J.; de Liefde Meyer, H. J. J. Organomet. Chem. **1975**, _94_, 23. (b) Blenkers, J.; de Liefde Meyer, H. J.; Teuben, J. H. J. Organomet.

Chem. **1981**, <u>218</u>, 383. (c) Erker, G.; Berg, K.; Kruger, C.; Muller, G.; Angermund, K; Benn, K.; Schroth, R. Angew. Chem. **1984**, <u>96</u>, 445.

(6) (a) Datta, S.; Wreford, S. S.; Beatty, R. P.; McNeese, T. J. Am. Chem. Soc. **1979**, <u>101</u>, 1053. (b) Datta, S.; Fischer, M. B.; Wreford, S. S. J. Organomet. Chem. **1980**, <u>188</u>, 353. (c) Beatty, R. P.; Datta, S.; Wreford, S. S. Inorg. Chem. **1979**, <u>18</u>, 3139.

(7) (a) Yasuda, H.; Nakamura, A. Rev. Chem. Intermed. **1986**, <u>6</u>, 365. (b) Morikawa, H.; Kitazume, S. Ind. Eng. Prod. Res. Dev. **1979**, <u>18</u>, 254. (c) Perry, D. C.; Farson, F. S.; Schoenberg, E. J. Polym. Sci. **1975**, <u>13</u>, 1071.

(8) (a) Cooper, W. In The Stereoorubbers; Saltman, W. M., Ed; Wiley: New York, 1977; p 21. (b) Quirk, R. P. Transition Metal Catalyzed Polymerizations, Alkenes and Dienes; Harwood Academic: London, 1983. (c) Boor, J., Jr. Ziegler Natta Catalysts and Polymerizations; Academic: New York, 1979.

(9) Akita, M.; Yasuda, H.; Nagasuna, K.; Nakamura, A. Bull. Chem. Soc. Jpn. **1983**, <u>56</u>, 554.

(10) (a) Chandrasekaran, E. S.; Grubbs, R. H.; Brubaker, C. H., Jr. J. Organomet. Chem. **1976**, <u>120</u>, 49. (b) Lau, C.-P.; Chang, B.-H.; Grubbs, R. H.; Brubaker, C. H., Jr. J. Organomet. Chem. **1981**, <u>214</u>, 325. (c) Bergbreiter, D. E.; Parsons, G. L. J. Organomet. Chem. **1981**, <u>208</u>, 47.

(11) (a) Teyssie, P.; Dawans, F.; Durand, J. P. J. Polym. Sci., Polym. Chem. Ed. **1970**, <u>8</u>, 979. (b) Natta, G.; Porri, L. Polymer Chemistry of Synthetic Elastomer; Interscience: New York, 1968; p 652.

(12) Many examples are known. See, for example: (a) Reetz,

M. T. Organotitanium reagents in Organic Synthesis; Springer:
Berlin, 1986.   (b) Bottrill, M.; Gavens, P. D.; McMeeking, J. In
Comprehensive Organometallic Chemistry; Wilkinson, G., Stone, F.
G. A., Abel, E. W., Eds.; Pergamon: London, 1982; Chapter 22.2.

(13) (a) Smith, G. M.; Suzuki, H.; Sonnenberger, D. C.; Day,
V. W.; Marks, T. J. Organometallics **1986**, 5, 402.   (b) Erker; G.;
Muhlenbernd, T.; Benn, R.; Rufinska, A. Organometallics **1986**, 5,
402.

(14) Hoberg, H.; Jenni, K.; Raabe, E.; Kruger, C.; Schroth,
G. J. Organomet. Chem. **1987**, 320, 325.

(15) Harlow, R. L.; Krusic, P. J.; McKinney, R. J.; Wreford,
S. S. Organometallics **1982**, 1, 1506.

(16) (a) Buchwald, S. L.; Watson, B. T.; Huffman, J. C. J.
Am. Chem. Soc. **1986**, 108, 7411.   (b) Buchwald, S. L.; Lum, R. T.;
Dewan, J. C. J. Am. Chem. Soc. **1986**, 108, 7441.   (c) Takahashi,
T.; Swanson, D. R.; Negishi, E. Chem. Lett. **1987**, 623.

(17) The term prone and supine are employed in this text to
describe the mode of diene orientation.   The conventional
notation exo and endo does not seem suitable to express the
present stereochemistry.

(18) (a) Ruh, S.; van Philipsborn, W. J. Organomet. Chem.
1977, 127, C59.   (b) Benn, R.; Schroth, G. J. Organomet. Chem.
1982, 228, 71.

(19) (a) Hunter, A. D.; Legzdins, P.; Nurse, C. R.;
Einstein, F. W. B.; Willis, A. L. J. Am. Chem. Soc. **1985**, 107,
1791.   (b) Hunter, A. D.; Legzdins, P.; Einstein, F. W. B.;
Willis, A. C.; Bursten, B. E.; Gatter, M. G. J. Am. Chem. Soc.
1986, 108, 3843.

(20) Marshall, J. L. Carbon-Carbon and Carbon-Proton NMR

Couplings, Verlag Chemie: FL, 1983.

(21) Benn R.; Rufinska, A. J. Organomet. Chem. **1987**, <u>323</u>, 305.

(22) Sorensen, O. W.; Freeman, R.; Frenkiel, T.; Maraci, T. H.; Scuck, R. J. Magn. Reson. **1982**, <u>46</u>, 180.

(23) Newton, M. D.; Schulmann, T. M.; Manus, M. M. J. Am. Chem. Soc. **1974**, <u>96</u>, 17.

(24) (a) Pearson, A. J. Aust. J. Chem. **1977**, <u>30</u>, 407. (b) Peason, A. J. Aust. J. Chem. **1976**, <u>29</u>, 1679.

(25) Caddy, P.; Green, M.; Obrien, E.; Smart, L. E.; Woodward, P. J. Chem. Soc., Dalton Trans. **1980**, 962.

(26) (a) Buchmann, K.; van Philipsborn, W. Org. Magn. Reson. **1976**, <u>8</u>, 648. (b) Olah, G. A.; Liang, G.; Yu, S. H. J. Org. Chem. **19976**, <u>41</u>, 2227.

(27) For example, see: Powell, P.; Russel, L. J. Chem. Res., Synop. **1978**, 283.

(28) Faller, J. W.; Rosan, A. M. J. Am. Chem. Soc. **1977**, <u>99</u>, 4858.

(29) Davidson, J. L.; Davidson, K.; Lindsell, W. E. J.Chem. Soc., Dalton Trans. **1986**, 677.

(30) van Soest, T. C.; van der Ent, A.; Royers, E. C. Cryst. Struct. Commun. **1973**, <u>2</u>, 527.

(31) Brookhart, M; Cox, K.; Cloke, F. G. N.; Green, J. C.; Green, M. L. H.; Hare, P. M.; Bashkin, J.; Derome, A. E.; Grebenik, P. D. J. Chem. Soc., Dalton Trans. **1985**, <u>42</u>, 3.

(32) Immiziri, A.; Allegra, G. Acta Crystallogr., Sect. B: Struct. Crystallogr. Cryst. Chem. **1969**, <u>B25</u>, 125.

(33) (a) Mills, O. S.; Robinson, G. Acta Crystalogr. **1963**, <u>16</u>, 758. (b) Whitting, D. A. Cryst. Struct. Commun. **1972**, <u>1</u>,

379. (c) McCall, J. M.; Morton, J. R.; Page, Y. L.; Preston, K. F. Organometallics **1984,** 3, 1299.

(34) Cohen, S. A.; Auburn, R. P.; Bercaw, J. E. J. Am. Chem. Soc. **1983,** 105, 1136.

(35) Fachinetti, G.; Floriani, C.; Marchetti, F.; Melini, M. J. Chem. Soc., Dalton Trans. **1978,** 1398.

(36) (a) de Cian, A.; Lhuilier, P. M.; Weiss, R. Bull. Soc. Chim. Fr. **1973,** 451. (b) Erker, G.; Engel, K.; Kruger, C.; Muller, G. Organometallics **1984,** 3, 128.

(37) Threlkel, R. S.; Bercaw, J. E.; Seidler, P. F.; Stryker, J. M.; Bergman, R. G. Org. Synth. **1987,** 65, 42.

(38) Llinas, G. H.; Mena, M.; Palacios, F.; Royo, P.; Serrano, R. J. Organomet. Chem. **1988,** 340, 37.

(39) (a) Yasuda, H.; Nakano, Y.; Natsukawa, K.; Tani, H. Macromolecules **1978,** 11, 586. (b) Fujita, K.; Ohnuma, Y.; Yasuda, H.; Tani, H. J. Organomet. Chem. **1976,** 113, 210. (c) Yasuda, H.; Nakamura, A. In Recent Advances in Anionic Polymerization; Hogen-Eisch, Smid, J., Eds.; Elsevier: New York, 1987; p 59.

(40) Stewart, J. M. X-ray 76, Report TR-446; University of Maryland: College Park, MD, 1976.

(41) Johnson, C. K. ORTEP-II, Report ORNL-5138; Oak Ridge National Laboratory: Oak Ridge, TN, 1974.

Chapter 3

Highly Selective Linear Dimerization of Conjugated Dienes
Catalyzed by Titanium-Diene Complexes

Introduction

The recent accelerated development in the chemistry of organo-early transition metal complexes is based on the isolation of many highly reactive olefin- or diene-complexes and alkylidene complexes of Ti, Zr, Hf, Nb, Ta, etc. Extensive studies on their molecular structures and chemical behavior have provided us much important informations about the stereochemistry of the intermediates and their reaction pathways.[1]

Although highly stereospecific polymerization of 1,3-butadiene has already been attained using a variety of transition metal catalysts, but regio- and stereoselective linear- or cyclo-oligomerization of <u>substituted</u> 1,3-dienes has still remained as a fundamental problem in the field of catalysis and organometallic chemistry. Indeed highly selective linear dimerization of a non-substituted diene, butadiene, providing either 1,3,6- or 1,3,7-octatriene has already been realized using various transition metal catalyst systems such as $[PdCl(C_3H_5)]_2/PhOH$,[2] $Ni[P(OC_2H_5)_3]_3/morpholine$,[3] $Pd[P(C_2H_5)_3]_3/CO_2$[4] etc., but these catalyst systems show relatively low activity and poor selectivity in the dimerization of mono-substituted dienes such as isoprene or 1,3-pentadiene. To effect the selective dimerization of mono-substituted dienes, some modification of the catalyst

components on the design of entirely new catalyst systems seems necessary.

Among the possible four isomers of linear isoprene dimers (head-to-head, head-to-tail, tail-to-head, and tail-to-tail), only the tail-to-tail and tail-to-head dimers have been prepared with fairly good delectivity as summarized below. Highly regio-selective catalytic dimerization of isoprene has first been realized by using $ZrCp_2$(isoprene) by our group,[5] i.e. isoprene is converted to 2,7-dimethyl-1,3,6-octatriene at 30°C and to 2,7-dimethyl-2,4,6-octatriene at 60 °C in good selectivity (>85%). The tail-to-head dimer was also obtained in our group by the catalysis of niobium-diene complexes.[6] These findings stimulated the author to examine the catalytic oligomerization of conjugated dienes using the titanium-diene complexes described in the previous chapter.

tail-to-tail

Pd(PPh$_3$)$_2$/maleic anhydride[7a]
Pd(acac)$_2$/PPh$_3$/m-MeOC$_6$H$_4$CHO[7b]
Pd(PR$_3$)$_4$/CO[7c]

tail-to-head

PdCl(C$_3$H$_5$)$_2$/NiCl$_2$(PPh$_3$)$_2$[10]

Cp$_2$Zr(isoprene) (30 °C)[5]
TiCl$_2$(p-tosyl)$_2$/AlEt$_2$Cl[8]

TiCl$_4$/P(OPh)$_3$/AlEt$_2$Cl[11a]
Zr(C$_3$H$_5$)$_4$/Al$_2$Et$_3$Cl$_3$[11b]
Zr(OEt)$_4$/AlEt$_2$Cl/PPh$_3$[11b]
Hf(OBu)$_4$/AlEt$_2$Cl[11c]
VO(OEt)$_3$/AlEt$_2$Cl[11d]

Cp$_2$Zr(isoprene) (60 °C)[5]
Cr(RN=CHCH=NR)$_2$[9]
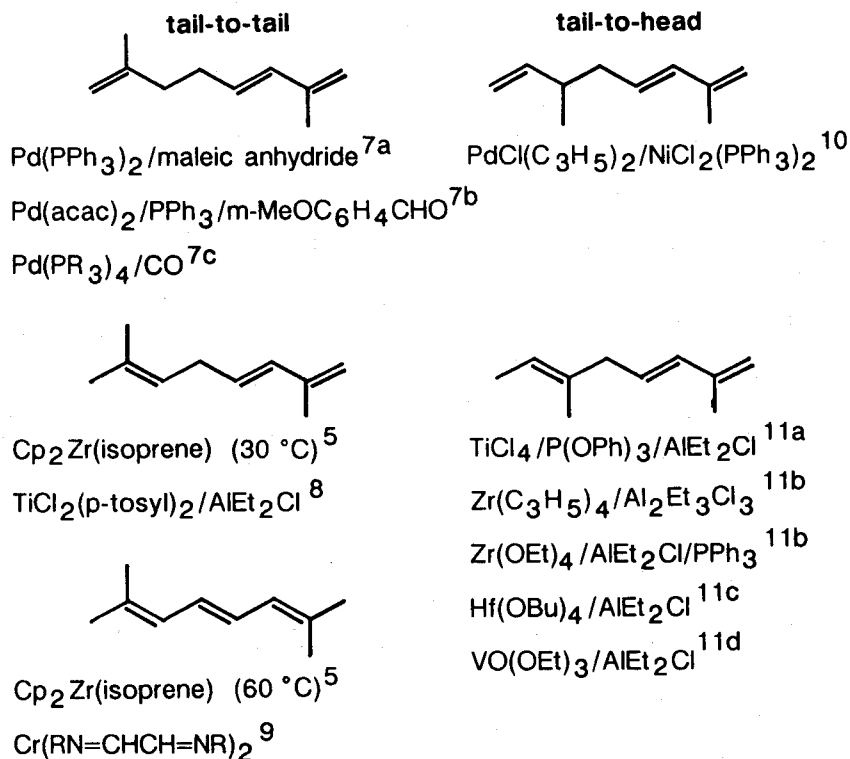
Results and Discussion

Catalysis of Titanium–Diene Complexes for Regioselective Dimerization of Isoprene. In a previous paper, Yasuda et al. have reported that a pure zirconium-diene complex of the type $ZrCp_2$(isoprene) can conduct the regio- and stereoselective catalytic dimerization of isoprene yielding tail-to-tail bonded dimers, i.e. (E)-2,7-dimethyl-1,3,6-octatriene at 30 °C and (E)-2,7-dimethyl-2,4,6-octatriene at ca. 65 °C.[5,12] Although the present $TiXCp^*$(diene) and related $TiCp^*_2$(diene) complexes exhibit no catalytic activity to initiate the dimerization or polymerization of conjugated dienes at 0-80 °C, we have found that the abstraction of the halide ligand on treatment with R MgX or Mg in the presence of excess isoprene is quite effective to generate an excellent catalyst for the selective dimerization of isoprene at 60 °C as summarized in Table I. Typically the nascent titanium species showed the catalysis with total turnover of 25, 8-10 times larger value compared with that observed for $ZrCp_2$-(isoprene). The titanium species generated in situ on reacting $TiCl_3Cp^*$ with (2-methyl-2-butene-1,4-diyl)magnesium (4:7), R MgX, or BuLi (2:7) show an increased activity for the linear dimerization of isoprene (total turnover 65-85). The most striking feature emerged in this catalytic reaction lies in the formation of a tail-to-head bonded isoprene dimer (2,6-dimethyl-1,3,6-octatriene; **1a**) with exceedingly high selectivity (99%) in place of the tail-to-tail bonded dimer (eq. 1).

Such a high selectivity has never been observed except for the above-noted zirconium-catalyzed reaction. Reduction of $TiBr_3Cp^*$ and TiI_3Cp^* at 60 °C also gives a catalyst that induces the same type of dimerization although these systems displayed a

$$\text{(structure)} \xrightarrow[\text{60°C}]{\text{"TiCp*"}} \text{(structure)} \qquad (1)$$
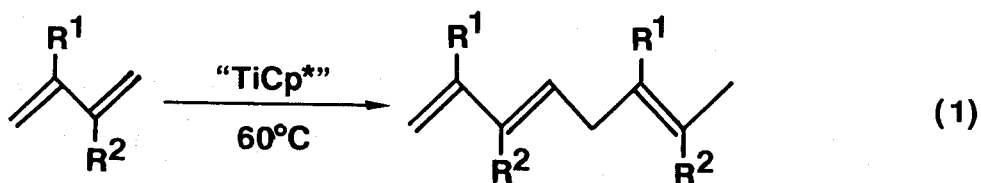
1a: $R^1 = CH_3$, $R^2 = H$

1b: $R^1 = R^2 = CH_3$

lower catalytic activity (total turnover 6-55). When the reaction temperature is raised to 80 °C, a conjugated triene, 2,6-dimethyl-2,4,6-octatriene (tail-to-head bonded dimer), is formed predominantly (>85%). Such a titanium-catalyzed multiple-bond isomerization has already been reported in cases of alkenes and unconjugated dienes. The corresponding tail-to-head dimeri-zation is also known by the catalysis of $Zr(OR)_4/AlClEt_2/donor$, but its selectivity is much lower due to the concomitant forma-tion of linear and cyclic oligomers.[11b)]

Replacement of the Cp* ligand with less bulky Cp ring always resulted in the catalytic conversion of isoprene into a mixture of (E)-2,6-dimethyl-1,3,6-octatriene (tail-to-head bonded dimer) and (E,E)-3,6-dimethyl-1,3,6-octatriene (head-to-head bonded dimer) in ca. 2:3-3:2 ratio, regardless of the reducing agents. Of particular importance is the fact that the titanium-catalyzed

$$\text{(structure)} \xrightarrow[\text{60°C}]{\text{"TiCp"}} \begin{array}{c} \text{1a} \\ + \\ \text{1c} \end{array} \qquad (2)$$
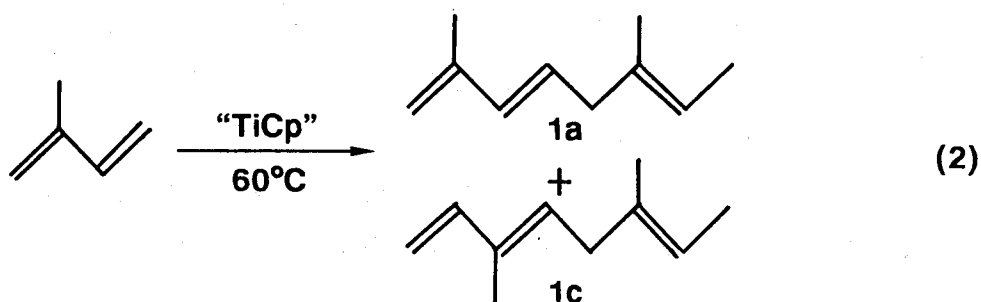
Table I. Titanium-Catalyzed Linear Dimerization of Isoprene.

catalyst system	Mg/Ti	max turnover no. (h^{-1})	turn-over	compositn of the dimer, %	
				1 a	1 c
TiClCp*(C_5H_8)/tBuMgCl	1.0	4	25	98	2
	2.0	0.5	3	98	2
TiClCp*(C_5H_8)/Mg(IP)	0.5	5	30	98	2
TiCl$_3$Cp*/tBuMgCl	3.0	21	46	99	1
TiCl$_3$Cp*/Mg(IP)	1.5	26	70	99	1
TiBr$_3$Cp*/Mg(IP)	1.5	30	55	99	1
TiI$_3$Cp*/Mg(IP)	1.5	1.5	6	99	1
TiCl$_3$Cp/tBuMgCl	3.0	18	57	51	49
TiCl$_3$Cp/Mg(IP)	1.5	22	89	52	48

[a] Reaction was carried out in benzene at 60 °C for 12 h under argon atmosphere with monitoring the conversion at regular intervals. Charged ratio; isoprene/Ti = 100.0 mol/mol.

dimerization completely suppresses the formation of the tail-to-tail bonded dimer. The drastic change may be ascribed to the difference in the oxidation state of metal species, i.e. d^0 species for the zirconium catalyst and d^1 species for the titanium catalyst. Actually the reduction of $TiClCp^*$(isoprene) with magnesium (the color changes from blue to purple) and the reduction of $TiCl_2Cp^*$ or $TiCl_3Cp^*$ with (2-methyl-2-butene-1,4-diyl)magnesium (1:1 and 2:3, respectively) both generate the same paramagnetic species as evidenced by the EPR spectroscopy. The g factor (1.999) for the resulting $TiCp^*$ species is in accord with those reported for titanium d^1 species as $TiCl_2Cp^*$(THF) (1.977), $TiCl_2Cp$ (1.974),[14] $TiCp(Me)_2$ (1.987), and $TiCp(Ph)_2$ (1.991).[15] Hyperfine coupling was not observed in the EPR signals even at 4 K. Reduction of $TiCl_3Cp$ with (2-methyl-2-butene-1,4-diyl)-magnesium also generates d^1 titanium species whose g value (1.992) nearly equals to those mentioned above. On hydrolysis of the product, 3-methyl-1-butene was obtained in good yield. Accordingly we can estimate the formation of $TiCp^*$(isoprene) (3) and TiCp(isoprene) in the presentsystems that should play an important role in the catalytic dimerization of dienes. Repeated attempts to isolate the low-valent $TiCp^*$(isoprene) or $TiCp^*$(buta-diene) species as single crystals have failed due to their great thermal instability especially in noncoordinating solvents such as pentane and hexane. Disproportionation or decomposition occurs promptly even at 0 °C in these solutions.

On the basis of the above noted regiochemistry, we can postulate a reaction mechanism for the catalytic dimerizationof isoprene. The mode of coordination may be given formally as shown in eq 4 and 5. In the initial step of the reaction, two

isoprene molecules coordinates to a low-valent "TiCp*" or TiCp*-(η^4-isoprene) species (eq 3) to generate the 13e intermediate **4**

"TiCp*"

$$+ \quad \longrightarrow \quad \textbf{3 or 8} \xleftarrow{\quad \text{C}_5\text{H}_8 \quad} \text{TiCp*}(\text{C}_5\text{H}_8) \qquad (3)$$

$$2\text{C}_5\text{H}_8 \qquad\qquad\qquad\qquad \textbf{2}$$

or **9** involving two η^2-coordinated dienes and succeeding oxidative coupling should give rise to metallacyclopentane species **5** or **10**. A similar reaction pathway has been proposed for the titanium-mediated olefin coupling leading to titanacyclopentanes.[16,17] Indeed a metallacycle that corresponds to **10** has been isolated in the case of platinum complexes. The β-hydride elimination on the species **6**, that is in equilibrium with **5**, followed by the hydrogen migration to the terminal CH_2 group may generate a transient titanium-diene complex (**8**). In the final stage of the catalytic cycle, the ligand exchange reaction may occur to release the tail-to-head bonded isoprene dimer. The proposed reaction pathway is essentially the same as that reported for $ZrCp_2$(isoprene)-catalyzed dimerization except for the regio-selectivity.[18] If the β-elimination proceeds on the species **7**, it must produce a head-to-tail bonded 1,3,6-octatriene derivatives (a natural product). However, this type of reaction did not occur to indicate the absence of an equilibrium between **5** and **7**.

On the other hand, generation of the intermediate **9** which gives rise to the head-to-head dimerization of isoprene may become possible when the bulkiness of the auxiliary ligand is sufficiently small (eq 9). In this case, two isoprene molecules

(4)

(5)

coordinates in η^2-manner at the more electron-rich C(1)-C(2) olefinic bond in place of the C(3)-C(4) bond. The succeeding β-hydrogen elimination and diene-diene exchange on the metal sphere finally release sterically rather unfavorable head-to-head bonded dimer.

Although the exact structure of transient species **4** and **9** remains unclear, the above concept provides us with a useful guideline for understanding of the regiochemistry emerged in the dimerization of various conjugated dienes. Indeed, the $TiCl_3Cp/RMgX$ (1:3) system also conducts the dimerization of 2,3-dimethylbutadiene at 60 °C leading to solely 2,3,6,7-tetramethyl-1,3,6-octatriene and the dimerization of (E)-1,3-pentadiene leading to a mixture of 6-methyl-2,4,7-nonatriene (tail-to-head bonded dimer) and 4-methyl-1,3,6-nonatriene (head-to-tail) in a ratio 81:19. The reaction pathway for these reactions may be inferred on the same ground as described in eq 8 and 9. Note that titanium- and zirconium-catalyzed dimerizations generally yield 1,3,6-octatriene derivatives, while palladium-catalyzed reaction always gives rise to 1,3,7-octatriene derivatives.[7]

Experimental Section

Catalytic Dimerization of Isoprene. To a benzene solution (1 mL) of $TiCl_3Cp^*$ (0.03g, 0.1 mmol) in a Schlenk type glass tube (10 mL, thick walled) was added isoprene (0.68g, 10 mmol) and then a THF suspension (0.3 mL) of (2-methyl-2-butene-1,4-diyl)magnesium (0.15 mmol) or i-PrMgBr (0.3 mmol). The color of the solution changed immediately from red to purple. The reaction tube was sealed in argon and kept at 60 °C for 6-12 h with shaking. After the reaction, the mixtire was separated by

distillation or gas chromatographically to obtain the pure sample of the isoprene dimer, 2,6-dimethyl-1,3,6-octatriene, in 70% conversion based on the charged isoprene.

2,6-Dimethyl-1,3,6-octatriene: ^{1}H NMR (CDCl$_3$) δ 6.16 (d, 1H, J=15.6 Hz, CH=), 5.59 (dt, 1H, J=15.6 and 6.4 Hz, =CH), 5.30 (q, 1H, J=6.6 Hz, CHMe=), 4.88 (s, 2H, CH$_2$), 2.83 (d, 2H, J=6.4 Hz, CH$_2$), 1.82 (s, 3H, CH$_3$), 1.65 (s, 3H, CH$_3$), 1.62 (d, 3H, J=6.6 Hz, CH$_3$); EIMS, m/z 136 (M$^+$). Anal. Calcd for C$_{10}$H$_{16}$: C, 88.16; H, 11.84. Found: C, 88.08; H, 11.89.

3,6-Dimethyl-1,3,6-octatriene: ^{1}H NMR (CDCl$_3$) δ 6.38 (dd, 1H, J=10.2 and 17.6 Hz, CH=CMe), 5.45 (t, 1H, J=7.4 Hz, =CH), 5.24 (q, 1H, J=6.0 Hz, CHMe=), 5.08 (d, 1H, J=17.6 Hz, CH$_2$=), 4.94 (d, 1H, J=10.2 Hz, CH$_2$=), 2.85 (d, 2H, J=7.4 Hz, CH$_2$), 1.78 (s, 3H, CH$_3$), 1.66 (s, 3H, CH$_3$), 1.61 (d, 3H, J=6.0 Hz, CH$_3$); EIMS, m/z 136 (M$^+$).

2,6-Dimethyl-2,4,6-octatriene: ^{1}H NMR (CDCl$_3$) δ 5.50 (t, 1H, J=16.0 Hz, =CHCMe), 6.38 (dd, 1H, J=16.0 and 8.0 Hz, CH=), 5.96 (d, 1H, J=8.0 Hz, MeC=CH), 5.41 (q, 1H, J=7.5 Hz, MeCH=), 1.80 (s, 9H, CH$_3$), 1.76 (d, 3H, J=7.5 Hz, CH$_3$); EIMS, m/z 136 (M$^+$).

Catalytic Dimerization of 2,3-Dimethylbutadiene. The catalytic dimerization was performed by the following procedure noted for the dimerization of isoprene. Total turnover after 6 h was 65-75.

2,3,6,7-Tetramethyl-1,3,6-octatriene: ^{1}H NMR (CDCl$_3$) δ 5.50 (t, 1H, J=6.2 Hz, CH=), 4.94 (d, 2H, J=9.1 Hz, CH$_2$=), 2.87 (d, 2H, J=5.9 Hz, CH$_2$), 1.86 (s, 3H, CH$_3$ at C(2)), 1.82 (s, 3H, CH$_3$ at C(3)), 1.65 (s, 3H, CH$_3$ at C(6)), 1.62 (s, 6H, CH$_3$ at C(6) and C(7)); EIMS, m/z (relative intensity) 164 (M$^+$, 100.0), 150 (M$^+$-

CH_2, 61.3).

Catalytic Dimerization of (E)–1,3–Pentadiene. The reaction was carried out in essentially the same manner as described above. When $TiCl_3Cp$/iPrMgBr (1:3) was added to (E)-1,3-pentadiene (100 equiv.) in benzene and the mixture was kept at 60 °C for 10 h with shaking, the following products were obtained in a ratio of 77:23 (turnover 45-55), while the $TiCl_3Cp^*$/iPrMgBr system showed very low catalytic activity (total turnover ca. 5, product ratio 80:20).

6–Methyl–2,4,7–nonatriene: ^{1}H NMR ($CDCl_3$) δ 5.35-5.65 (m, 6H, CH=), 2.69 (m, 1H, CH at C(6)), 1.65 (bs, 6H, CH_3 ay C(1) and C(9)), 0.99 (d, 3H, J=7.6 Hz, CH_3 at C(6)); EIMS< m/z 136 (M^+).

4–Methyl–1,3,6–nonatriene: ^{1}H NMR ($CDCl_3$) δ 6.68 (dt, 1H, J=16.1 and 10.8 Hz, CH= at C(2)), 6.05 (m, 2H, CH= at C(6) and C(7)), 5.40 (m, 1H, CH at C(3)), 5.15 (m, 2H, CH_2=), 2.18 (d, 2H, J=6.2 Hz, CH_2), 2.12 (dq, 2H, J=7.8 and 6.1 Hz, CH_2 atC(8)), 1.64 (s, 3H, CH_3), 0.94 (t, 3H, CH_3); EIMS, m/z 136 (M^+).

EPR Measurement. (C_5R_5)$TiCl_3$ (R=H, Me; 0.1 mmol) dissolved in benzene (10 mL) was reduced with (2-methyl-2-butene-1,4-diyl)-magnesium (0.15 mmol) at 25 °C. The solution thus obtained was transfered into an EPR tube (5 mm i.d.) via a syringe in argon, and the tube was sealed. EPR measurements were carried out on a JEOL FE-1X spectrometer with 100 KHz field modulation in conjunction with a cylindrical TE_{011} cavity in the temperature range of 4-320 K. The g value was obtained in a conventional method by using Mn^{2+} in MgO as a standard.

References

1) (a) Cardin, D. J.; Lappert, M. F.; Raston, C. L.; Riley, P. I., in Wilkinson, G.; Stone, F. G. A.; Abel, E. W., eds., Comprehensive Organometallic Chemistry, Pergamon Press, Vol. 3, Ch. 23, 1982. (b) Yasuda, H.; Tatsumi, K.; Nakamura, A. Acc. Chem. Res. **1985**, <u>18</u>, 120. (c) Pez, G. P.; Armor, J. N. Advan. Organomet. Chem. **1981**, <u>29</u>, 2.

2) (a) Smutny, E. J. J. Am. Chem. Soc. **1967**, <u>89</u>, 6793. (b) Takahashi, S.; Shibano, T.; Hagihara, N. Tetrahedron Lett. **1967**, 2451.

3) Heimbach, P. Angew. Chem., Int. Ed. Engl. **1968**, <u>7</u>, 882.

4) (a) Musco, A.; Silvani, A. J. Organomet. Chem. **1975**, <u>88</u>, C41. (b) Alderson, T.; Jenner, E. L.; Rindsey, R. V. J. Am. Chem. Soc. **1965**, <u>87</u>, 5368.

5) Yasuda, H.; Kajihara, Y.; Nagasuna, K.; Mashima, K.; Nakamura, A. Chem. Lett. **1980**, 719.

6) Okamoto, T.; Yasuda, H.; Nakamura, A.; Kai, Y.; Kanehisa, N.; Kasai, N. J. Am. Chem. Soc. **1988**, <u>110</u>, 5008.

7) (a) Takahashi, S.; Hagihara, N. Kogyo Kagaku Zasshi **1969**, <u>72</u>, 1637. (b) Anteunis, M.; DeSmet, A. Synthesis **1974**, 800. (c) Musco, A. J. Mol.Catal. **1976**, <u>1</u>, 443.

8) Itakura, J.; Tanaka, H. Macromol. Chem. **1969**, <u>123</u>, 274.

9) tom Dieck, H.; Kinzel, A. Angew. Chem., Int. Ed. Engle. **1979**, <u>18</u>, 324.

10) Yagi, H.; Tanaka, E.; Ishiwatari, H.; Hidai, M.; Uchida, Y. Synthesis **1977**, 334.

11) (a) Mitsubishi Petrochem., Co. Ger. Pat. 2061352 (1971). (b) Uchida, Y.; Furuhata, K.; Yoshida, S. Bull. Chem.

Soc. Jpn. **1971**, <u>44</u>, 1966. (c) Misono, A.; Uchida, Y.; Furuhata,
K.; Yoshida, S. Bull. Chem. Soc. Jpn. **1969**, <u>42</u>, 1383. (d)
Uchida, Y.; Furuhata, K.; Ishiwatari, H. Bull. Chem. Soc. Jpn.
1971, <u>44</u>, 1118.

12) (a) Bestian, H.; Klauss, K. Angew. Chem., Int. Ed.
Engl. **1963**, <u>2</u>, 224. (b) Antonsen, D. H.; Warren, R. W.; Johnson,
R. H. Ind. Eng. Chem. Prod. Res. Dev. **1964**, <u>3</u>, 3111.

13) Data were collected in the present work. See for the
preparation procedure: Nieman, J. W.; Teuben, J. H. J.
Organomet. Chem. **1984**, <u>262</u>, 157.

14) Bartlet, P. D.; Seide, D. J. Am. Chem. Soc. **1961**, <u>83</u>,
581.

15) Kenworthy, J. G.; Myatt, J.; Todd, P. F. J. Chem. Soc.
B **1970**, 791.

16) Lauher, J. W.; Hoffman, R. J. Am. Chem. Soc. **1976**, <u>98</u>,
1729.

17) Ammeter, J. H.; Burgi, H. B.; Thibeault, J. C.; Hoffman,
R. J. Am. Chem. Soc. **1978**, <u>100</u>, 3686.

18) Yasuda, H.; Nakamura, A. Angew. Chem., Int. Ed. Engl.
1987, <u>26</u>, 723.

—67—

Chapter 4

Structural Features of Low-Valent Titanium-Allyl Complexes

Introduction

Much effort has been devoted during the last 30 years on the chemistry of organo-titanium complexes to understand the characteristics,[1] since they are known to display an exceedingly high catalytic activity in the polymerization or oligomerization of conjugated dienes.[2,3] η^3-Allyl titanium species is regarded to be a key intermediate in those diene conversion reactions. However, the structural studies on the η^3-allyl complexes of early transition metals, especially those of Ti(III), have been poorly developed due to their paramagnetic nature in addition to difficulty in handling of these compounds. The only one Ti(III)-allyl complex, $TiCp_2$(1,2-dimethylallyl), is reported for its structure by X-ray analysis, but the structural parameters of the complex has only low precision for the detailed discussion.[5] It is of fundamental importance to reveal the molecular structure of a series of η^3-allyl titanium complexes in order to understand their structural and chemical characteristics.

In this point of view, X-ray structure analyses of a series of titanium-η^3-allyl complexes have been carried out.

Results and Discussion

(a) Synthesis of Titanium-η^3-Allyl Complexes.

The mixed ring Ti-allyl complex, $TiCpCp^*(allyl)$ ($Cp^*=C_5Me_5$), was first prepared accoding to eq. 1 and 2. The reaction of $TiCp^*Cl_3$ with one equivalent of CpNa in THF gave the mixed ring titanocene dichloride, $TiCpCp^*Cl_2$, in 90% yield as red-purple crystals. The mixed ring titanocene-allyl complex was obtained
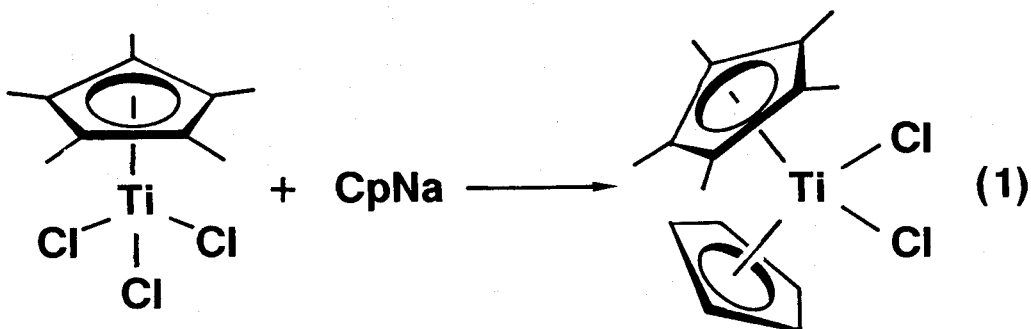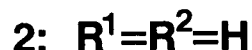

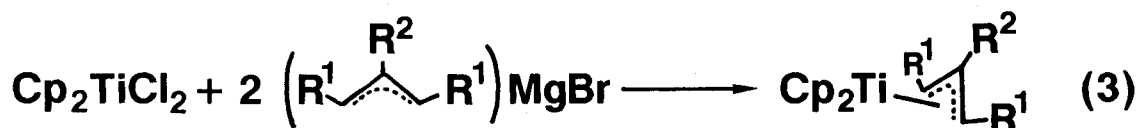by the reaction of $TiCpCp^*Cl_2$ with 2 equivalents of allyl Grignard reagent. Recrystallization from hexane/THF (10:1) gave the complex (1) as purple crystals in 80% yield.
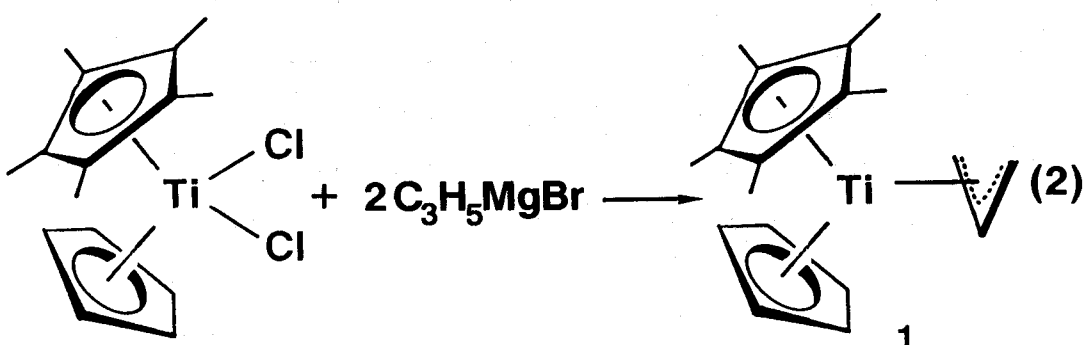
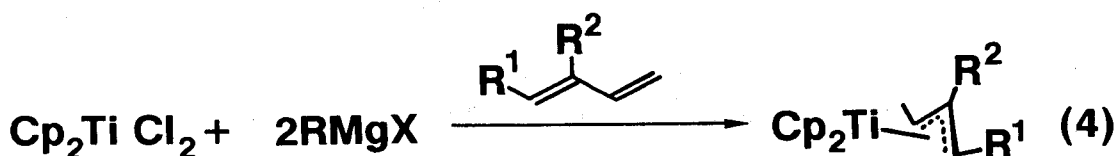The titanium-η^3-allyl complexes of the type, $TiCp_2(R)$ (R=alyll, 1-methylallyl, 2-methylallyl, and 1,3-dimethylallyl), were prepared by reaction of $TiCp_2Cl_2$ with 2 equivalents of

allylmagnesium bromide or its higher analogous in THF (eq. 3) according to the method reported by Martin and Jellinek with slight modification.   The reaction mixture was extracted with

$$Cp_2TiCl_2 + 2 \left(R^1 \diagdown \overset{R^2}{\diagdown} R^1 \right) MgBr \longrightarrow Cp_2Ti \diagdown \overset{R^1}{\underset{R^1}{\diagdown}} R^2 \quad (3)$$

2: $R^1 = R^2 = H$

3: $R^1 = Me, R^2 = H$

4: $R^1 = H, R^2 = Me$

hexane at 60 °C to separate the magnesium salts completely. The single crystals suitable for X-ray analysis were obtained by recrystallization of the products from hexane/THF (5:1) solution.

Complex 3 along with $TiCp_2$(1,2-dimethylallyl) (5) are also available in high yields from an alternative route as shown in eq. 4, i.e. the hydrometalaion of 1,3-pentadiene or isoprene to a transient $TiCp_2$(H) species generated in situ on treating $TiCp_2Cl_2$ with 2 equivalents of RMgX (R=Et, i-Pr) or BuLi.

$$Cp_2Ti\,Cl_2 + 2RMgX \xrightarrow{R^1 \diagdown \overset{R^2}{\diagdown}\diagup} Cp_2Ti \diagdown \overset{R^2}{\underset{R^1}{\diagdown}} \quad (4)$$

R=Et, i-Pr

3: $R^1 = Me, R^2 = H$

5: $R^1 = H, R^2 = Me$

(b) X-ray Structure Analyses of Titanium-Allyl Complexes.

The molecular structure of η^3-C_3H_5 complex of titanium is the most important in a series of titanium-allyl complexes.

Thus, the X-ray structure analysis of complex **1** was carried out. The ORTEP diagram of complex **1** is shown in Figure 1. The coordination geometries around titanium atom of **1** together with **3** and **4** are summarized in Table I.

The crystal structure of **1** involves the crystallographic mirror symmetry, which passes through the titanium atom, the central
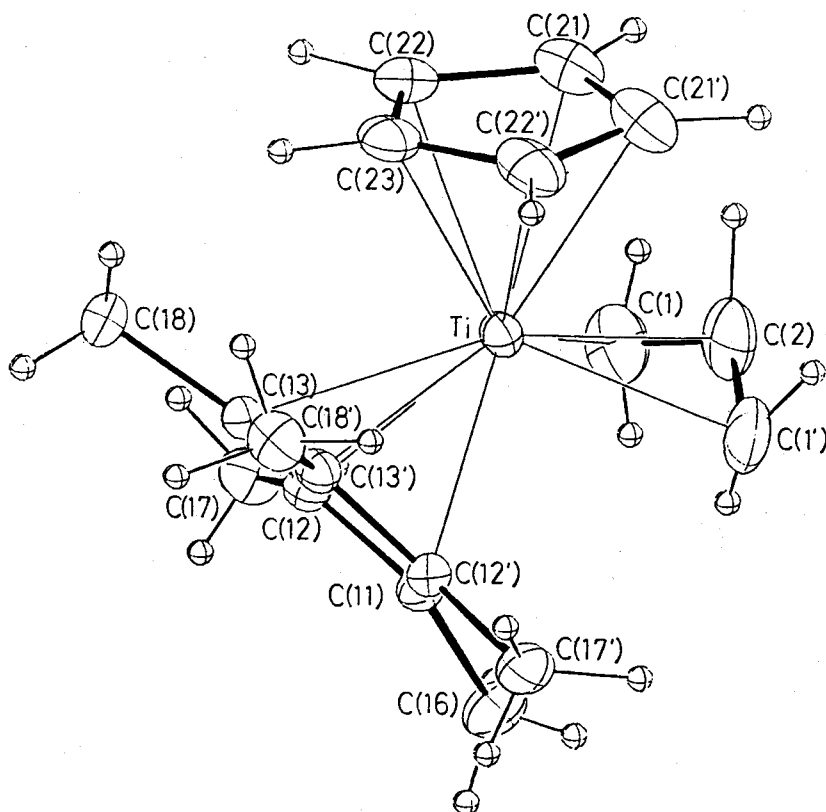

Figure 1. Molecular Structure of Complex **1**.

C(2) carbon of the allyl ligand, and the center of gravity of two cyclopentadienyl groups. Two cyclopentadienyl ligands (Cp and Cp*: Cp=C$_5$H$_5$, Cp*=C$_5$Me$_5$) assume staggered configration to release their interatomic interaction. Additionally, the Cp group takes sutable position to minimize steric congestion by locating the C(21)-C(21') bond nearly parallel to the allyl C(1)...C(1') interatomic axis, while the C(11)-C(12) bond in Cp* group is

oriented so that C(11) atom fills the space under C(2) in allyl ligand. Thus, the coordination geometries of cyclopentadienyl groups and allyl ligand are complementary to each other to minimize the steric repulsion among them. This type of geometries are very common as found in the related complexes **3** and **4**, and also in the reported complex, $TiCp_2$(1,2-dimethylallyl).

The structure analysis of a more simple complex, $TiCp_2(C_3H_5)$ (**2**), has failed because of the presence of packing and/or conformational disorder of cyclopentadienyl and allyl ligands in the crystal lattice.[7]

To clarify the effect of substituent(s) on allyl group, structure analyses of the complexes **3** and **4** were also demonstrated. The molecular structures of **3** and **4** are shown in Figure 2 and 3, respectively. The crystal lattices of both complexes **3** and **4** include two crystallographically independent molecules and their molecular structure are found to be essencially the same as confirmed by their structural parameters.

The whole geometries of complexes **1** compare very closely with that of **3**. The angles Φ_1, Φ_2, and Φ_3 are the angles around the titanium atom made by the CCP1, CCP2, and M1 (CCP means centroid of Cp ligand, and M1 is the midpoint of C(1) and C(3) in allyl ligand). Sum of these angles is about 360°, to indicate that the vectors connecting the titanium atom and CCP1, CCP2, and M1 are in a plane. The coordination geometries of the ligands around the titanium atom are also possible to correlate to the angles γ, δ, and ϵ. The summation of these angles becomes 180°. The allyl ligand in complex **1** and **3** is roughly normal to the Cp(1) ligand, while that of complex **4** is bended away from the titanium atom (δ=99.9°).
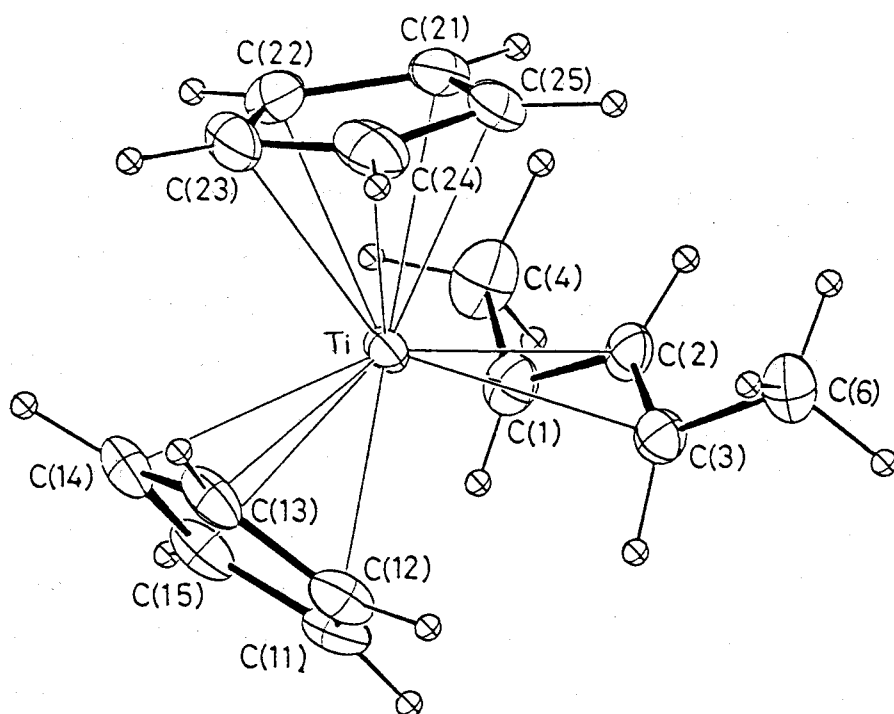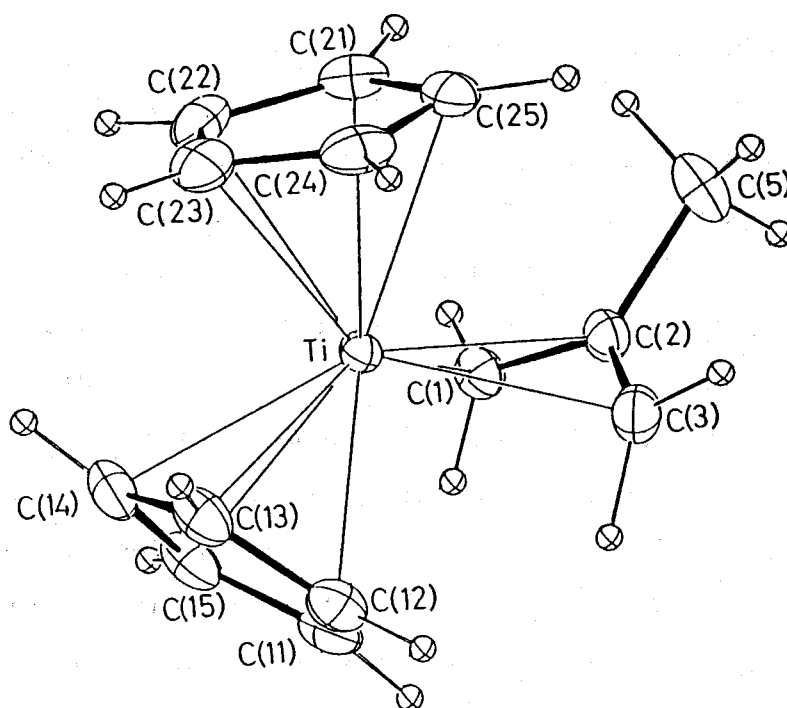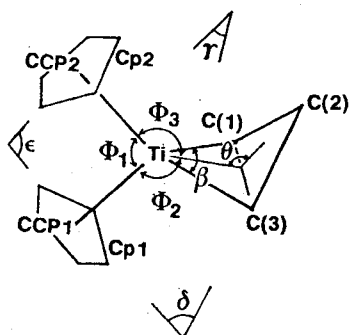
Figure 2. Molecular Structure of Complex **3.**

Figure 3. Molecular Structure of Complex **4.**

Table I. Coordination Geometry around the Titanium Atom

	1	3-1	3-2	4-1	4-2
Ti-CCP1,[a] Å	2.094	2.072	2.082	2.088	2.090
Ti-CCP2, Å	2.083	2.071	2.078	2.070	2.066
Ti-M1,[b] Å	2.033	2.073	2.059	2.045	2.046
C(1)...C(3), Å	2.469	2.526	2.524	2.458	2.446
β,[c] deg	62.5	62.0	62.2	62.0	61.7
θ,[d] deg	114.7	112.3	113.3	121.5	120.2
Φ_1,[e] deg	132.7	132.4	132.7	131.5	131.4
Φ_2, deg	113.3	110.5	110.8	111.1	111.0
Φ_3, deg	114.0	117.1	116.5	117.4	117.6
γ,[f] deg	39.0	38.9	38.0	30.0	30.9
δ,[f] deg	91.5	91.6	92.1	100.2	99.5
ϵ,[f] deg	49.5	49.6	49.9	49.8	49.6
TI-C(1) Å	2.379	2.432	2.388	2.395	2.367
Ti-C(2) Å	2.360	2.376	2.382	2.464	2.451
Ti-C(3) Å	2.379	2.404	2.424	2.378	2.400
C(1)-C(2) Å	1.381	1.385	1.387	1.410	1.403
C(2)-C(3) Å	1.381	1.392	1.404	1.392	1.383

[a]CCP: centroid of Cp ligand. [b]M1: midpoint of C(1) and C(3). [c]β: bite angle, C(1)-Ti-C(3). [d]θ: bent angle. [e]Φ: angles formed by the bonds among CCP1,CCP2,M1, and Ti.
[f]γ,δ,ϵ,: angles formed by the planes of two Cp groups and allyl ligand.

The bent angle (θ) defined by the dihedral angle between Ti-C(1)-C(3) plane and C(1)-C(2)-C(3) plane is one of the important geometrical parameters. Smaller θ value (av. 112.8°) in terminally substituted allyl complex (3) and larger value (av. 120.9°) in centrally substituted allyl complex 4 were observed as compared with the parent-allyl complex 1 (114.7°). These results reflect the severe interatomic repulsions among the methyl substituent(s) on the allyl ligand and Cp groups.

The bite angles (β), defined by C(1)-Ti-C(3), are almost the same in complexes 1, 3, and 4 (61.7-62.5°). Small bite angles and large bent angles are also observed in other early-transition metal allyl complexes such as $ZrCp^*(C_8H_8)(C_3H_5)$ (β=59°, θ=112°),[8] $Zr(C_8H_8)(OBu^t)(C_3H_5)$ (β=58°, θ=113°),[9] and $V(CO)_3(Me_4As_2C_6H_4)(MeCHCHCH_2)$ (β=62°, θ=116°).[10] In late-transition metal allyl complexes, the bite angle (β) varies from 65° in $Ru(NO)(PPh_3)(C_3H_5)$[11] to 75° in $Ni(PMe_3)(C_3H_5)_2$,[12] and the bent angle (θ) changes from 112° in $Pd(C_6H_8N_2)Cl(C_3H_5)$[13] to 99° in $Ir(COD)[P(OMe)_3](C_3H_5)$.[14] Thus, the smaller bite angle and larger bent angle are the characteristics in early-transition metal allyl complexes, and the late-transition metal allyl complexes tend to have larger bite angle and smaller bent angle.

The substituion on the central carbon of allyl ligand has a considerable influence over the whole geometry of the complex. Table II summarizes the nonbonded atomic contacts among Cp/Cp* and allyl ligands. All of these carbons in allyl ligand (C(1), C(2), and C(3)) have the close contacts with facing C(11), C(12), C(15), C(21), and C(25) atoms in the Cp/Cp* ligands. The shortest contact in each molecule is that between C(2) atom and C(21)

or C(25) atom in the Cp(2) group. The contact distances between C(5) (methyl group on C(2) in complex **4**) and C(21) or C(25) (3.152-3.265 Å) are quite shorter than those between C(4)/C(6) (terminal methyl groups in 1,3-dimethylallyl ligand) and C(21)/C(25) atoms (3.392-3.500 Å). Thus, the nonbonded repulsion

Table II. Nonbonded Atomic Contacts Between Cp/Cp* and Allyl Ligands

	1	3-1	3-2	4-1	4-2
C(1)...C(11)	3.225 Å	3.153 Å	3.161 Å	3.175 Å	3.128 Å
C(12)	3.254	3.188	3.224	3.300	3.199
C(21)	3.124	3.273	3.201	3.201	3.172
C(2)...C(11)	3.589	3.505	3.535	3.594	3.567
C(21)	2.958	3.129	2.971	3.113	3.158
C(25)		2.985	3.141	3.136	3.074
C(3)...C(11)		3.165	3.175	3.166	3.172
C(15)		3.243	3.223	3.139	3.241
C(25)		3.189	3.246	3.192	3.241
C(4)...C(21)		3.500	3.401		
C(5)...C(21)				3.201	3.265
C(25)				3.230	3.152
C(6)...C(25)		3.392	3.446		

between the Cp ring and methyl group on the 2-methylallyl ligand in **4** causes the unique coordination geometries, i.e. 1) large δ value, 2) large θ value, and 3) longer Ti-C(2) bond length than Ti-C(1)/C(3) lengths.

Experimental Section

All operations were conducted with standard Schlenk techniques under an argon atmosphere. Tetrahydrofuran and hexane were dried over Na/K alloy, distilled, and degassed before use. Alkyl halides were dried over $CaCl_2$ and distilled under an argon atmosphere. Grignard reagents were prepared by the reaction of activated magnesium with 3-bromo-1-propene, 1-bromo-2-butene, 2-bromo-3-pentene, or 3-bromo-2-methyl-1-propene. $TiCp_2Cl_2$ was obtained by the established method. $TiCp^*Cl_3$ was prepared by the reaction of $TiCl_4$ with $C_5Me_5SiMe_3$ (see Chapter 2).

Preparation of $TiCpCp^*Cl_2$.

To a stirred solution of $TiCp^*Cl_3$ (5.8 g, 20 mmol) in THF (200 mL) was dropwise added a THF solution of CpNa (1.76 g, 20 mmol) at 0°C. The color of the solution turns purple from red-orange during the addition. After the solution was stirred for 1 h at ambient temperature, the solvent was removed in vacuo to dryness. The residue was extracted with $CHCl_3$ (200 mL) and the salt was separated from the extracts by filtration. Concentration and cooling to -20 °C of the extracts gave $TiCpCp^*Cl_2$ as red-purple crystals in 82% yield. Anal. Calcd for $C_{15}H_{20}Cl_2Ti$: C, 56.46; H, 6.32. Found: C, 56.33; H, 6.32. ^{1}H NMR ($CDCl_3$) δ 6.24 (s, 5H, C_5H_5), 2.20 (s, 15H, C_5Me_5).

Preparation of Titanium-Allyl Complexes 1-5.

Method A. Preparation Using Allylmagnesium Bromide.

A solution of allylmagnesium bromide (5 mmol) in diethyl-ether (10 mL) was dropwise added to a solution of $TiCpCp^*Cl_2$ (0.8 g, 2.5 mmol) in THF (30 mL) with magnetic stirring at 0 °C.

After stirring for 30 min at ambient temperature, solvent was evaporated to dryness in vacuo. Hexane (40 mL) was added, and heated to 60°C for 10 min to separate the magnesium salt completely. The precipitated salts were removed by centrifugation. Concentration and cooling of the hexane extracts gave $TiCpCp^*(C_3H_5)$ (1) as purple crystals in 76% yield.

The complexes 2-5 were obtained in a simmilar manner by using $TiCp_2Cl_2$ and appropriate Grignard reagents as starting materials.

Method B. Preparation by Hydrotitanation of 1,3-Dienes.

Typical procedure as follows. To a THF solution (30 mL) of $TiCp_2Cl_2$ (0.5 g, 2 mmol) was added a THF solution of isoprene (0.27 g, 4 mmol). An ethereal solution of i-PrMgCl (2.5 M, 1.6 mL, 4 mmol) was dropwise added to the mixture with vigorous stirring at 0°C. The color of the solution turned immediately to purple from red. After stirring at ambient temperature for 15 min, solvent was evaporated to dryness in vacuo. The residue was extracted with 40 mL of hexane. The extracts were kept at 60 °C for 10 min to precipitate the magnesium salt completely. After removal of the salts by centrifugation, the extracts were concentrated and cooled to -20 °C to give $TiCp_2$(1,2-dimethylallyl) (5) in 84% yield as purple crystals.

The preparation method B is applicable for the synthesis of 1-methylallyl, 1,3-dimethylallyl, and 1,2-dimethylallyl complexes.

X-ray Analyses of Titanium-Allyl Complexes.

The X-ray analyses of 1-4 have been done in cooperation with Prof. Y. Kai, Prof. N. Kasai, and Mr. J. Chien of Faculty of Engineering, Osaka University.

Air sensitive single crystals of the complexes **1-4** were sealed in thin-walled glass capillary tube under argon. All X-ray experiments were carried out at 20 °C on a Rigaku automated four-circle diffractometer with graphite monochromatized MoKα radiation. The unit cell parameters were determined by a least-squares fit to 2θ values of 25 strong higher angle reflections. The crystal data and experimental conditions for **1**, **3**, and **4** are summarized in Table III. No significant intensity decay of the standard reflections were observed during the data collection. The intensity data were collected for the usual Lorentz and polarization effects but not for absorption. The crystal struc-tures were solved by the conventional heavy atom method and were refined by the full-matrix least-squares by the use of XRAY-76 system[15] including the observed reflections [|Fo|>3σ(Fo)]. After anisotropic refinement of the non-hydrogen atoms, all hydrogen atoms were located in the difference Fourier maps with the help of geometric calculations and were refined isotropic-ally.

Table III. Crystallographic and Experimental Data for **1**, **3**, and **4**.

Compound	**1**	**3**	**4**
allyl ligand	allyl	1,3-dimethylallyl	2-methylallyl
formula	$C_{18}H_{25}Ti$	$C_{15}H_{19}Ti$	$C_{14}H_{17}Ti$
F. W.	289.2	247.2	233.2
system	orthorhombic	monoclinic	orthorombic
space group	Pnma	$P2_1/n$	Pbca
a, Å	9.633(1)	13.353(2)	15.299(4)
b, Å	12.743(1)	7.674(1)	25.797(2)
c, Å	12.718(1)	25.543(2)	12.014(1)
β, deg		90.92(1)	
V, Å^3	1561.2(3)	2617.2(6)	4742(1.3)
Z	4	8	16
D_{calcd}, gcm^{-3}	1.231	1.254	1.306
F(000), e	620	1048	1968
μ(MoKα), cm^{-1}	5.5	6.4	7.0
cryst size, mm	0.80x0.35x0.25	0.75x0.60x0.40	0.75x0.55x0.50
T, °C	20	20	20
2θ limits, deg	$4<2\theta<60$	$4<2\theta<60$	$4<2\theta<60$
scan type	$\theta-2\theta$	$\theta-2\theta$	$\theta-2\theta$
scan speed, deg min^{-1} in 2θ	4.0	4.0	4.0
scan width, deg in 2θ	2.0+0.70tan	2.0+0.70tan	2.0+0.70tan
bkgd counting	5	5	5
unique data	2372	7622	6899
reflectns obsd	1627	5730	5333
no. of params refined	147	442	402
R(F)	0.065	0.069	0.057
R_w(F)	0.097	0.093	0.078

Diffraction data were collected with a Rigaku automated four-circle diffractometer using graphite-monochromatized MoKα radiation.

References

1) (a) Reetz, M. T. Organotitanium Reagents in Organic Synthsis; Springer: Berlin, 1986. (b) Bottrill, M.; Gevens, P. D.; Mcmeeking, J. In Comprehensive Organometallic Chemistry; Wilkinson, G.; Stone, F. G. A.; Abel, E. W., Eds.; Pergamon: London, 1982; Chapter 22.2.

2) (a) Yasuda, H.; Nakamura, A. Rev. Chem. Intermed. **1986,** <u>6</u>, 365. (b) Marikawa, H.; Kitazume, S. Ind. Eng. Prod. Res. Dev. **1979,** <u>18</u>, 254. (c) Perry, D. C.; Farson, F. S.; Schoenberg, E. J. Polym. Sci. **1975,** <u>13</u>, 1071. (d) Quirk, R. P. Transition Metal Catalyzed Polymerizations, Alkenes and Dienes; Harwood Academic: London, 1983. (e) Boor, J., Jr. Ziegler-Natta Catalysts and Polymerizations; Academic: New York, 1979.

3) (a) Akita, M.; Yasuda, H.; Nagasuna, K.; Nakamura, A. Bull. Chem. Soc. Jpn. **1983,** <u>56</u>, 554. (b) Chandrasekaran, E. S.; Grubbs, R. H.; Brubaker, C. H., Jr. J. Organomet. Chem. **1976,** <u>120</u>, 49. (c) Lau, C.-P.; Chang, B.-H.; Grubbs, R. H.; Brubaker, C. H., Jr. J. Organomet. Chem. **1981,** <u>214</u>, 325. (d) Bergbreiter, D. E.; Parsons, G. L. J. Organomet. Chem. **1981,** <u>208</u>, 47.

4) (a) Dolgoplosk, B. A.; Tinyakova, Y. I. Polym. Sci. USSR (Engl. Transl.) **1978,** <u>19</u>, 285. (b) Porri, L.; Gallazzi, M. C.; Destri, S.; Bolognesi, A. Makromol., Chem. Rapid. Commun. **1983,** <u>4</u>, 485.

5) Helmholdt, R. B.; Jellinek, F.; Martin, H. A. A. Vos. Recl. Trav. Chim. Pays-Bas, **1967,** <u>86</u>, 1263.

6) (a) Martin, H. A.; Jellinek, F. J. Organomet. Chem. **1967,** <u>8</u>, 115. (b) Martin, H. A.; Jellinek, F. J. Organomet. Chem. **1966,** <u>6</u>, 293.

7) Crystallographic data of $TiCp_2(C_3H_5)$ (2): $C_{13}H_{15}Ti$,

F.w.=219.2, monoclinic, Cc, a=13.319(3), b=7.618(1), c=11.982(3) $\overset{\circ}{A}$, β=114.55(2)°, V=1105.9(4) $\overset{\circ}{A}{}^3$, Z=4, D_{calcd}=1.316 gcm^{-3}, F(000)=460, μ(MoKα)=7.4 cm^{-1}. The full-matrix least-squares refinment gave the R(F) index of 0.099 for the 1167 observed reflections.

8) Higjcock, W. J.; Mills, R. M.; Spencer, J. L.; Woodward, P. J. Chem. Soc., Chem. Commun. **1982**, 128.

9) Braver, D. J.; Kruger, C. Organometallics **1982**, _1_, 204.

10) Frunke, U.; Weiss, E. J. Organomet. Chem. **1977**, _139_, 305.

11) Schoover, M. W. Inorg. Chem. **1978**, _17_, 3050.

12) Goddard, R.; Kruger, C.; Mark, F.; Stansfield, R.; Zhang, X. Organometallics **1985**, _4_, 285.

13) Bauley, P. M. J. Organomet. Chem. **1978**, _144_, C52.

14) Muetterties, E. L.; Tau, K. D.; Kirner, J. F.; Harris, T. V.; Stark, J.; Thompson, M. R.; Day, V. W. Organometallics **1982**, _1_, 1562.

15) Stewart, J. M. X-ray 76, Report TR-446; University of Maryland: College Park, MD, 1976.

Chapter 5

Synthesis and Unique Structure of Yb-Al Heterobimetallic Complexes and Their Catalysis for Ethylene-MMA Block Copolymerization

Introduction

During the past decade, f-block lanthanide organometallic chemistry has shown unprecended development.[1] Although great tendency of organolanthanides to form ate-complex with LiX, MgX_2, AlX_3 etc. has hampered isolation of salt-free lanthanide compounds, this problem has more recently solved by the use of cyclopentadienyl or analogous ligand as ancillary ligand. Thus, a lot of salt- and/or donor-free lanthanide complexes are now available.

Extensive studies by Evans, Andersen, Marks, Teuben, Schumann, Watson et al. proved quite unique reactivities and catalyses of organolanthanide complexes which differ markedly both from main group metal compounds and d-block transition metal complexes, e.g. multiple bond such as $C=C$, $C\equiv C$, $C\equiv O$, and $N=N$ cleavage and reorganization reactions,[2,3] Ziegler-Natta type polymerization of ethylene,[4] C-H activations of hydrocarbons,[5] and Grignard type insertion of electrophiles.[6]

The success in isolation of organolanthanide compounds prompted chemists to examine their complexation with main group organometallic compounds to find new type of olefin polymerization catalysts as well as new reagents effective in organic synthesis.

Synthesis of heterobimetallic compounds obtained from group 3A and 4A metallocene compounds and appropriate main group organometallic compounds in many cases involve a double alkyl,[7] ' halogeno,[8] or hydrido[9] bridges such as $Cp_2M(\mu-CH_3)_2AlR_2$ (M=Ti, Y, Sm, Gd, Dy, Ho, Yb),[7] $Cp_2Ti(\mu-Cl)_2AlR_2$,[8] $Cp_2Ti(\mu-H)_2BH_2$,[9] and $Cp_2Ti(\mu-Cl)(\mu-R)AlR_2$.[10] The complex with a single alkyl bridge is known only in the case of $Cp^*_2Yb(\mu-CH_3)BeCp^*$.[11]

This chapter describes the synthesis of the first example of the single ethyl-bridged lanthanide(II)-aluminum(III) complex, $YbCp^*_2(\mu-C_2H_5)Al(C_2H_5)_2(THF)$ and its X-ray crystallographic analysis together with its catalytic activity in ethylene polymerization and novel ethylene-methyl methacrylate block copolymerization.

Result and Discussion

1. **Preparation of Novel Ytterbium-Aluminum Heterobimetallic Complexes.** The bis(tetrahydrofuran) adduct of permethylated ytterbocene, $YbCp^*_2(THF)_2$ (1), was found to easily react with one equivalent of trialkylaluminum in toluene at 0 °C to give mono-(tetrahydrofuran) adduct, $YbCp^*_2(THF)$ (2) (eq 1). Complex 2 is isolated as orange crystals in high yield.

$$\text{1} \quad + \quad \text{AlR}_3 \quad \xrightarrow{\text{Tol.}} \quad \text{2} \qquad (1)$$
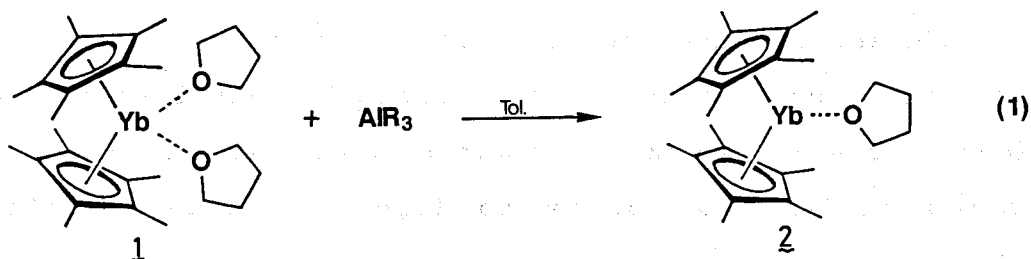
Further addition of one equivalent of $Al(C_2H_5)_3$ to $YbCp^*_2$-(THF) (2) in toluene at 0 °C resulted in the formation of a new compound. Recrystallization of the product in hexane at -20 °C

gave the complex **3a** displayed in eq. 2 as green crystals in 62%

$$3a \quad R = Me$$
$$3b \quad R = Et$$
$$3c \quad R = iBu$$
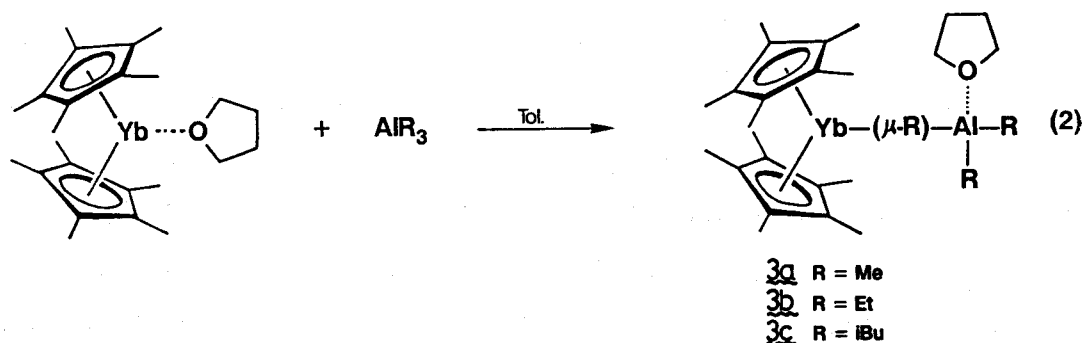
yield. In a simmilar manner, the corresponding adducts, $YbCp^*_2$-$(\mu-CH_3)Al(CH_3)_2(THF)$ (**3b**) and $YbCp^*_2(\mu-i-C_4H_9)Al(i-C_4H_9)(THF)$ (**3c**), were also obtained as violet and green crystals in good yields by the addition of $Al(CH_3)_3$ and $Al(i-C_4H_9)_3$, respectively, as confirmed by the ^{1}H NMR studies (see experimental).

The variable temperature ^{1}H NMR studies were carried out to find dynamic structure of the complexes **3a-c**. Interestingly, three alkyl groups were magnetically equivalent at temperatures from 60 °C to -100 °C. Only upfield shift of the aluminum-ethyl and the Cp^* methyl resonances and downfield shift of the THF signals were observed on lowering the temperature. The electron impact mass spectroscopy (EIMS) was also ineffective in structure determination of the complexes **3a-c**. Only the signals of $YbCp^*_2$ together with AlR_3 were observed in the EIMS spectra. These results indicate that the complexes **3a-c** have rather weak bonds between the two metal components.

2. X-ray Structure Analysis of $YbCp^*_2(\mu-C_2H_5)Al(C_2H_5)_2(THF)$

(3a). In order to establish the exact molecular structure, an X-ray crystallographic analysis of the complex **3a** has been carried out. Figure 1 shows an ORTEP diagram of the complex **3a** with the numbering scheme of selected atoms. The bond lengths and angles are listed in Table II. The molecule consists of $YbCp^*_2$ and $Al(C_2H_5)_3(THF)$ components. Thus, the added $Al(C_2H_5)_3$ pulled out the THF molecule from $YbCp^*_2(THF)$ during the reaction. The ytterbium atom is tri-coordinated if the Cp^* ligand is considered to occupy one coordination site and the ethyl group is bound to ytterbium only at the CH_2 position. The aluminum atom shows a distorted tetrahedral geometry, since a tetrahydrofuran molecule is coordinated to the metal.

The most intriguing structural feature of **3a** lies in the mode of its $Yb-(\mu-C_2H_5)-Al$ linkage. The Yb-C(1) distance of 2.854(18) Å is the longest value among the bonds reported for alkylytterbium complexes, i.e. $YbCp^*_2(\mu-CH_3)BeCp^*$ (2.766(4) Å),[11] $(YbCp_2(\mu-CH_3))_2$ (2.51 Å),[12] and $YbCp_2(\mu-CH_3)_2Al(CH_3)_2$ (2.609(23) Å).[7] The Yb-C(2) distance (2.939(21) Å) is slightly longer than the Yb-C(1) distance but is still within the bonding range. The close proximity of C(2) to Yb may necessarily result from the electron deficient bonding of the C(1) carbon bridging over Yb and Al atoms. The Yb-C(1)-C(2) angle of 76.6° is significantly small even compared with the corresponding angles (85-88°) reported for typical complexes with agostic interaction.[13] The Yb-C(1)-Al angle (177.7°) is comparable to the corresponding angle observed for $YbCp^*_2(\mu-CH_3)BeCp^*$ (177.4°). The four atoms, Yb, C(1), C(2), and Al are nearly coplanar and the dihedral angle between Yb-C(1)-C(2) and Al-C(1)-C(2) planes is 2.1°.
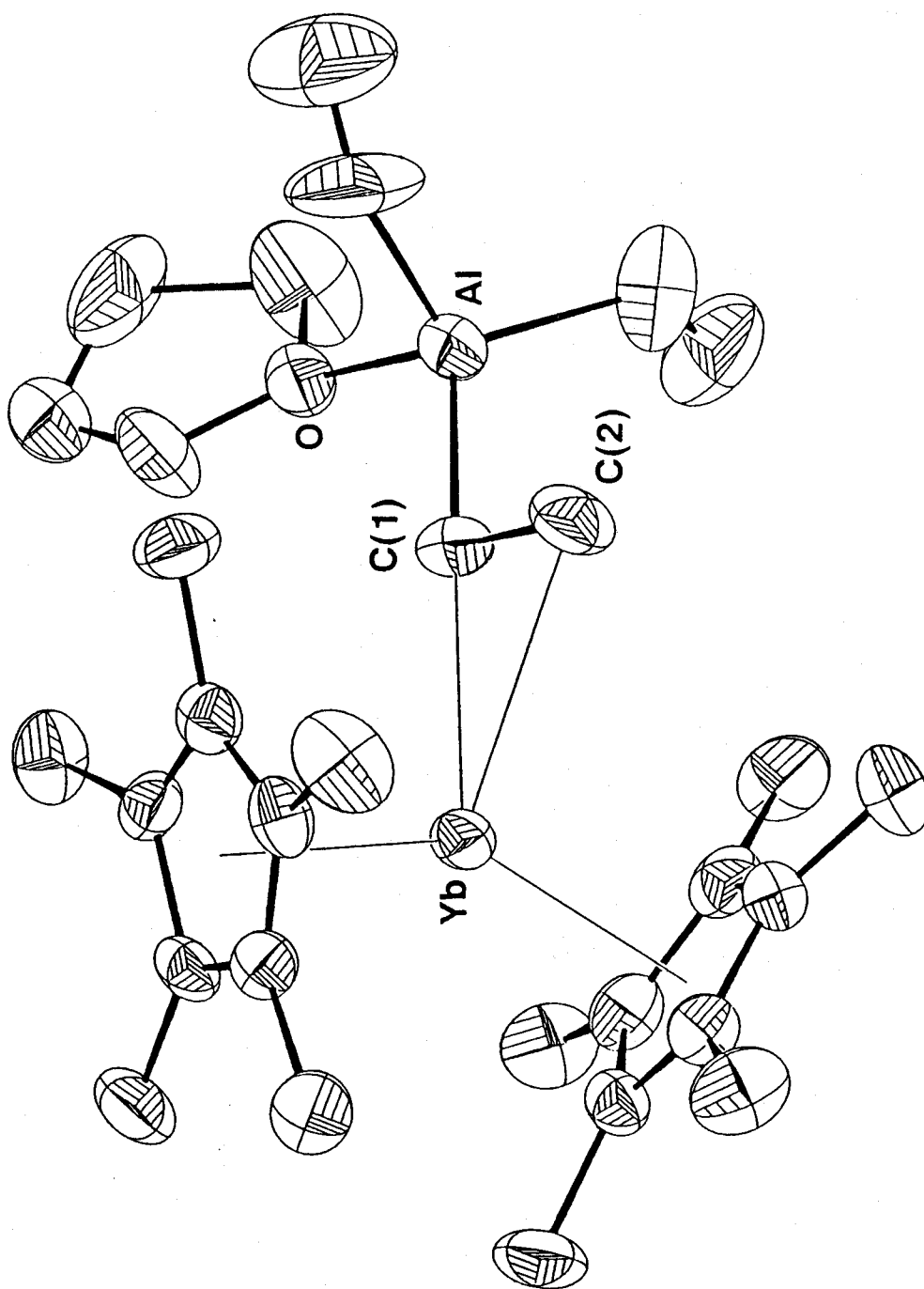
Figure 1. Molecular Structure of **3a**.

Table II. Selected Bond Lengths and Angles for **3a**.

Yb–C(1)	2.854(18)	C(1)–C(2)	1.943(15)
Yb–C(2)	2.939(21)	Al–C(1)	1.996(19)
Yb–CCP1	2.397(1)	Al–C(2)	2.889(22)
Yb–CCP2	2.388(1)	Al–O	1.943(15)
Yb–C(Cp) av.2.679(18)			

CCP: Centroid of Cp* ring.

C(1)–Yb–C(2)	32.6(5)	Yb–C(1)–Al	177.2(9)
C(1)–Yb–CCP1	105.1(4)	Yb–C(1)–C(2)	76.6(9)
C(1)–Yb–CCP2	111.6(4)	Al–C(1)–C(2)	105.3(12)
C(2)–Yb–CCP1	109.5(4)	Yb–C(2)–Al	112.6(7)
C(2)–Yb–CCP2	104.5(4)	CCP1–Yb–CCP2	142.82(3)
ϕ_1	20.4	θ	177.9
ϕ_2	22.4		

θ: dihedral angle between the planes defined by
Yb, C(1), C(2) and Al, C(1), C(2).

ϕ: dihedral angle between the Yb–C(1)–C(2) plane
and Cp* plane.

A slight lengthening of the C(1)-C(2) bond (1.628(27) $\overset{\circ}{A}$) as compared with the conventional non-bridged ethyl C-C bonds in $K[Al(C_2H_5)_3]F$ (1.523(22) $\overset{\circ}{A}$)[14] and $LiAl(C_2H_5)_4$ (1.523(12) $\overset{\circ}{A}$)[15] is suggestive of a very weak agostic interaction for the bond between the Yb and C(2) methyl group, because the agostic interaction generally brings about the shortening of the ethyl C-C bond (by 0.06-0.08 $\overset{\circ}{A}$).[13] The result of low temperature ^{1}H NMR studies also supports this concept. The Al-C(1)-C(2) angle (105°) is significantly smaller than the conventional $AlCH_2CH_3$ angle observed, for example, in $LiAl(C_2H_5)_4$ (109°),[15] but is comparable with the value reported for $SmCp^*_2(\mu-C_2H_5)_2Al(C_2H_5)_2$ (104°).[16] The Yb-C(Cp^*) distances (av. 2.679(17) $\overset{\circ}{A}$) and (Cp^*-centroid)-Yb-(Cp^*-centroid) angle (142.8°) are nearly identical with those reported for $YbCp^*_2$(donor) adducts.[17]

3. Catalysis of $YbCp^*_2(\mu-C_2H_5)Al(C_2H_5)_2$(THF) (3a).

(a) Polymerization of Ethylene.

During the investigation of the reactivity of complexes 3a-c, we have observed good catalysis of 3a in polymerization of ethylene in toluene at 25 °C. For example, 1000 equivalents of ethylene are converted to polyethylene (Mw=136000) in 98% yield by allowing the reaction at 25 °C for 8 h under atmospheric pressure (Table III). The characteristic of this catalyst is that high molecular weight polyethylene could be obtained with relatively narrow molecular weight distribution under mild conditions (25 °C, 1 atm).

The ytterbium-aluminum species generated in situ on reacting

Table III. Ethylene Polymerization Catalyzed
by Lanthanide/Aluminum System.

Catalyst Systems	Activity Kg/mol·h	$Mw/10^3$	Mw/Mn
$Cp_2^*Yb(\mu\text{-}Et)AlEt_3(THF)$	24	1363	2.16
$Cp_2^*Yb(THF)/AlEt_3(1:1)$	4.9	17.7 2.4	1.54 2.21
(1:3)	2.1	0.5	1.30
$Cp_2^*Sm \cdot AlEt_3(THF)$	21	404	4.2
$Cp_2^*Sm(THF)/AlEt_3(1:1)$	7.8	198 1.6	1.76 2.05
(1:3)	4.9	254 1.9	3.17 2.41
$Cp_2^*Eu(THF)/AlEt_3$	no catalysis		
$Cp_2^*Yb(THF)$	no catalysis		

25°C , 8h, in toluene , catalyst; 0.1mol%

$YbCp^*_2(THF)$ with $Al(C_2H_5)_3$ showed a marked decrease in activity for ethylene polymerization. When $YbCp^*_2(THF)$ (2) and $Al(C_2H_5)_3$ were mixed in a 1:1 ratio, bimodal polyethylene was obtained. In case of a 1:3 ratio, no high molecular weight polyethylene was obtained and only the formation of oligomers (Mw=500) was observed.

It is well known that lanthanide-alkyl complexes react with alkylaluminum reagent to give bis-alkyl bridged dimer (eq 3).[4]

$$A_nLn\text{-}R' \quad + \quad AlR_3 \quad \longrightarrow \quad A_nLn \diagdown_{R}^{R'} Al \diagdown_{R}^{R} \qquad (3)$$

A_n: ancillary ligand

The exchange reaction between the bridging alkyls and terminal alkyls occurs rapidly in solution. In the present catalyst systems ($YbCp^*_2(THF)/nAl(C_2H_5)_3$), the exchange reaction may occur between the ytterbium-polymer chain and an ethyl group of the excess alkylalminum reagent (Scheme 1). Thus, the presence of excess aluminum reagent may induce undesired chain transfer in these systems.
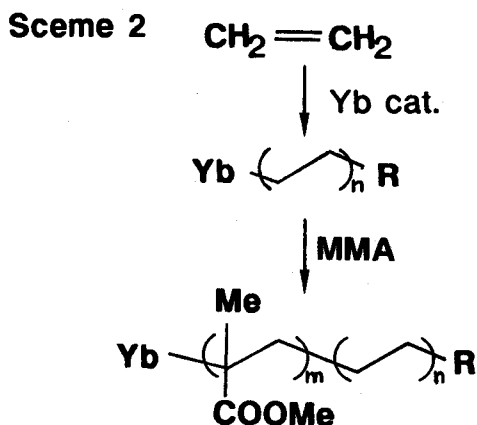
Scheme 1

$$Yb\text{-}CH_2\text{-}\textcircled{P}$$
$$+$$
$$Al(CH_2CH_3)_3$$

$$\textcircled{P} \text{---} CH_2 \diagup Yb \diagdown_{CH_2}^{CH_2} Al \diagup \text{---} CH_3$$

$$Yb\text{-}CH_2CH_3$$
$$+$$
$$(\textcircled{P}CH_2)Al(CH_2CH_3)_2$$
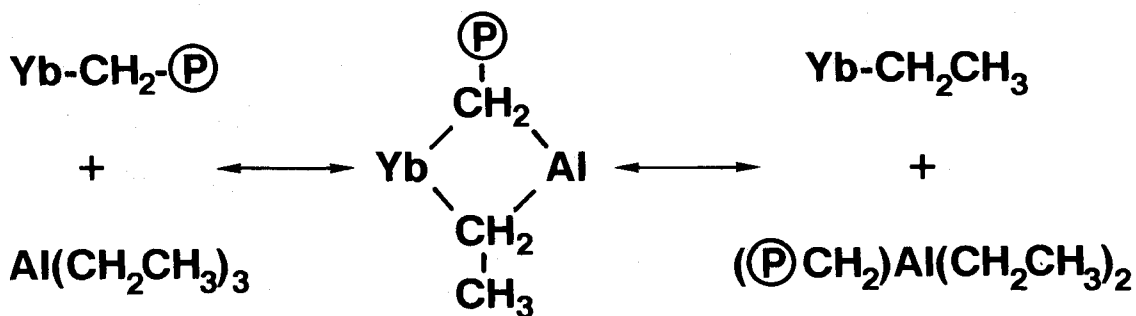
$\textcircled{P}$: polymer chain

The YbCp$^*_2$(THF) (2) itself shows no catalytic activity for ethylene polymerization, and this fact indicates that the interaction of alkylaluminum with Yb species is requisite for initiation of the polymerization. To obtain useful information about the initiation process, a reaction of YbCp$^*_2(\mu$-C$_2$H$_5$)Al(C$_2$H$_5$)$_2$-(THF) (3a) with ethylene was monitored by ^{1}H NMR. After 10 min, the ethyl signals of the triethylaluminum became very complicated, and the Cp* methyl resonance was broadened ($v_{1/2}$=60 Hz). This result indicates that a paramagnetic Yb(III)-alkyl species may be produced via the alkyl- or hydride-transfer reaction from triethylaluminum to the Yb(II) center. In fact, the formation of a trivalent lanthanide-alkyl complex, SmCp$^*_2$(CH$_3$)/AlCH$_3$, by the addition of excess AlCH$_3$ (100 eq.) to SmCp$^*_2$(THF) is reported, the reaction mechanism being unknown. The YbCp$^*_2$(CH$_3$)(ether) synthesized from separate route indeed shows extremely high activity for the polymerization of ethylene.[18]

Similar complexation with AlR$_3$ was also observed in samarium systems. The SmCp$^*_2$(THF)/Al(C$_2$H$_5$)$_3$ 1:1 adduct isolated as green solid shows nearly the same activity compared with the complex 3a. The Sm-Al species generated in situ exhibits much reduced activity as observed in the Yb-Al systems. In the case of the corresponding europium complex, EuCp$^*_2$(THF)/Al(C$_2$H$_5$)$_3$, no catalysis was observed. This may be ascribed to the relatively low redox potencial of the europium metal compared with those of samarium and ytterbium.

(b) Block Copolymerization of Ethylene with Methyl Methacrylate.

Improvement of chemical and physical properties of poly-ethylene, especially by the introduction of polar functional groups to the main chain or chain end, is one of most important problems in industrial polymer chemistry. We have therefore examined the copolymerization of ethylene with various polar monomers using $YbCp^{*}_2(\mu-C_2H_5)Al(C_2H_5)_2(THF)$ (3a) as a catalyst. As a result, we have found that complex 3a showed a good cataly-sis for AB type block copolymerization of ethylene with methyl methacrylate (MMA). That is to say, after polymerization of ethylene by complex 3a, poly(MMA) unit was bond to the poly-ethylene living end by repeated insertion of MMA (Scheme 2).

Sceme 2

$$CH_2 = CH_2$$

$$\downarrow \text{ Yb cat.}$$

$$Yb \overset{}{\underset{n}{(\diagup\diagdown)}} R$$

$$\downarrow MMA$$

$$Yb \overset{Me}{\underset{COOMe}{\Big(}\overset{}{|}\Big)_m} \overset{}{(\diagup\diagdown)_n} R$$

The results were summarized in Table IV. As the M_n of poly-ethylene before addition of MMA increases, the M_n for poly(MMA) part in resulted block copolymer decreases. These results may be caused by the heterogeneity of the system due to insolubility (precipitation) of polyethylene in toluene. Gel permeation chro-matographic analyses of the polymer show unimodal spectral pattern. This is indicative of the formation of block copolymer and not the mixture of homopolymers of ethylene and MMA (Figure

V). IR spectrum of the block copolymer is shown in Figure VI together with that of polyethylene and poly(MMA). The absorption bands of the copolymer consist of the sum of the absorption of polyethylene and poly(MMA), indicating the absence of ethylene-MMA random copolymer. Addition of MMA before polymerization of ethylene completely inhibits the ethylene polymerization, and only poly(MMA) was obtained (M_n=960000, rr=76%).

It is well known that polar monomer generally acts as inhibitor in Ziegler-Natta type polymerization, and incorporation of polar monomers to polyolefin chain has not been realized. Thus, the present method may provide a nice strategy for modification of polyethylene leading to a polymer with better chemical and physical properties, e.g. easy closs linking property.

Table IV. Block Copolymerization of Ethylene with MMA.

Reaction time b (min)	Mw/10³	Mw/Mn	Mn for Poly(MMA) unit	ethylene/MMA ratio in polymers
60	923	2.22	4800	690/1
120	963	2.15	3400	1000/1
180	1256	2.20	1100	4100/1

a)MMA was added after the polymerization of ethylene was carried out for a fixed time.

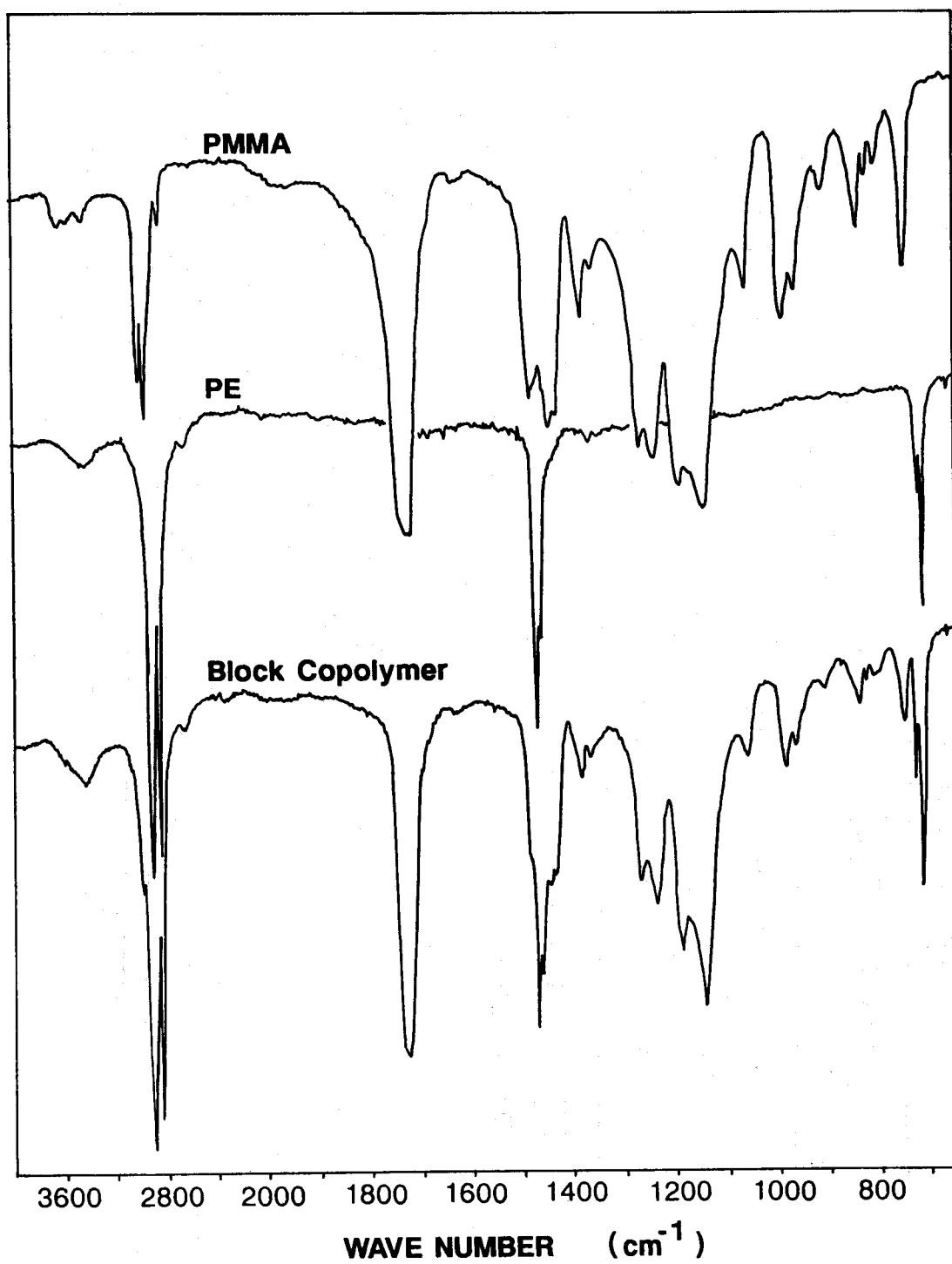b)Data for polymerization of ethylene at 25°C in toluene.
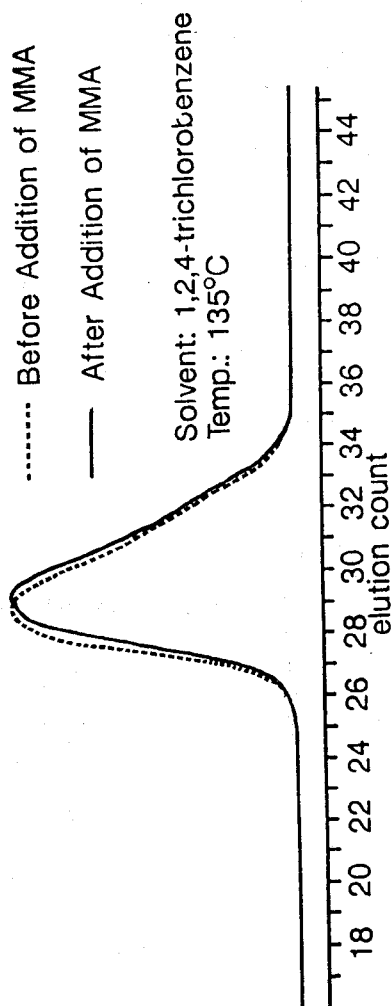
Figure 2. GPC Curve of Ethylene-MMA Block Copolymer (CHCl₃ Insoluble Fraction)

Figure 3. IR Spectrum of Ethylene-MMA Block Copolymer.

Experimental Section

General Remarks

All operations were conducted with standard Schlenk techniques under an argon atmosphere. Toluene and n-hexane were dried over Na/K alloy, distilled, and degassed before use. Anhydrous $YbCl_3$ was obtained from Yb_2O_3 by literature method. $YbCp^*_2(THF)_2$ and $SmCp^*_2(THF)_2$ were prepared according to the procedures repored by Andersen and Evans, respectively. Methyl methacrylate was purified with reference to the literature and dried over molecular sieves 4A and distilled just before use. Trialkylaluminum and ethylene were obtained commercially. NMR spectra were recorded on a JEOL GSX-270 or a Varian XL-100 spectrometer. Mass spectra were obtained on a JEOL 01SG-2 spectrometer at 30 eV. Gel permeation chromatgraphy was carried out on an Waters ALC/GPC 150C using a column packed with SHODEX GPC A-80M/S. Melting points were measured on a Yamato melting point apparatus model MP-21 and were uncorrected.

Preparation of $YbCp^*_2(THF)$ (2).

To a stirred solution of $YbCp^*_2(THF)_2$ (1.17 g, 2 mmol) in toluene (40 mL) was added a toluene solution of $Al(C_2H_5)_3$ (2 mmol) at 0 °C. The color of the solution changed from red to orange during the addition of $Al(C_2H_5)_3$. The reaction mixture was allowed to warm up to 20 °C, and stirred for 30 min. After the solvent was removed by trap-to-trap distillation, the product was extracted with hexane (40 mL) and purified by recrystallization at -20 °C to give $YbCp^*_2(THF)$ in 85 % yield as orange crystals. ^1H NMR (C_6D_6) δ 2.06 (s, 30H, C_5Me_5), 3.35 (m,

4H, THF), 1.39 (m, 4H, THF); EIMS (30 eV), m/z (relative intensity) 444 ($M^+-C_4H_8O$, 100.0, species with ^{174}Yb), 309 ((C_5Me_5Yb)$^+$, 71.0, species with ^{174}Yb), 174 ($^{174}Yb^+$, 45.8).

preparation of $YbCp^*_2(\mu-R)AlR_2(THF)$ (3a-c).

A solution of $Al(C_2H_5)_3$ (1.0 mmol) in toluene (1 mL) was dropwise added to a stirred toluene solution (20 mL) of $YbCp^*_2$-(THF) (0.516 g, 1.0 mmol) at 0 °C. The color of the solution turned greenish brown from orange. After stirring the solution for 30 min at ambient temperature, solvent was removed in vacuo. Resulted green crystalline solid was extracted with hexane (30 mL). The hexane solution was concentrated to ca. 9 mL and cooled to -20 °C to give $YbCp^*_2(\mu-C_2H_5)Al(C_2H_5)_2(THF)$ (3a) as green crystals; yield 62%. mp 115 °C(dec.); EIMS (30 eV), m/z (relative intensity) 444 (($YbCp^*_2$)$^+$, 100.0, species with ^{174}Yb), 309 (($YbCp^*$)$^+$, 71.2, species with ^{174}Yb), 174 ($^{174}Yb^+$, 41.3).

In essentially the same manner, $YbCp^*_2(\mu-CH_3)Al(CH_3)_2(THF)$ (3b) and $YbCp^*_2(\mu-i-C_4H_9)Al(i-C_4H_9)_2(THF)$ (3c) were prepared as violet and green crystals in 50-60% yields by the addition of $Al(CH_3)_3$ and $Al(i-C_4H_9)_3$, respectively.

3b: mp 143 °C (dec.); EIMS (30 eV), m/z (relative intensity) 444 (($YbCp^*_2$)$^+$, 100.0, species with ^{174}Yb), 309 (($YbCp^*$)$^+$, 69.8, species with ^{174}Yb), 174($^{174}Yb^+$, 40.5).

3c: mp 48 °C (dec.); EIMS (30 eV), m/z (relative intensity) 444 (($YbCp^*_2$)$^+$, 100.0, species with ^{174}Yb), 309 (($YbCp^*$)$^+$, 72.2, species with ^{174}Yb), 174 ($^{174}Yb^+$, 41.0).

X-ray Crystallographic Analysis of $YbCp^*_2(\mu-C_2H_5)Al(C_2H_5)_2(THF)$ (3a).

Air sensitive single crystal of **3a** was sealed in a thin-walled glass capillary tube under argon. All X-ray experiments were carried out on a Rigaku automated four-circle diffractometer with graphite-monochromatized $MoK\alpha$ radiation. The unit cell parameters at 20 °C were determined by a least-squared fit to 2θ values of 25 strong higher angle reflections. The crystal data and experimental conditions are summarized in Table V. No significant intensity decay of the standard reflections was observed during the data collection. The intensity data were collected for the usual Lorentz and polarization effects but not for absorption. The crystal structure was solved by the conventional heavy-atom method and was refined by the full-matrix least-squares method as implemented in the X-ray SYSTEM by the use of observed reflections [$|Fo| > 3\sigma(Fo)$].

Polymerization of Ethylene

Typical procedure: $YbCp^*_2(\mu-C_2H_5)Al(C_2H_5)_2(THF)$ (0.0252 g, 0.04 mmol) was dissolved in thoroughly degassed toluene (40 mL). Then ethylene was bubbled into the solution cooled to -78 °C from a rubber baloon (1 L). The reaction mixture was allowed to warm up to room temperature, and stirred at there for 4 h. During the reaction, the color of the solution turned to yellow-orange from red-orange. White solid polyethylene began to precipitate after 15 min and all of the monomers was consumed in 4 h. The resulting suspension was poured into MeOH (500 mL). Filtration followed by drying of the white solid gave polyethylene as a white powder (1.2 g, 96% conversion).

Block Copolymerization of Ethylene with Methyl Methacrylate.

Ethylene was introduced to the toluene solution (40 mL) of YbCp$^*_2$(μ-C_2H_5)Al(C_2H_5)$_2$(THF) (0.0252 g, 0.04 mmol) at -78 °C. The reaction mixture was allowed to warm slowly and stirred at ambient temperature. After the fixed periods, methyl methacrylate (MMA, 1 mL) was added with a syringe at this temperature. After stirring for 1 h, the reaction was terminated by pouring the reaction mixture into MeOH (500 mL). Filtration followed by drying gave white polymeric products. The white polymer was refluxed in CHCl$_3$ for 24 h to give white powder by filtration. The powder was dissolved in 1,2,4-trichlorobenzene (50 mL) at 160 °C, and the resulting clear solution was poured into CHCl$_3$ to remove the CHCl$_3$ soluble fraction (MMA homopolymer) completely. The white precipitate powder was washed with CHCl$_3$ and dried under reduced pressure to give an ethylene-MMA block copolymer.

Table V. Crystallographic and Experimental Data for **3a**

Formula	$C_{30}H_{53}OAlYb$
F.W.	629.77
System	Orthorhombic
Space Group	$P2_12_12_1$
a, $\overset{\circ}{A}$	13.354(2)
b, $\overset{\circ}{A}$	19.629(3)
c, $\overset{\circ}{A}$	12.372(2)
V, $\overset{\circ}{A}^3$	3240.8(8)
Z	4
D_{calcd}, g cm^{-1}	1.290
F(000), e	1296
$\mu(MoK_\alpha)$, cm^{-1}	30.8
crysttal size	0.2X0.4X0.4
T, °C	20
2θ Limits, deg	4-60
scan type	$\theta-2\theta$
Scan Speed, deg min^{-1}	4.0
Unique Data	5218
Reflections	3621
Observed	
No. of Parameters	
R(F)	0.077
$R_w(F)$	0.079

References

1) (a) Baker, E. C.; Halstead, G. W.; Raymond, K. N. Struct. Bonding (Berl.) **1976**, 25, 23. (b) Cernia, E.; Mazzei, A. Inorg. Chem. **1974**, 10, 239. (c) Hayes, R. G.; Thomas, J. L. Organomet. Chem. Rev., A **1971**, 7, 1. (d) Marks, T. J. Adv. Chem. Ser. **1976**, 150, 232. (e) Marks, T. J. Acc. Chem. Res. **1976**, 9, 223. (f) Tsutsui, M.; Ely, N.; Dubois, R. Acc. Chem. Res. **1976**, 9, 217.

2) (a) Evans, W. J.; Drummond, D. K. J. Am. Chem. Soc. **1988**, 110, 2772. (b) Evans, W. J.; Haghes, L. A.; Drummond, D. K.; Atwood, J. L. J. Am. Chem. Soc. **1986**, 108, 1722.

3) (a) Evans, W. J.; Grate, J. W.; Choi, H. W.; Bloom, I.; Hunter, W. E.; Atwood, J. L. J. Am. Chem. Soc. **1985**, 107, 3728. (b) Evans, W. J.; Drummond, D. K.; Chamberlain, L. R.; Doedens, R. J.; Bott, S. G.; Zhang, H.; Atwood, J. L. J. Am. Chem. Soc. **1988**, 110, 4983.

4) Watson, P. L. J. Am. Chem. Soc. **1982**, 104, 337.

5) Watson, P. L. J. Chem. Soc., Chem. Commun. **1983**, 276.

6) For example, see, (a) Hou, Z.; Fujiwara, Y.; Jintoku, T.; Mine, N.; Taniguchi, H. J. Org. Chem. **1987**, 52, 3524. (b) Evans, W. J.; Drummond, D. K. J. Am. Chem. Soc. **1988**, 110, 2772. (c) Imamoto, T.; Takeyama, T.; Koto, H. Tetrahedron Lett. **1986**, 27, 3243.

7) Holton, J.; Lappert, M. F.; Ballard, D. G. H.; Pearce, R.; Atwood, J. L.; Hunter, W. E. J. Chem. Soc., Dalton Trans. **1979**, 45.

8) Natta, G.; Corradini, P.; Bassi, I. W. J. Am. hem. Soc. **1958**, 80, 755.

9) Melmed, K. M.; Coucouvanis, D.; Lippard, S. J. Inorg. Chem. **1973**, 12, 232.

10) Tebbe, F. N.; Parshall, G. W.; Reddy, G. S. J. Am. Chem. Soc. **1978**, 100, 3611.

11) Burns, C. J.; Andersen, R. A. J. Am. Chem. Soc. **1987**, 109, 5853.

12) Holton, J.; Lappert, M. F.; Ballard, D. G. H.; Pearce, R.; Atwood, J. L.; Hunter, W. E. J. Chem. Soc., Chem. Commun. **1976**, 480.

13) (a) Dawoodi, Z.; Green, M. L. H.; Mtetwa, V. S. B.; Prout, K. J. Chem. Soc., Chem. Commun. **1982**, 802. (b) Brookhart, M.; Green, M. L. H.; Pardy, R. B. J. Chem. Soc., Chem. Commun. **1983**, 691. (c) Koga, N.; Obara, S.; Morokuma, K. J. Am. Chem. Soc. **1984**, 106, 4625.

14) Allegra, G.; Perego, G. Acta Crystallogr. **1964**, 16, 872.

15) Gertis, R. L.; Dickerson, R. E.; Brown, T. L. Inorg. Chem. **1964**, 3, 872.

16) Evans, W. J.; Chamberlein, L. R.; Jiller, J. W. J. Am. Chem. Soc. **1987**, 109, 7209.

17) (a) Tilley, T. D.; Andersen, R. A.; Spencer, B.; Zalkin, A. Inorg. Chem. **1982**, 21, 2647. (b) Watson , P. L. J. Chem.Soc., Chem. Commun. **1980**, 652. (c) Wayda, A. L.; Dye, J. L. Organometallics **1984**, 3, 1605.

18) (a) Jeske, G.; Lauke, H.; Mavermann, H.; Swepston, P. N.; Schumann, H.; Marks, T. J. J. Am. Chem. Soc. **1985**, 107, 8091. (b) Watson, P. L.; Herskovitz, T.

Chapter 6

Highly Syndiotactic Living Polymerization of Methyl Methacrylate

Catalyzed by Organolanthanide(II) Complexes

Introduction

Recent rapid progress in the field of organolanthanide chemistry has enabled us to percieve the unique structures and intriguing chemical vehavior of organolanthanide complexes, that have never been observed for d transition metal complexes.[1] In the previous chapter, the author described about the catalyses of novel Yb-Al heterobimetallic complex, $YbCp^{*}_{2}(\mu-C_{2}H_{5})Al(C_{2}H_{5})_{2}$-(THF). This complex catalyzes the polymerization of methyl methacrylate (MMA) with fairly high syndiotacticity.

Although the syndiotactic polymerization of MMA has been attained by several catalyst systems such as t-BuMgBr, $Al(CH_{2}-CH_{3})_{3}/PPh_{3}$ etc. under severe conditions (-90--110 °C), and the obtained polymer has low molecular weights (<3000) and relatively wider polydispersity (1.18-1.63).[2] To develop the new catalyst systems which produce mono-disperse, high molecular weight, and highly syndiotactic poly(MMA) under mild conditions is the most important subject for both polymer chemistry and industrial purpose.

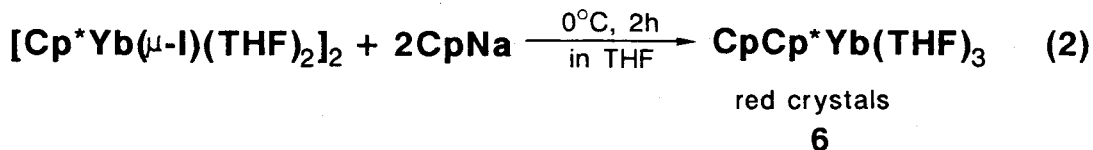## Preparation of Lanthanide (II) Complexes.

Following divalent organolanthanide complexes were tested for polymerization of MMA. $YbCp^*_2(THF)_2$ (1),[3] $YbCp^*_2(pyridine)_2$ (3),[4] and $SmCp^*_2(THF)_2$ (4)[5] were obtained by the known methods. $YbCp^*_2(THF)$ (2) and $YbCp^*_2(\mu-C_2H_5)Al(C_2H_5)_2(THF)$ (5) were prepared by the reaction of $Al(C_2H_5)_3$ with $YbCp^*_2(THF)_2$ or $YbCp^*_2(THF)$, respectively as described in chapter 5. The mixed ring ytterbocene, $YbCpCp^*(THF)_3$ (6), was obtained by the following procedure.

Alkali metal salt free mono(pentamethylcyclopentadienyl)-ytterbium iodide, $[YbCp^*(\mu-I)(THF)_2]_2$ (7), was prepared by the redistribution reaction of $YbCp^*_2(THF)_2$ (1) and YbI_2 (eq. 1).

$$Cp^*_2Yb(THF)_2 + YbI_2(THF)_2 \xrightarrow[\text{in THF}]{0°C, 4h} [Cp^*Yb(\mu\text{-}I)(THF)_2]_2 \quad (1)$$

yellow crystals

7
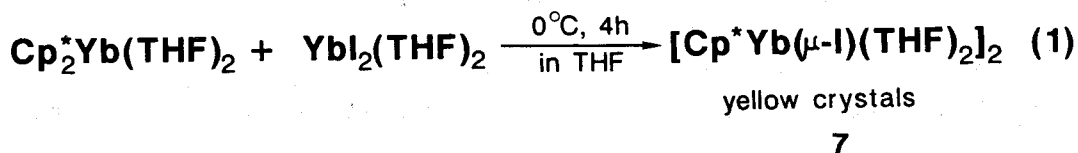
The yellow crystals of **7** react with one equivqlent of CpNa in THF to give salt-free $YbCpCp^*(THF)_3$ (6) in 80% yield as red crystals (eq. 2). From the ^1H NMR of **6**, presence of three THF molecules

$$[Cp^*Yb(\mu\text{-}I)(THF)_2]_2 + 2CpNa \xrightarrow[\text{in THF}]{0°C, 2h} CpCp^*Yb(THF)_3 \quad (2)$$

red crystals

6

per ytterbium atom is evident. Presumably, one of these THF molecules is incorporated as crystal solvent.

Living Polymerization of MMA with Ln(II) Complexes.

Polymerization of MMA was examined in various conditions using organolanthanide (II) complexes 1-6 as catalyst. All the lanthanide complexes employed here were thoroughly purified by repeated recrystallization and are isolated as air sensitive single crystals. Monomer and solvents were thoroughly dried and degassed before use. The reaction proceeds in a homogeneous state during all stages of polymerization until reaction completes. Table I summaizes the results of polymerizations catalyzed by typical Ln(II) complexes at 0 °C.

Figure 1. Lanthanide(II) Catalysts for Syndiotactic Polymerization of MMA

Cp$_2^*$Yb(THF)$_2$ **1**   Cp$_2^*$Yb(THF) **2**   Cp$_2^*$Yb(py)$_2$ **3**   Cp$_2^*$Sm(THF)$_2$ **4**

Cp$_2^*$Yb(μ-Et)AlEt$_2$(THF) **5**   CpCp*Yb(THF)$_2$ **6**
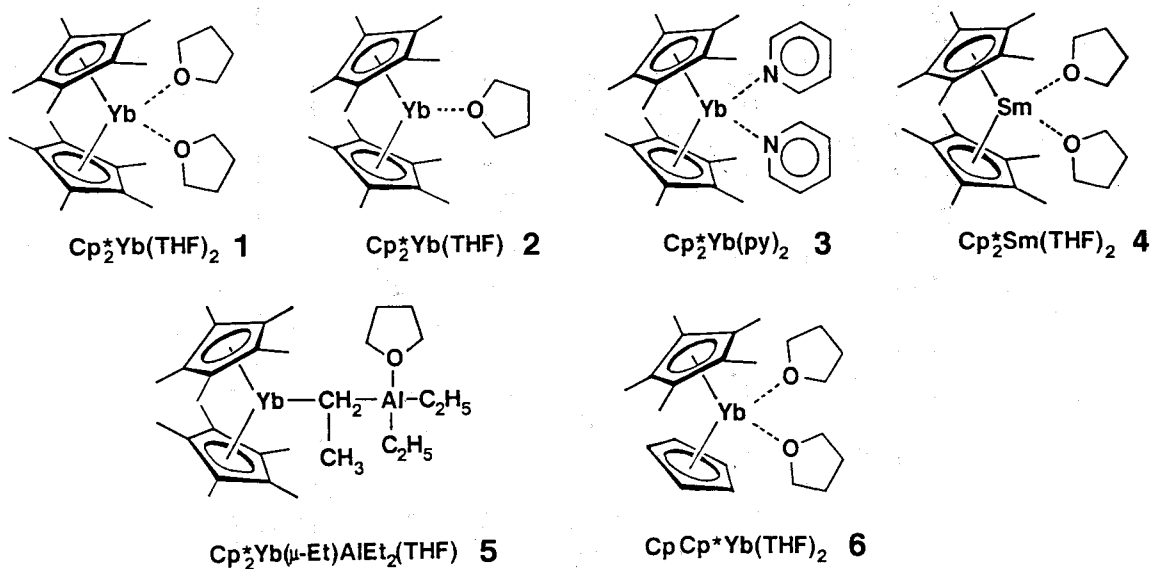
Table I. Ln(II) Catalyzed Polymerization of MMA in Toluene at 0°C

Catalysts	Time(min)	$Mw/10^3$	Mw/Mn	Tacticity(%)			Yield(%)
				rr	rm	mm	
$Cp^*_2Yb(THF)$	30	160	1.13	83.1	16.9	0	96
$Cp^*_2Yb(THF)_2$	60	320	1.09	86.0	14.0	0	96
$Cp^*_2Yb(py)_2$	60	39	1.13	72.1	26.3	1.6	77
$Cp^*_2Yb(\mu\text{-Et})AlEt_2(THF)$	20	960	2.28	77.6	20.4	2.0	98
$CpCp^*Yb(THF)_3$	60	240 68	1.11 1.19	76.5	21.5	2.0	65
$Cp^*_2Sm(THF)_2$	60	70	1.10	83.2	16.1	0.7	40

catalyst; 0.2mol%

These reactions involve following marked features, i.e. 1) highly syndiotactic poly(MMA) were formed in quantitative yield, 2) polydispersity of the resulted polymers are exceedingly narrow in comparison with reported values, 3) polymerization occurs very rapidly in a living manner leading to high molecular weight poly-(MMA) with narrow molecular weight distribution. Any catalyst system has not yet satisfy the whole items 1)-3). Although several catalyst systems, i.e. Grignard reagents such as i-BuMgBr, t-BuMgBr, and (m-vinylbenzyl)MgCl, and $Al(C_2H_5)_3 \cdot PPh_3$, are known to produce highly syndiotactic poly(MMA) (rr=94.3-96.6%) in relatively low yield.[2,6] Molecular weight of these polymers is generally much smaller ($1.1-1.8 \times 10^3$) and polydispersity is wider (1.2-1.8) as compared with the present systems.

In general, the syndiotacticity is known to vary greatly depending upon the polymerization temperature. The effect of polymerization temperature to syndiotacticity as well as polydispersity was examined. The results are shown in Figure 2. The syndiotacticity increased up to 91.2% from 77% by changing the temperature from 25 °C to -40 °C in line with general trend. The polydispersity shows no variation during these reactions.

Concequently we can readily estimate that the present polymerization occurs in a living fashion. To ascertain the living polymerization mode, conversion vs. Mn together with conversion vs. polydispersity were plotted as shown in Figure 3. Both plots gave straight lines irrespective of the catalyst concentration, in confirmation of living polymerization. The efficiency of catalyst is 25% in case of 0.5 mol% of catalyst concentration, while the efficiency decreased to 24 and 14% in cases of 0.2 and 0.1 mol%, respectively. This is presumably due

to the action of trace amount of water and oxygen in the system. Actually, the addition of water and dried oxygen to the polymerization system resulted in enlargement of Mw/Mn. Consequently strict elimination of these impurities is essential to realize the ideal living polymerization (conventional drying over CaH_2 is insufficient for this purpose since monomer and solvent contain ca. 30 ppm water as revealed by Karl Fischer titration as well as gaschromatographic analysis).

The extent of syndiotacticity of the present poly(MMA) was easily determined with reference to the reported pentad assignment.[7] ^{13}C NMR spectra of a polymer obtained by complex 1 (at -40 °C) and that of conventional atactic polymer prepared by AIBN are shown in Fig 4. Signals at 178.2, 177.8, and 176.9 ppm are assigned to mrrr, rrrr, rmrr, respectively. The ratio of these signals is 9:82:9 for the polymer obtained by 1, i.e. 91%

Figure 2. Catalytic Behavior of Cp$_2^*$Yb(THF)$_2$ at Various Temperature

in toluene
catalyst; 0.2mol%
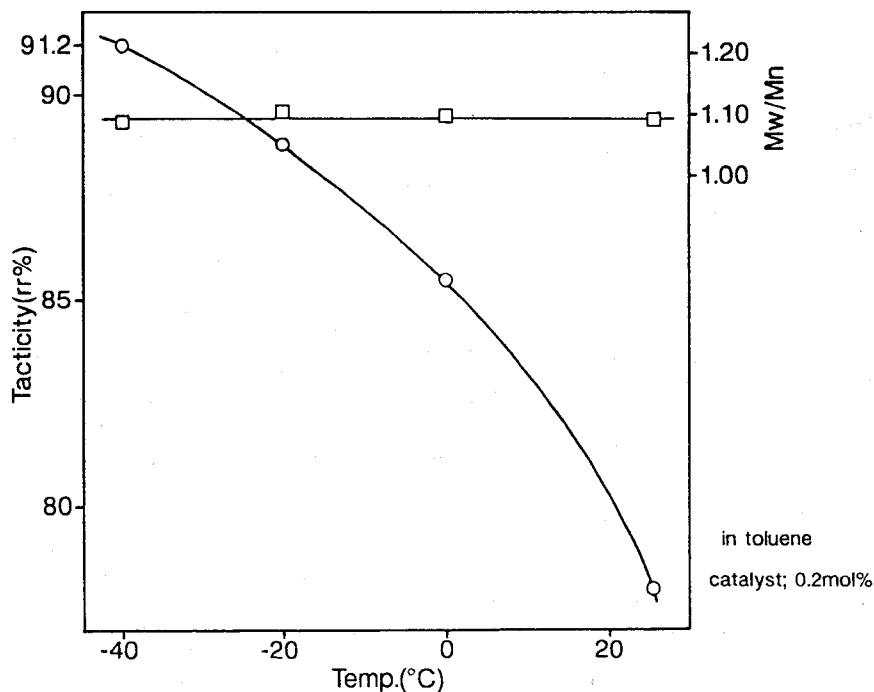
Figure 3. Conversion-Mn and Conversion-Mw/Mn Plots

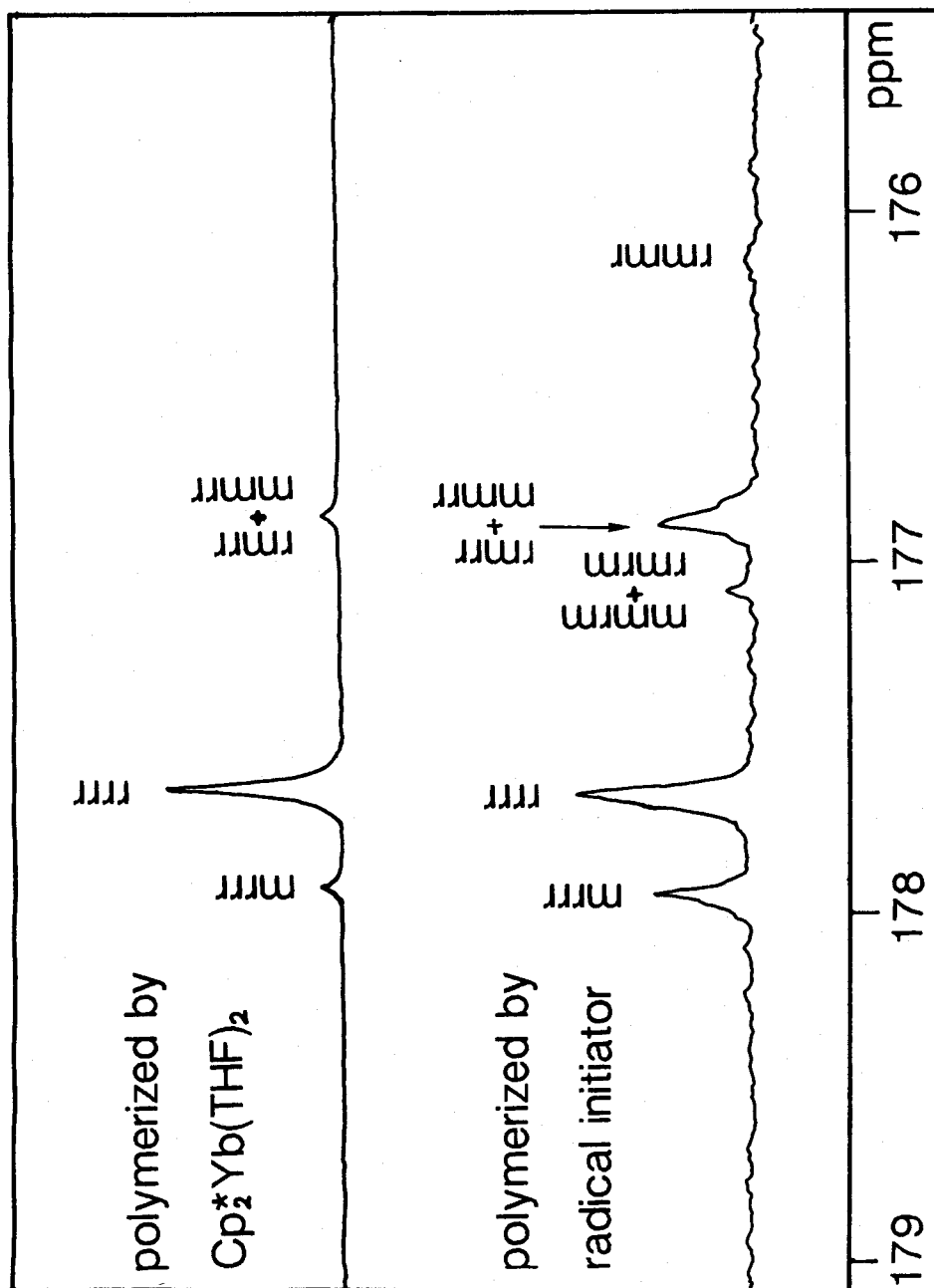at 0°C, in toluene
catalyst; $Cp_2^*Yb(THF)_2$
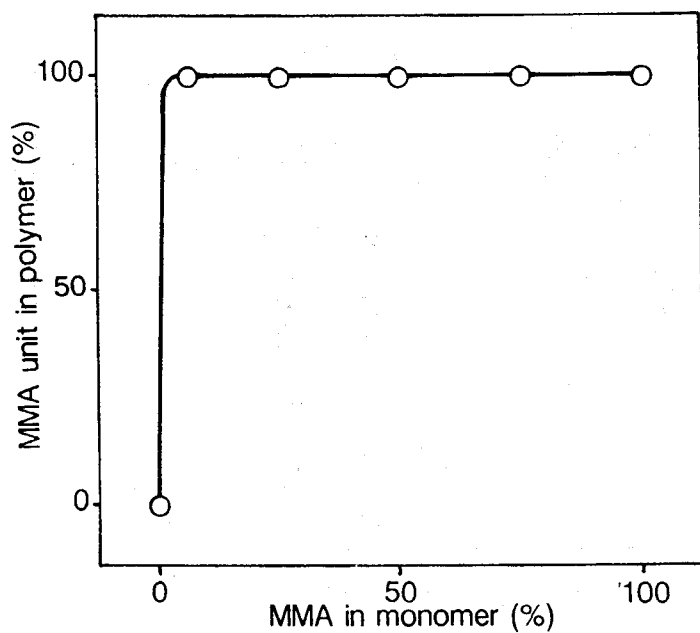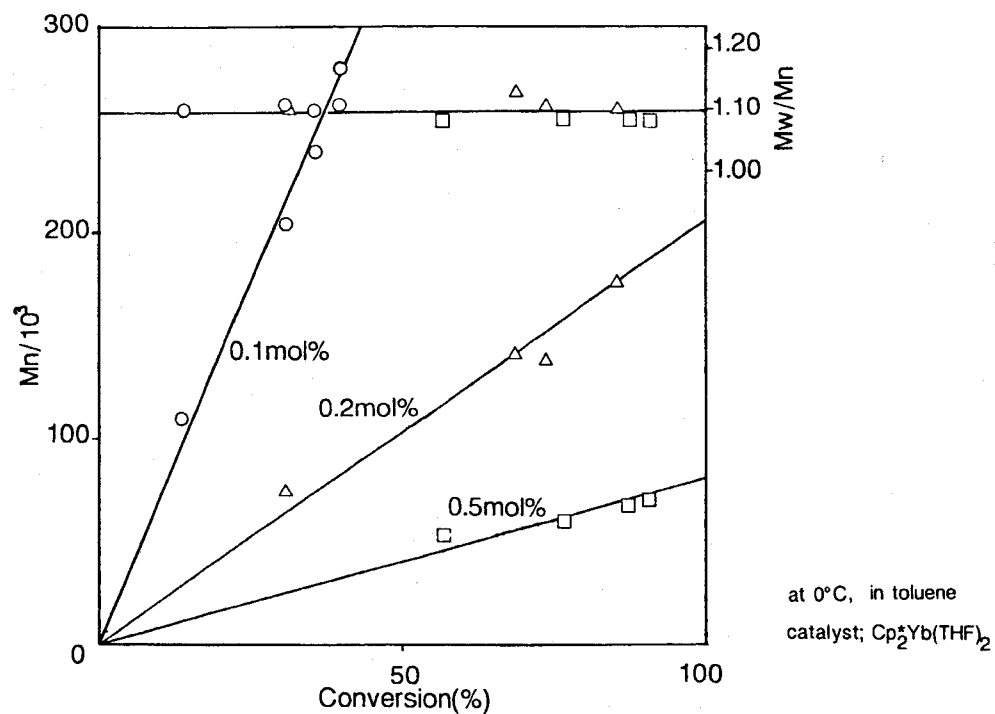
Figure 4. Copolymerization of MMA with styrene

Figure 5. Carbonyl Region of ^{13}C NMR of PMMA.

syndiotacticity by triad assignment.

To clarify the polymerization mechanism, copolymerization of MMA with styrene was carried out at various monomer ratio. Interestingly, no styrene monomer was incorporated to the poly-(MMA) chain end at any monomer ratio (Figire 5). This result indicates that the polymerization of MMA catalyzed by organo-lanthanide(II) complexes proceeds through anionic mechanism.

Experimental   Section

Materials.

YbCp$^*_2$(THF)$_2$ (1), YbCp$^*_2$(pyridine)$_2$ (3), and SmCp$^*_2$(THF)$_2$ (4) were prepared by the established methods. YbCp$^*_2$(THF) (2) and YbCp$^*_2$(μ-Et)AlEt$_2$(THF) (5) were obtained according to the methods described in chapter 5. Commercially obtained methyl methacrylate was purified by the following procedure. After removing of inhibitor by shaking MMA with 5% NaOH, MMA was dried over CaH$_2$ for 8 h and distilled under argon onto CaH$_2$ through Widmer Column for two times. Since the obtained MMA still contains ca. 30 ppm of water, the MMA was dried over molecular sieves under an argon atmosphere, and finally degassed and purified by trap-to-trap distillation just before use.

Preparation of Mixed Ring Ytterbocene.

To a stirred solution of YbI$_2$ (10 mmol) in THF (250 mL) was added a 20 mL of THF solution of YbCp$^*_2$ (5.87 g, 10 mmol) at 20 °C. After stirring for 2 h at this temperature, the solution was filtered and the filtrate was concentrated to ca. 50 mL to give [YbCp*(μ-I)(THF)$_2$]$_2$ as yellow crystalline solid (7.2 g, 81%). The yellow [YbCp*(μ-I)(THF)$_2$]$_2$ (5.8 g, 5 mmol) was dissolved in

THF (100 mL) and THF solution of CpNa (0.88 g, 10 mmol) was drop-wise added to the solution at 0 °C. After being stirred for 2 h, solvent was evaporated to dryness. The residue was extracted with 60 mL of toluene and the salt was separated with a centrifugation under argon. The toluene was removed in vacuo and the residual solid was recrystalized from THF/hexane (1:1) to afford YbCpCp*(THF)$_3$ as red crystals in 76% yield. ^{1}H NMR (C$_6$D$_6$) δ 6.08 (s, 5H, C$_5$H$_5$), 2.26 (s, 15H, C$_5$Me$_5$), 3.42 (m, 12H, THF), 1.39 (m, 12H, THF).

Syndiotactic Living Polymerization of MMA Catalyzed by Lanthanide(II) Complexes.

A toluene solution (5 mL) of MMA (1.0g, 10 mmol) was cooled to -78 °C. The solution was added to YbCp$^*_2$(THF)$_2$ (5.87 mg, 0.01 mmol) in toluene (15 mL) with stirring at -78 °C. The reaction vessel was sealed and kept at -40 °C for 15 h. The reaction mixture was poured into MeOH (500 mL). The obtained polymer was dissolved in CHCl$_3$ and purified by precipitation into MeOH. After drying under reduced pressure at 100 °C for 12 h, the molecular weight of the polymer was measured by gel permeation chromatograph together with light scattering method.

Reference

1) (a) Evans, W. J. Polyhedron **1987**, <u>6</u>, 803. (b) Evans, W. J. Adv. Organomet. Chem. **1985**, <u>24</u>, 131.

2) (a) Cao, Z.; Ute, K.; Kitayama, T.; Okamoto, Y.; Hatada, K. Kobunshi Ronbunshu **1986**, <u>43</u>, 435. (b) Hatada, K.; Nakanishi, H.; Ute, K.; Kitayama, T. Polym. J. **1986**, <u>18</u>, 581. (c) Joh, Y.; Kotake, Y. Macromolecules **1970**, <u>3</u>, 337.

3) Tilley, T. D.; Andersen, R. A.; Spencer, B.; Ruben, H.; Zalkin, A.; Templeton, D. H. Inorg. Chem. **1980**, <u>19</u>, 2999.

4) Tilley, T. D.; Andersen, R. A.; Spencer, B.; Zalkin, A. Inorg. Chem. **1982**, <u>21</u>, 2647.

5) Evans, W. J.; Grate, J. W.; Choi, H. W.; Bloom, I.; Hunter, W. E.; Atwood, J. L. J. Am. Chem. Soc. **1985**, <u>107</u>, 941.

6) (a) Cao, Z.; Okamoto, Y.; Hatada, K. Kobunshi Ronbunshu **1986**, <u>43</u>, 857. (b) Abe, H.; Imai, K.; Matsumoto, M. J. Polym. Sci. **1968**, <u>C23</u>, 469. (c) Koide, N.; Iimura, K. Polym. Prepr., Am. Chem. Soc., Div. Polym. Chem.**1979**, <u>20</u>, 558. (d) Hatada, K.; Ute, K.; Shinozaki, T.; Kitayama, T. Polym. Bull. **1988**, <u>19</u>, 231.

7) Moad, G.; Solomon, D. H.; Spurling, T. H.; Johns, S. R.; Willing, R. I. Aust. J. Chem. **1986**, <u>39</u>, 43.

Chapter 7

Facile Synthesis and Structural Features of Alkyne Complexes of Alkylniobocene: $NbCp_2(R)(alkyne)$

Introduction

Intramolecular migration of metal hydride or metal alkyl to the coordinated C-C unsaturation is considered to be the pivotal step in the initiation or propagation of the Ziegler-Natta type polymerization process.[1]   However, only limited evidence for this type of intramoleculer migration have been reported.[2,3] The reason is that the alkyl complex resulted from the migration reaction is generally unstable in the absence of substrate with C-C unsaturation, i.e. β-H elimination or reductive elimination occurs.

A concerted mechanism via a cyclic transition state has been proposed for the insertion of olefins into the M-H bond and β-H elimination of M-R since the insertion occurs ordinarily in a cis-fashion.[4]   The kinetic studies regarding ring size effect in the rate of thermal decomposition of platinum(II) metallacyclo-alkanes[5] and the lack of β-H elimination from metal-norbornyl complexes[6] suggest that a planar arrangement of the four atoms (M-C-C-H), in which the H and olefin locate in the cis position, is crucial in alkyl-metal bond formation and the β-H elimination.[7,8]

$NbCp_2(H)(CH_2=CH_2)$ may be a useful starting material for detailed study on the intramolecular migration reactions, since these complexes have fairly good thermal stability so that these
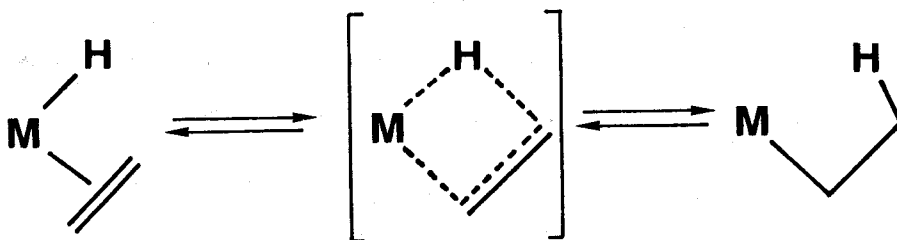
are able to be isolated as diamagnetic crystalline compounds. The cis- and planar arrangement of the coordinated olefin toward Nb-H has already been well confirmed on the basis of X-ray crystallography.

Yasuda et al. have already reported that a series of conjugated diene exhibit good reactivity towards $NbCp_2(H)(CH_2=CH_2)$ and give rise to the formation of allylic compounds, $NbCp_2(\eta^3-CHR^1-CR^2-CHR^3)$, as a result of olefin-diene ligand exchange followed by hydrometallation.[9] Since alkyne molecules are in many cases known to show higher or identical π-donating property, the reactions of variety of alkynes with the Nb(H)(olefin) complexes have been examined here.

This chapter describes the mode of reactions between $NbCp_2(H)(CH_2=CH_2)$ and various alkynes leading to novel alkyl(alkyne) complexes and typical examples of the molecular structures of the resulting complexes.

Results and Discussion

1.   Reaction of Mono-Substituted Alkynes with $NbCp_2(H)$-(ethylene)

The ethylene complex of hydridoniobocene, $NbCp_2(H)(CH_2=CH_2)$, was found to readily react with a variety of mono-substituted alkynes such as propyne, 1-butyne, and phenylacetylene. The reaction proceeds cleanly in toluene at 60 °C. The color of the solution turns green from yellow during the reaction. The products could be isolated as air-sensitive pale yellow crystals in ca. 70 % yield by repeating recrystallization of the product from thoroughly degassed hexane (contamination of decomposed compounds less than 0.2 % causes the color of the product to green). Their EIMS spectral and elemental analyses data are consistent with those formulated by $NbCp_2(CH_2CH_3)(RC\equiv CH)$ (see Experimental Section). The reaction proceeds following eq. 1 as identified on

1. $R=CH_3$
2. $R=CH_2CH_3$
3. $R=Ph$
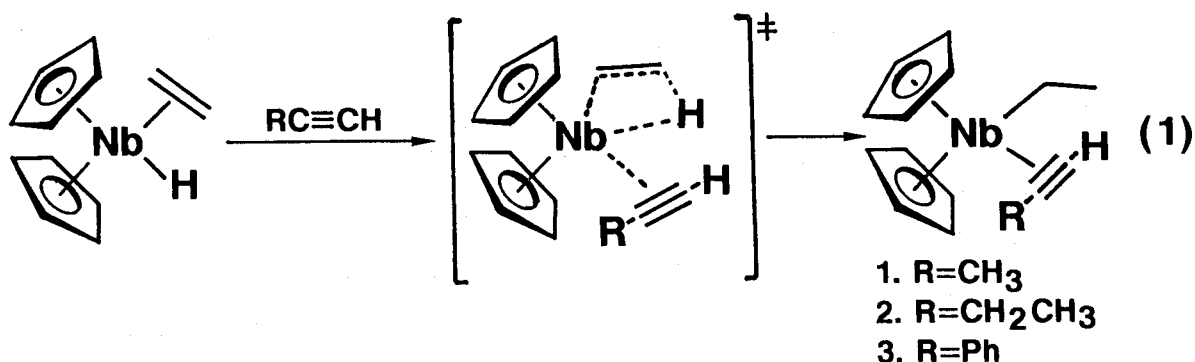
the basis of N M R studies. The attack of alkyne resulted in intramolecular migration of Nb-hydrido group to the ligated ethylene accompanied by coordination of the incoming alkyne to the metal.

The mode of this reaction corresponds well to that for reactions of $NbCp_2(H)(CH_2=CH_2)$ with CO and isonitrile which give rise

to the formation of $NbCp_2(CH_2CH_3)(donor)$.[3a]   All   of the result-
ing   products, $NbCp_2(CH_2CH_3)(CH_3C{\equiv}CH)$ (1), $NbCp_2(CH_2CH_3)$-
$(CH_3CH_2C{\equiv}CH)$ (2), and $NbCp_2(CH_2CH_3)(PhC{\equiv}CH)$ (3) comprise of two
geometrical isomers, exo and endo (Figure 1), as confirmed by the

Figure 1   **exo**   **endo**
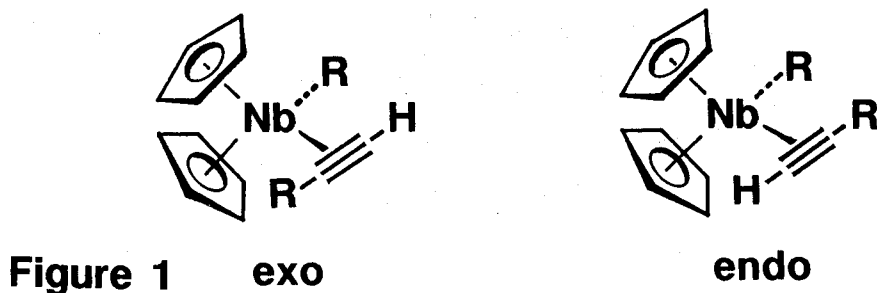
NMR studies. ^{1}H and ^{13}C NMR parameters are summarized in Table I
and II, respectively. In general, alkyne CH proton signals of
exo-isomer (6.2-7.2 ppm) show upfield shift as compared with
alkyne CH resonances of endo-isomer (8.1-9.1 ppm). Most striking
is the predominant formation of the exo-isomer. This trend
sharply contrasts to the behavior of the starting alkene comp-
lexes, which prefer the endo-structure. This drastic change of
the favorable structure between the alkene and alkyne complexes
may arise from the difference in steric interaction among the Cp
groups, Nb-alkyl, and the substituents on the ligated alkenes or
alkynes. Figure 2explains the steric conjestions for the alkene
and alkyne complexes. A close contact is considered for the
alkene complex between the alkyl substituent of the ligated
alkene and Cp, while for the alkyne complex a severe steric
interaction is expected between the alkyl substituent and Nb-R.
In fact, the exo-content increases as increasing bulkiness of the
alkyl substituent in the latter complex.

Figure 2
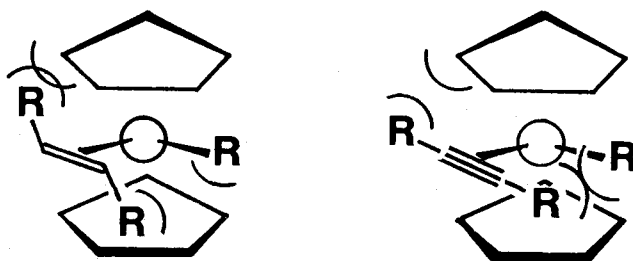
The assignment of the exo- and endo-isomers of the alkyne complexes was made on the basis of 2D-NOESY experiment. Typically the spectrum of $NbCp_2(CH_2CH_3)(CH_3C\equiv CH)$ (1) is shown in Figure 3, which displays cross peaks among the proton peaks: CH(exo-propyne)-CH_2 and CH_3 (exo-$NbCH_2CH_3$), CH_3(endo-propyne)-CH_2 and CH_3 (endo-$NbCH_2CH_3$). Thus, steric repulsion between Nb-alkyl and substituent on the alkyne plays an important role in determining the exo-geometry.

Exceptional is the reaction of bulky alkynes, such as t-butylacetylene and trimethylsilylacetylene, with $NbCp_2(H)$-$(CH_2=CH_2)$. The reaction gives rise to the formation of a hydridoniobocene(alkyne) complex, $NbCp_2(H)(RC\equiv CH)$ (6: R=t-Bu, 7: R=$Si(CH_3)_3$), selectively in high yields. This type of complexation was identified by the ^{1}H NMR measurement in addition to the EIMS spectrum. The proton signals at higher field (-0.08--0.9 ppm) are reasonably assigned to Nb-H on the basis of signal ratio and chemical shift. The proton-proton coupling between acetylenic hydrogen of the coordinated alkyne and Nb-H indicates the formation of the exo-isomer as a sole product. The chemical

Table I. ^{1}H NMR Parameters for Nb-Alkyne Complexes.

Complexes	H^1	Chemical Shift (coupling Constants, Hz) H^2	H^3	H^4
NbCp$_2$(R^{1}CCH^2)(CH$_2^3$CH$_3^4$)				
1 R=CH$_3$ exo(79%)	2.59 (d,1.74)	6.79 (d,1.74)	2.06 (q,7.15)	1.86 (t,7.15)
endo(21%)	2.37 (d,1.73)	8.09 (d,1.73)	1.83 (q,5.78)	1.76 (t,5.78)
2 R=CH$_2$CH$_3$ exo(81%)	2.74 (dq,1.54,7.23) 1.35 (t,7.23)	6.78 (d,1.54)	2.02 (q,7.05)	1.82 (t,7.05)
endo(19%)	2.63 (dq,1.36,7.30) 1.22 (t,7.30)	8.14 (d,1.36)	2.01 (q,6.22)	1.80 (t,6.22)
3 R=Ph exo(93%)	7.2-7.7 (m)	7.15 (s)	2.11 (q,7.15)	1.88 (t,7.15)
endo(7%)	7.2-7.7 (m)	8.19 (s)	1.83 (q, 7.05)	1.57 (t,7.05)
NbCp$_2$(R^{1}CCH^2)(H^3)				
4 R=t-Bu exo(100%)	1.80 (s)	7.52 (d,8.21)	-0.08 (d,8.21)	
5 R=SiMe$_3$ exo(100%)	0.36 (s)	9.18 (d,7.90)	-0.77 (d,7.90)	

$NbCp_2(R^1CCR^2)(CH_2^3CH_3^4)$			
6 R=CH₃	2.43(exo) (s)	1.98 1.97 $J_{33'}=-27.15$ $J_{3'4}=7.47$	$J_{34}=7.84$ 1.91
$NbCp_2(R^1CCR^2)(H^3)$			
7 R=Ph	7.2-8.3 (m)	7.2-8.3 (m)	-0.23 (s)

Spectra (500 MHz) measured in C_6D_6 at 25 °C were analyzed by computer simulation.

Table II. ^{13}C NMR Parameters for Nb-Alkyne Complexes.

Complexes	C^1	C^2	C^3	C^4	C^5	C^6
NbCp$_2$(R^{1}C^{2}C^{3}H)(C^{5}H$_2$C^{6}H$_3$)						
1 R=CH$_3$ exo(79%)	21.8	158.8	127.0	—	13.8	21.0
endo(21%)	11.9	137.2	138.4	—	14.3	21.4
2 R=CH$_2$CH$_3$ exo(81%)	30.5 / 23.0	165.7	126.5	—	14.3	20.9
endo(19%)	20.3 / 20.9	144.0	137.5	—	14.1	21.3
3 R=Ph exo(93%)	120–140	160.1	124.6	120–140	14.2	20.8
endo(7%)	120–140	138.0	137.0	120–140	14.3	23.0
NbCp$_2$(R^{1}C^{2}C^{3}H)(H)						
4 R=t-Bu exo(100%)	37.2 / 32.3	165.6	116.0	—	—	—
5 R=SiMe$_3$ exo(100%)	1.1	144.7	147.8	—	—	—
NbCp$_2$(R^{1}C^{2}C^{3}R^4)(C^{5}H$_2$C^{6}H$_3$)						
6 R=Me	20.0(exo)	147.9	130.2	9.6(endo)	12.7	21.6
NbCp$_2$(R^{1}C^{2}C^{3}R^4)(H)	120–140	149.2	139.0	120–140	—	—
7 R=Ph	120–140	149.2	139.0	120–140	—	—

Chemical Shift(ppm)

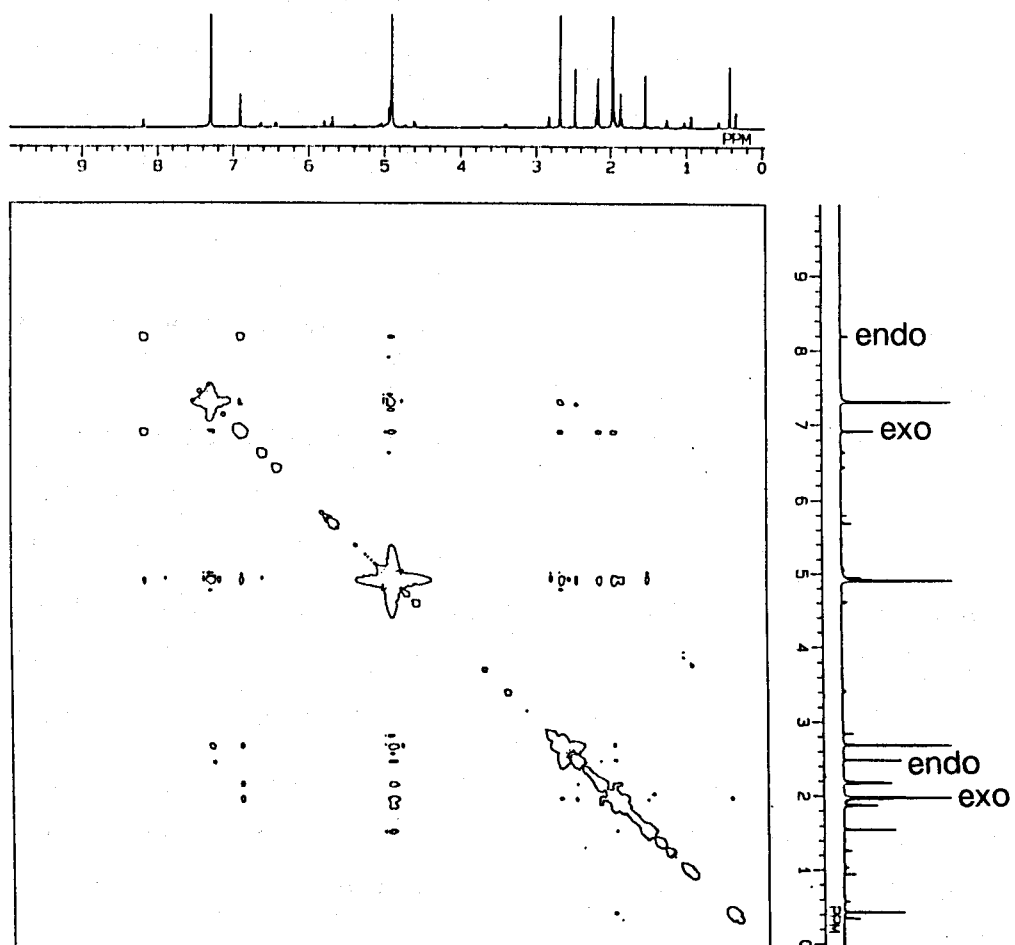Data were collected at 67.5 MHz in C$_6$D$_6$ at 25 °C.

Figure 3. NOESY- Spectrum of Complex **1**

shift value of the CH resonance also agree well with those for the exo-isomer of alkyne complexes, (1)-(5). This type of complexation may result from the strong π-donating property of the alkynes which allows the replacement of the coordinated alkene with an alkyne prior to the hydride transfer to the coordinated alkene. The exo-preference is therefore concluded to steric congestion between the hydrido and t-Bu- or Si(CH$_3$)$_3$- group in line with the geometry observed in alkyl(alkyne) complexes (1)-(5).
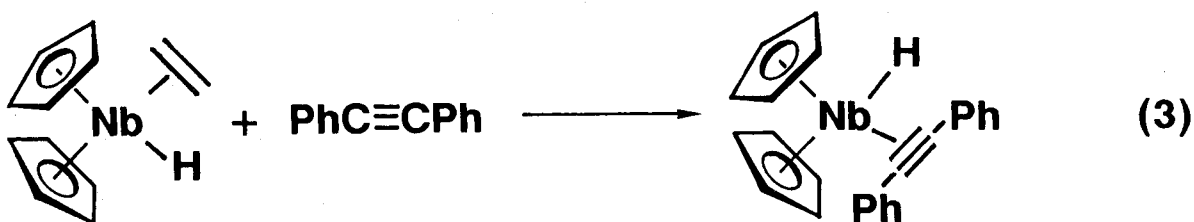
2. Reaction of Disubstituted Alkynes with NbCp$_2$(H)-(ethylene).

Reactions of disubstituted alkynes with NbCp$_2$(H)(ethylene) were explored to understand the steric as well as electronic effect to the reaction mode. Although disubstituted alkyne ligands are expected to show large steric contact with both Cp and Nb-H in access to the metal (due to the linear structure), 2-butyne was found to react smoothly with NbCp$_2$(H)(ethylene) to give an ethylniobocene(2-butyne) complex, NbCp$_2$(CH$_2$CH$_3$)-(CH$_3$C$\equiv$CCH$_3$) (6), as the sole product in 70% yield at 60 °C in toluene (eq. 2). ^{1}H NMR and EIMS spectral data support this

$$\text{(2)}$$
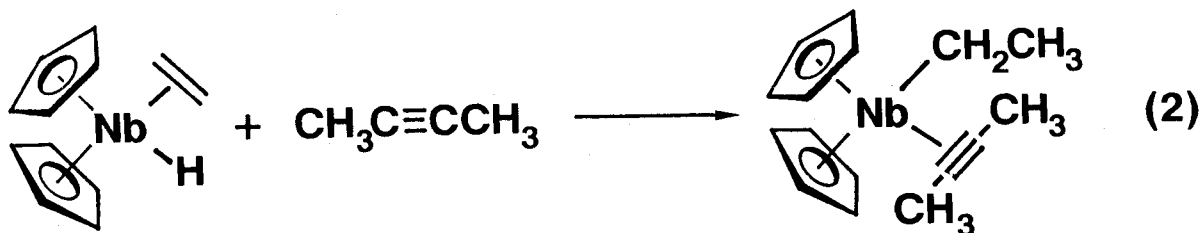
constitution. An attempt to prepare the corresponding alkyl-(alkyne) complexes by reaction of $NbCp_2Cl$(alkyne)[10] with Grignard reagent has failed because of the formation of complexed mixture.[11] Geometrical isomers are absent for complex **6**. However, the Nb-ethyl group shows very complicated ^1H NMR spectral pattern as shown in Figure 4, while Nb-ethyl group of $NbCp_2$-$(C_2H_5)(CH_3C\equiv CH)$ shows the normal A_2B_3 pattern. A detail analysis of the 500 MHz spectrum reveals the abnormal proton-proton couplings, which may be the result of the agostic interaction between one of the protons in Nb-CH_2 group and Nb. Indeed computer simulation of the spectrum confirms the ABC_3 pattern: J_{AB}=-27.15, J_{AC}=7.85, J_{BC}=7.43 Hz. The large J_{AB} geminal coupling of CH_2 group should originate from the small H–C–H angle. From the Karplus's correlation plot for geminal protons,[12] the value of the H–C–H angle is calculated to be ca. 101°. Actually, the H–C–H angle of 100° was confirmed by the X-ray crystallographic analysis of the complex **6** (vide infra).

Diphenylacetylene reacts with $NbCp_2(H)$(ethylene) in a different manner. Ethylene-alkyne ligand exchange reaction occurs predominantly in this case. ^1H NMR and EIMS spectra of the resulting product suppot the constitution (eq. 4).
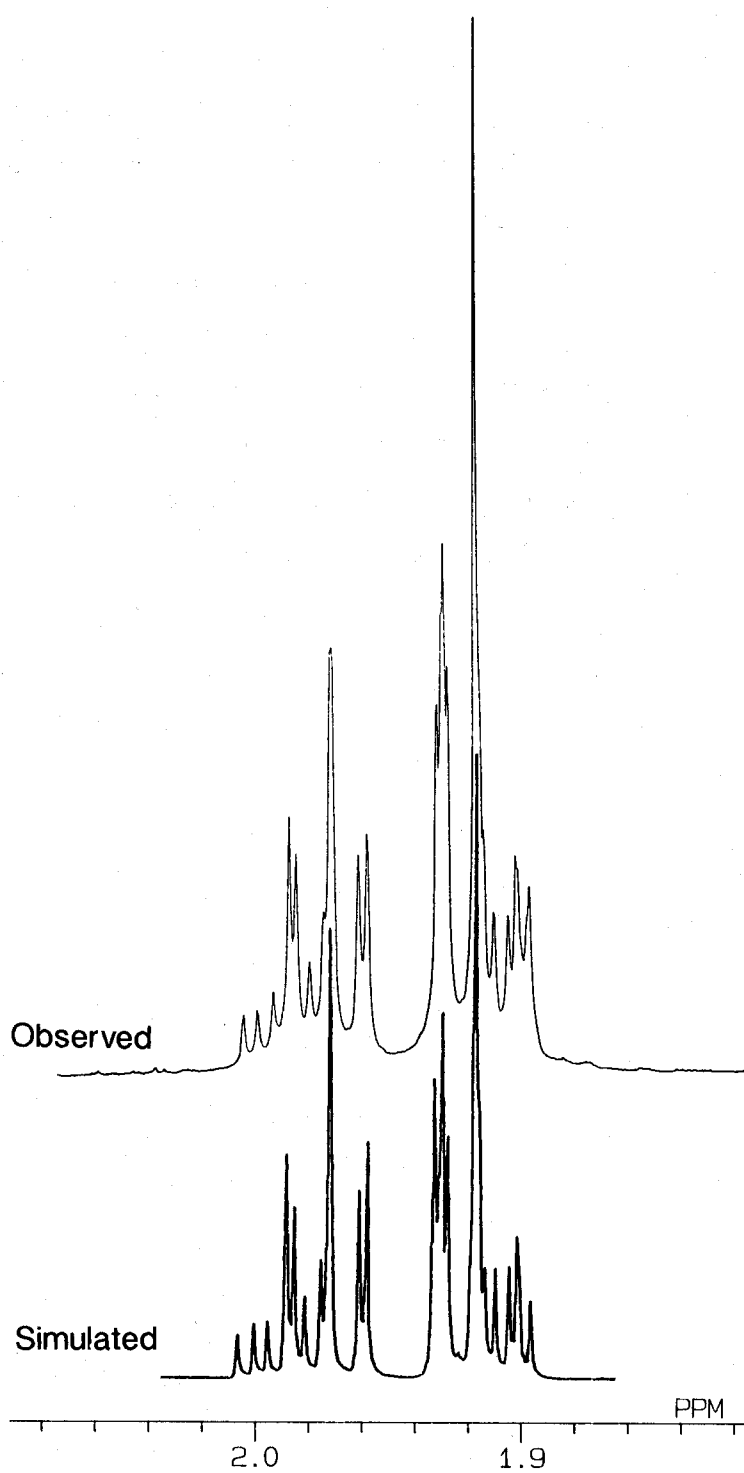

$$\text{Nb} \diagdown \text{H} + \text{PhC}\equiv\text{CPh} \longrightarrow \text{Nb} \diagup \text{Ph} \qquad (3)$$

Observed

Simulated

Figure 4. 500 MHz ¹H-NMR Spectrum of **6** (ethyl region).

3. X-ray Structure Analyses of Niobium-Alkyne Complexes

(a) Molecular Structure of $NbCp_2(H)[(CH_3)_3CC{\equiv}CH]$ (4).

To establish the exact structure of novel hydrido(alkyne)-niobocene complexes, X-ray crystallographic analysis of complex **4** was carried out. The molecular structure of **4** was shown in Figure 5, and IV, respectively.

Obviously, complex **4** has exo geometry in line with the result of NMR studies. The Nb-C(2) distance of 2.160(5) A is the shortest among those reported for $NbCp(CO)(PhC{\equiv}CPh)_2$ (av. 2.20 Å)[13] and $NbCp(CO)(C_4Ph_4)(PhC{\equiv}CPh)$ (2.23 Å)[14] together with those of $NbCp_2(H)(Me_3SiC{\equiv}CH)$ (5) (2.164(7) Å) and $NbCp_2(CH_2CH_3)(CH_3C{\equiv}CCH_3)$ (6) established in this work (vide infra). The Nb-C(1) distance of complex **4** (2.191(4) Å) is slightly long as compared with that of Nb-C(2), presumably due to steric interaction between bulky t-Bu group and Cp ligands. The C(1)-C(2) distance of 1.288(6) Å is lengthened from that of the non-coordinated alkyne molecules (ca.1.20 Å), and both t-Bu group and H(2) on alkyne ligand are bent away from the metal ($\angle$C(2)-C(1)-C(3)=137.6° and $\angle$C(1)-C(2)-H(2)=116(2)°). That is to say, there exists a pronounced participation of metallacyclo-2-propene structure.

The Nb-H(2) distance (1.632(79) Å) is comparable with that in $NbCp_2(H)_3$ (av. 1.65 Å).[15] However, the C(2)-Nb-H(1) angle (70.8°) is spread as compared with that of $NbCp_2(H)_3$ (av. 63°), probably due to the steric repulsion between H(1) and H(2) atoms together with the steric hindrance of bulky t-Bu substituent on the alkyne ligand.

Nb-C(Cp) distances (av. 2.433(7) Å) is significantly longer than those of $NbCp_2(H)_3$[15] and $NbCp_2(CH_2CH_3)(CH_2{=}CH_2)$[16]
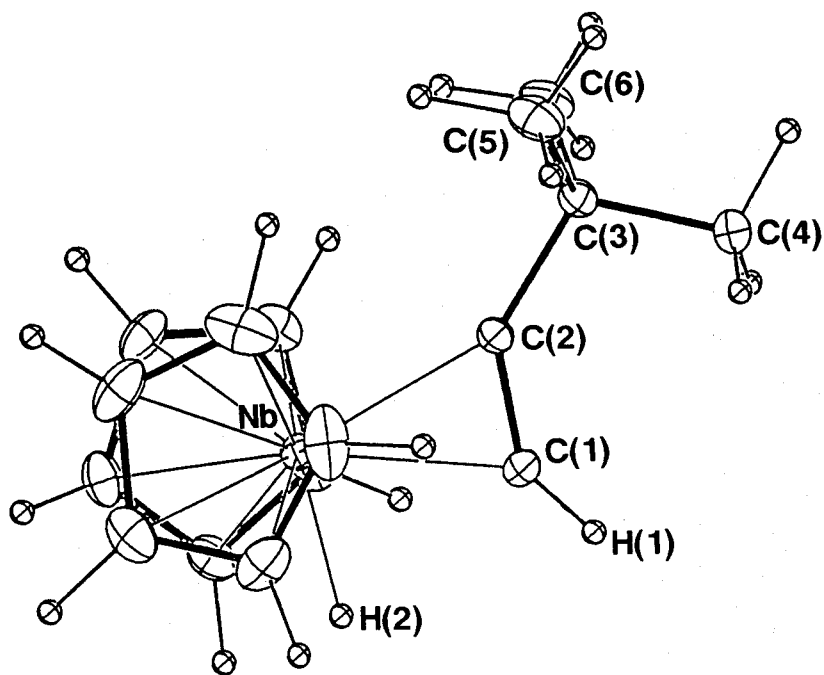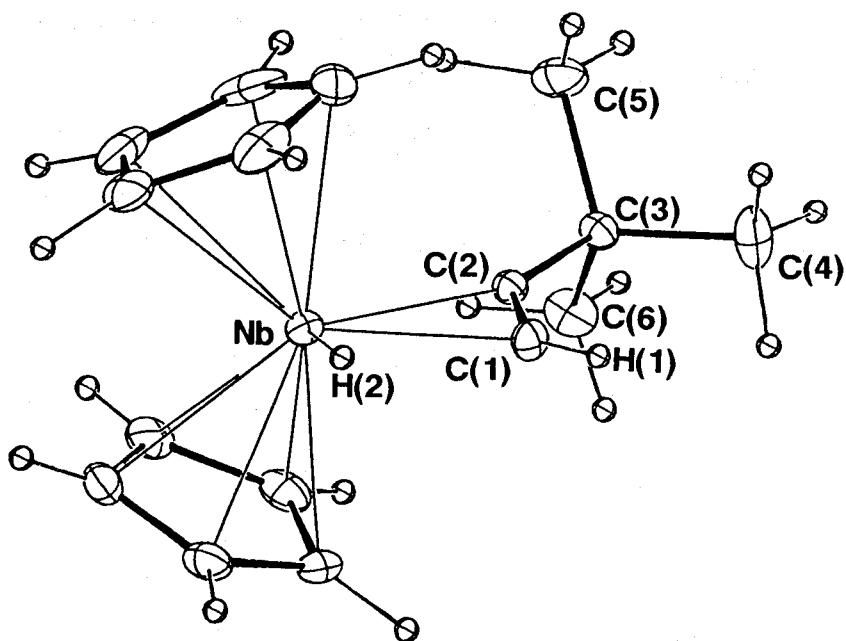
Figure 5. Molecular Structure of 4

(2.375(4)-2.402(5) Å). This may caused by the strong electron donating character of the alkyne ligand.

(b)   Structure Analysis of $NbCp_2(H)(Me_3SiC\equiv CH)$ (5).

To understand details of steric effect of the alkyne substituent, the molecular structure of $NbCp_2(H)(Me_3SiC\equiv CH)$ (5) was determined by the X-ray analysis. Resulted ORTEP diagram[17] of **5** is shown in Figure 6. Selected bond distances and angles are listed in Table III and IV, respectively.

The whole geometry of the complex **5** is virtally identical with that of the complex **4**. Both Nb-C(1) and Nb-C(2) distances [2.210(6) and 2.164(7) Å, respectively] are slightly longer than those in **4**, reflecting the steric hindrance of exo-substituent on the alkyne ligand. Furthermore, shortening of C(1)-C(2) bond (1.279(9) Å) and enlargement of the bending angles ($\angle$Si-C(2)- C(1)=141.5(5)°, $\angle$C(2)-C(1)-H(1)=128(5)°) were observed in complex **5**, indicating the enhanced triple bond character beside complex **4**.

The dihedral angle between the two cyclopentadienyl planes (46.1°) is enlarged as compared with that of **4**. This may be arised from larger steric repulsion between trimethylsilyl group and Cp ligands in the present molecule.

The Nb-H(2) distance (1.634(87) Å) compares closely with those of $NbCp_2(H)_3$ (1.65 Å)[15] and complex 5 (1.632(79) Å) and that H(2)-Nb-C(1) angle (71.1°) is nearly equal to that of complex **4** (70.8°).
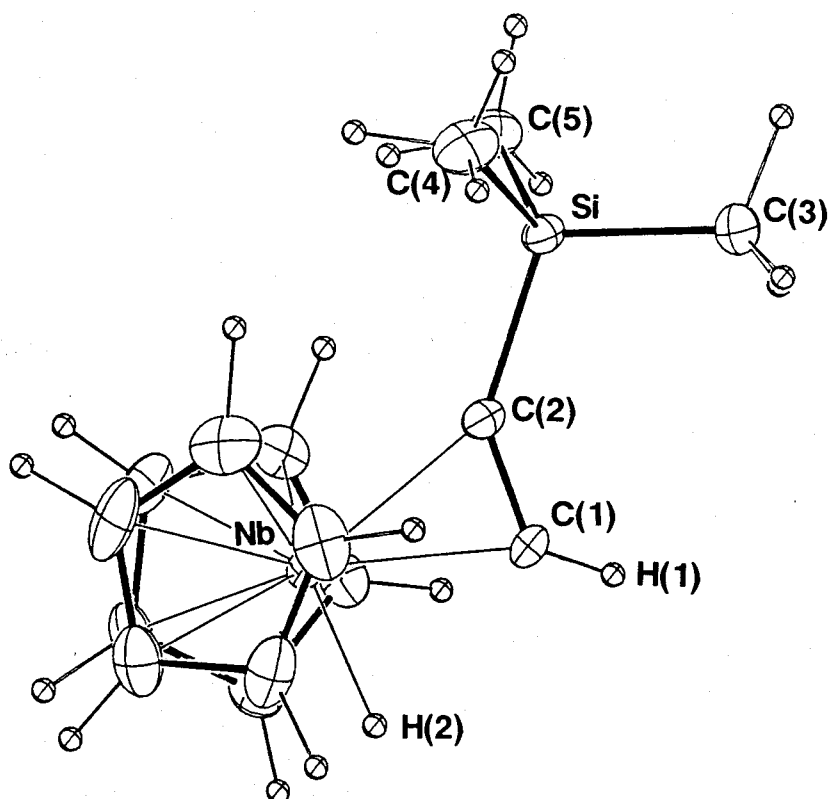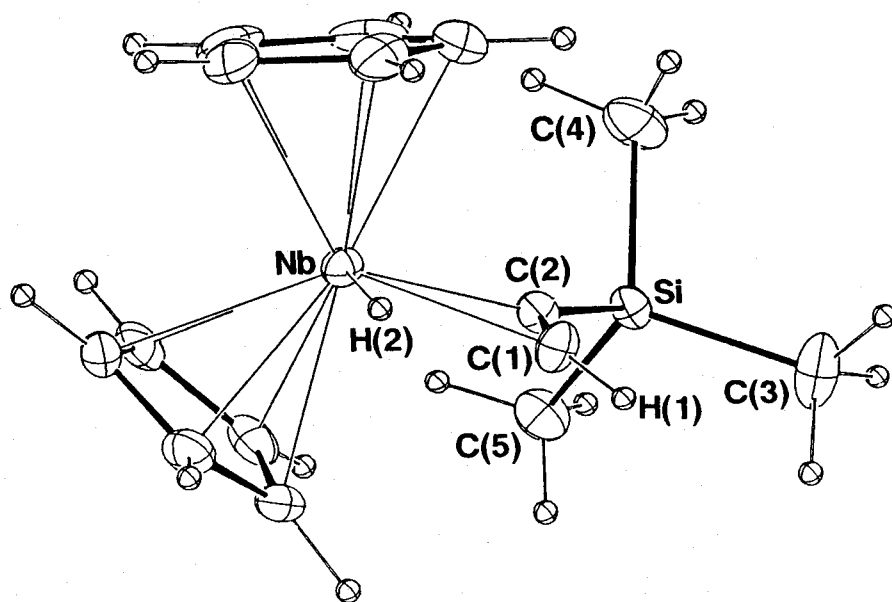
Figure 6. Molecular Structure of 5

Table III. Selected Bond Distances for Complexes **4** and **5**.

	4	**5**		**4**	**5**
Nb–C(1)	2.160(5)	2.164(7)	C(1)–C(2)	1.288(6)	1.279(9)
Nb–C(2)	2.191(4)	2.210(6)	C(1)–H(1)	0.92(7)	0.87(9)
Nb–H(2)	1.63(8)	1.63(9)	C(2)–C(3)/Si	1.525(6)	1.849(7)
Nb–CCP1	2.059(0)	2.105(0)	NbC(Cp)av.	2.433(7)	2.416(10)
Nb–CCP2	2.138(0)	2.108(0)			

Table IV. Selected Bond Angles for Complexes **4** and **5**.

	4	**5**
C(1)–Nb–C(2)	34.43(17)	33.97(25)
C(1)–Nb–H(2)	70.8(28)	71.1(31)
C(2)–Nb–H(2)	104.2(28)	105.1(31)
Nb–C(1)–H(1)	142.9(42)	152.9(57)
Nb–C(1)–C(2)	74.11(28)	74.97(42)
Nb–C(2)–C(1)	71.47(28)	71.07(41)
Nb–C(2)–C(3)/Si	150.82(31)	147.47(35)
C(2)–C(1)–H(1)	142.0(43)	128.1(57)
C(1)–C(2)–C(3)/Si	150.82(31)	141.46(55)
CCP1–Nb–CCP2	138.06(1)	134.86(2)
CCP1–Nb–C(1)	107.82(12)	112.02(18)
CCP1–Nb–C(2)	108.11(12)	107.92(16)
CCP2–Nb–C(1)	113.98(12)	112.91(18)
CCP2–Nb–C(2)	108.00(12)	106.67(16)
CCP1–Nb–H(2)	103.5(28)	99.6(31)
CCP2–Nb–H(2)	87.5(28)	98.4(31)
M1–Nb–H(2)	87.61(28)	88.3(31)

(c) Molecular Structure of NbCp$_2$(C$_2$H$_5$)(CH$_3$C≡CCH$_3$) (6).

As a typical example of the alkyl(alkyne) complexes of niobium, NbCp$_2$(C$_2$H$_5$)(CH$_3$C CCH$_3$) (6) was subjected to the crystallographic analysis. The molecular structure is shown in Figure 7 by two ORTEP drawings with numbering scheme. Selected bond distances and angles are listed in Table V and VI, respectively. Crystallographic data of the complexes 4, 5, and 6 are summarized in the experimental section (Table VII).

The C(1)-C(2) distance of 1.230(17) Å is slightly lengthened compared with the conventional C-C triple bond (1.204 Å), and this value is the shortest value among the bond distances reported for niobium-alkyne complexes, i.e. NbCp(CO)(PhC≡CPh)$_2$ (1.33 and 1.37 Å)[13] and NbCp(CO)(C$_4$Ph$_4$)(PhC CPh) (1.26 Å).[14] Two methyl groups of alkyne, C(3) and C(4), are again bent away from niobium atom and the angles, C(3)-C(1)-C(2) and C(4)-C(2)-C(1), are 141(1)° and 147(1)°, respectively. The observed rather large bent angles may arise from the steric repulsion between the Cp ligand and the exo-methyl group on alkyne as well as between the ethyl group and endo-methyl group. Nb-C(1) and Nb-C(2) distances (2.167(11) and 2.170(13) Å, respectively) are slightly shorter than those reported for NbCp(CO)(PhC CPh)$_2$ (av. 2.19 Å) and NbCp-(CO)(C$_4$Ph$_4$)(PhC≡CPh) (av. 2.29 Å).[14] Nb-C(3) distance, 2.311(11) Å is comparable with the value reported for closely related compound, NbCp$_2$(CH$_2$CH$_3$)(CH$_2$=CH$_2$) (2.316(8) Å).[16]

The most intriguing feature lies in the existence of an agostic interaction between Nb and H(51), whose distance (2.360(132) Å) is remarkably shorter than Nb-H(52) distance (2.664(95) Å) (cf. corresponding Nb···H nonbonding distances in NbCp$_2$(CH$_2$CH$_3$)(CH$_2$=CH$_2$) are 2.67(10) and 2.82(8) Å). The Nb-C(5)-
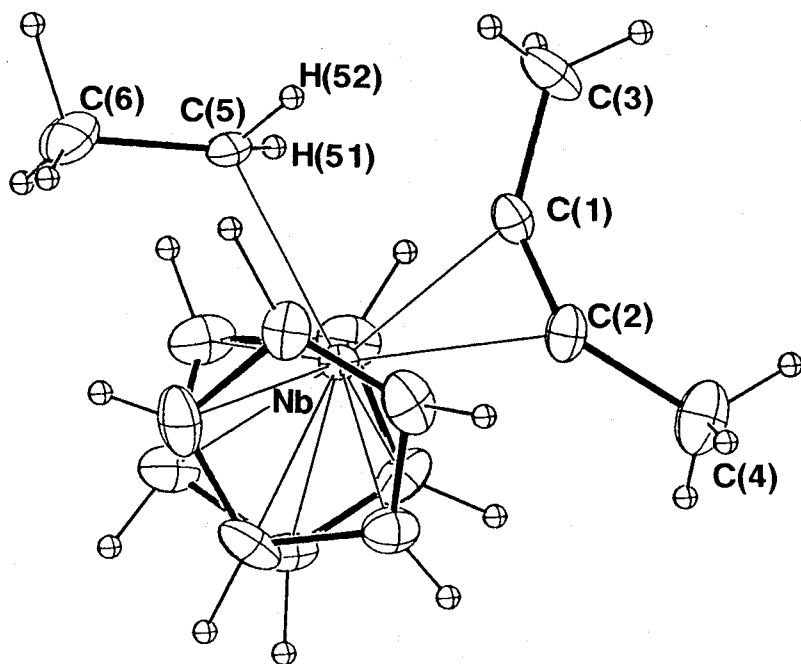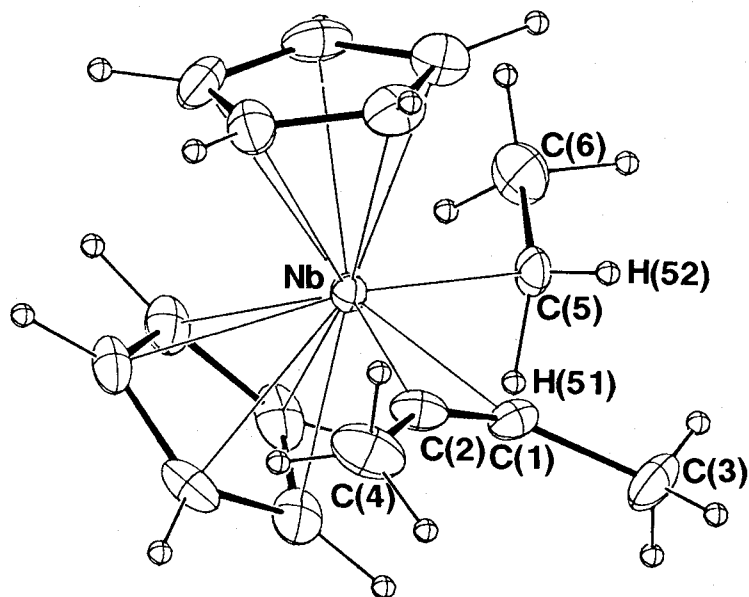
Figure 7. Molecular Structuer of **6**

Table V.   Selected Bond Distances of Complexe 6

Nb-C(1)	2.167(11)	C(1)-C(2)	1.230(17)
Nb-C(2)	2.170(13)	C(1)-C(3)	1.473(20)
Nb-C(5)	2.311(11)	C(2)-C(4)	1.514(24)
Nb-H(51)	2.36(13)	C(5)-C(6)	1.532(24)
Nb-H(52)	2.66(10)	C(5)-H(51)	0.90(10)
Nb-CCP1	2.112(1)	C(5)-H(52)	0.90(10)
Nb-CCP2	2,512(1)	Nb-C(Cp)av.	2.450 (15)

Table VI. Selected Bond Angles for Complex 6.

C(1)-Nb-C(2)	32.95(44)	H(51)-C(5)-H(52)	100(61)
C(1)-Nb-C(5)	76.57(40)	C(6)-C(5)-H(51)	122.5(70)
C(2)-Nb-C(5)	109.04(45)	C(6)-C(5)-H(52)	122.3(62)
C(5)-Nb-H(51)	27.0(32)	CCP1-Nb-CCP2	131.36(3)
Nb-C(1)-C(2)	73.67(78)	CCP1-Nb-C(1)	109.46(28)
Nb-C(1)-C(3)	145.06(93)	CCP1-Nb-C(2)	106.60(35)
Nb-C(2)-C(1)	73.39(78)	CCP1-Nb-C(5)	102.88(28)
Nb-C(2)-C(4)	139.9(11)	CCp2-Nb-C(1)	116.06(28)
C(2)-C(1)-C(3)	141.3(12)	CCP2-Nb-C(2)	102.43(35)
C(1)-C(2)-C(4)	146.7(14)	CCP2-Nb-C(5)	103.34(28)
Nb-C(5)-C(6)	120.46(99)	M1-Nb-C(5)	92.82(28)
Nb-C(5)-H(51)	79.0(69)		
Nb-C(5)-H(52)	103.1(61)		

H(51) angle of 79° is quite smaller than the angle of Nb-C(5)-H(52) (103°). These results clearly indicate the existence of α-hydrogen agostic interaction between Nb atom and H(51),consistent with the ^{1}H NMR studies (vide supra). C(5)-H(51) distance of 1.092(132) Å is slightly longer than C(5)-H(52) distance (0.903(96) Å).The four atoms, Nb, C(1), C(2), and C(5) are near-ly coplanar within 0.08 Å.

The Nb-C(Cp) distances (av. 2.450(15) Å) and the dihedral angle between the two Cp planes (49.13°) are larger than those of NbCp$_2$(H)$_3$ and NbCp$_2$(CH$_2$H$_5$)(CH$_2$=CH$_2$) (2.375(4)-2.402(5) Å, 38.4-47.6°). These values are reflected from the steric crowding between the ethyl group and the alkyne ligand.

Experimental Section

General Procedure

All reactions and other manipurations were performed under argon by using a standard Schlenk techniques. Solvents were dried over Na/K alloy, distilled, and thoroughly degassed before use. Pure NbCp$_2$(H)(CH$_2$=CH$_2$) was obtained as reported previous-ly.[18] ^{1}H NMR were recorded on a JEOL GX-500 (at 500 MHz) or JEOL GSX-270 (at 270 MHz) spectrometers and analyzed with a Varian spin simuration program. ^{13}C NMR were run on a JEOL GSX-270 spectrometer at 67.5 MHz. Mass spectra were recorded on a JEOL DX-300 spectrometer at 30-70 eV.

Preparation of NbCp$_2$(CH$_2$CH$_3$)(CH$_3$C≡CH) (1).

A benzene solution (10 mL) of propyne (0.2g, 5 mmol) was added to NbCp$_2$(H)(CH$_2$=CH$_2$) (0.63 g, 2.5 mmol) dissolved in thoroughly deoxygenated benzene (20 mL). The mixture was heated to 60 °C in a sealed Schlenk tube, kept there for 1 h, and then

evaporated to dryness. The residue was extracted with degassed hexane (30 mL), and the extract was filtered, concentrated and cooled to -20 °C to induce the precipitation of $NbCp_2(C_2H_5)$-($CH_3C\equiv CH$) as dark green solids. Recrystallization from absolute hexane gave pale-yellow crystals in 60% yield (about 0.1% contamination of decomposed compounds make the color of the crystals green). mp. 133 °C. EIMS m/z (relative intensity) 292 (M^+, 11.6), 252 (M^+-CH_3CCH, 11.2), 224 ($[NbCp_2H]^+$, 100.0). Anal. Calcd for $C_{15}H_{19}Nb$: C, 61.65; H, 6.56. Found C, 59.35; H, 5.65.

Analogous complexes containing 1-butyne (2), or phenyl-acetylene (3) can also be prepared in a similar manner.

(2): mp. 104 °C. EIMS m/z (relative intensity) 306 (M^+, 7.4), 252 ($M^+-C_2H_5CCH$, 16.4), 224 ($[NbCp_2H]^+$, 100.0). Anal. Calcd for $C_{16}H_{21}Nb$: C, 62.75; H, 6.91. Found: C, 63.89; H, 7.18.

(3): mp. 135 °C. EIMS m/z (relative intensity) 354 (M^+, 17.6), 252 ($M^+-PhCCH$, 49.0), 224 ($[NbCp_2H]^+$, 100.0). Anal. Calcd for $C_{20}H_{21}Nb$: C, 67.80; H, 5.97. Found: C, 68.97; H, 5.40.

Preparation of $NbCp_2(H)(t-BuC\equiv CH)$ (4).

To a benzene solution (30 mL) of $NbCp_2(H)(CH_2=CH_2)$ (0.63 g, 2.5 mmol) was added $t-BuC\equiv CH$ (0.25 g, 3 mmol). The reaction vessel was sealed and warmed up to 50 °C. The reaction mixture was kept at this temperature for 30 min (prolonged heating causes thermal decomposition). The color of the solution turns to green from yellow during the reaction. Solvents were removed in vacuo and the residue was extracted with 40 mL of hexane. Concentration and cooling to -20°C gave $NbCp_2(H)(t-BuC\equiv CH)$ as green crystalline solids. Repeating recrystallization from thoroughly degassed hexane gave the complex as pale-yellow crystals in 65%

yield. mp. 150 °C dec. EIMS m/z (relative intensity) 306 (M^+, 14.6), 224 ([$NbCp_2H$]$^+$, 100.0).

The trimethylsilylacetylene complex, $NbCp_2(H)(Me_3SiC\equiv CH)$ (5), could be prepared in essentially the same procedure as described for 4.

(5): mp. 162°C dec. EIMS m/z (relative intensity) 322 (M^+, 18.6), 224 ([$NbCp_2H$]$^+$, 100.0).

Preparation of $NbCp_2(CH_2CH_3)(CH_3C\equiv CCH_3)$ (6).

The internal alkyne complex of ethylniobocene was prepared in a similar method for the terminal alkyne complex of ethyl-niobocene. In this case, prolonged reaction time (2 h) is required for good yields.

(6): yield 81%. mp. 157 °C. EIMS m/z (relative intensity) 306 (M^+, 7.3), 252 ($M^+ - CH_3CCCH_3$, 30.5), 224 ([$NbCp_2H$]$^+$, 100.0). Anal. Calcd for $C_{16}H_{21}Nb$: C, 62.75; H, 6.91. Found: C, 62.12; H, 6.88.

The reaction of diphenylacetylene with $NbCp_2(H)(CH_2=CH_2)$ gave diphenylacetylene complex of hydridoniobocene, $NbCp_2(H)-(PhC\ CPh)$ (7) in 90% yield as pale-yellow crystals.

(7): mp. 105 °C. EIMS m/z (relative intensity) 402 (M^+, 100.0), 224 ([$NbCp_2H$]$^+$, 75.0). Anal. Calcd for $C_{24}H_{21}Nb$: C, 71.65; H, 5.26. Found: C, 69.76; H, 5.33.

Structure Determination of 4, 5, and 6.

A single crystal of 4, 5, and 6 sealed in a glass capillary was mounted on a Rigaku automated four-circle diffractometer. Relevant crystal and data statistics are summarized in Table IX. The unit-cell parameters at 20 °C were determined by a least squares fit to 2θ values of 25 strong higher angle reflections for all the complexes. Every sample showed no significant

intensity decay during the data collection.

The crystal structure were solved by the conventional heavy-atom method as implemented in the XRAY SYSTEM[19] by the use of observed reflections [|Fo| > 3σ(Fo)]. After anisotropic refinement of the non-hydrogen atoms, all hydrogen atoms were located on the difference Fourier maps with the help of geometrical calculations and were refined isotropically.

Table VII. Summary of Crystallographic and Experimental Data for Complexes **4, 5,** and **6.**

	$C_{16}H_{21}Nb$	$C_{15}H_{21}SiNb$	$C_{16}H_{21}Nb$
Formula	$C_{16}H_{21}Nb$	$C_{15}H_{21}SiNb$	$C_{16}H_{21}Nb$
Formula Weight	306.32	322.32	306.2
System	Monoclinic	Monoclinic	Orthorhombic
Space Group	$P2_1$	$P2_1$	$P2_12_12_1$
$a/\text{Å}$	6.307(1)	6.149(4)	12.930(6)
$b/\text{Å}$	14.428(3)	14.727(4)	14.498(7)
$c/\text{Å}$	8.218(2)	8.579(5)	7.590(5)
$\beta/°$	105.96(1)	104.78(5)	
$V/\text{Å}^3$	688.2(2)	751.1(6)	1422.8(1.2)
Z	2	2	4
$D_{calcd}/\text{g cm}^{-1}$	1.478	1.657	1.574
$F(000)$, e	316	332	632
$\mu(MoK\alpha)/\text{cm}^{-1}$	9.1	10.6	6.1
2θ range/°	4°-60°	4°-60°	4°-60°
No. of Reflections Measured	2047	2282	2566
No. of Reflections Observed	2007	2184	2253
No. of Variables	237	237	238
R	0.027	0.034	0.048
R_w	0.040	0.059	0.053
Crystal Size	0.55X0.45X0.50	0.20X0.30X0.20	0.50X0.80X0.20
Crystal Color	Yellow-green	Yellow-green	Yellow
Scan Speed/° min^{-1}	4	4	4

References

1) Bottril, M.; Gavens, P. D.; Kellard, J. W.; McMeeking, J. In Comprehensive Organometallic Chemistry; Wilkinson, G.; Stone, F. G. A.; Abel, E. W., Eds.; Pergamon: London, 1982; Chapter 22.5.

2) Roe, D. C. J. Am. Chem. Soc. **1983**, 105, 7771.

3) (a) Doherty, N. M.; Bercaw, J. E. J. Am. Chem. Soc. **1985**, 107, 2670. (b) Labinger, J. A.; Schwartz, J. J. Am. Chem. Soc. **1971**, 97, 1596. (c) Klazinga, A. H.; Teuben, J. H. J. Organomet. Chem. **1979**, 165, 31. (d) Tebbe, F. N.; Parshall, G. W. J. Am. Chem. Soc. **1971**, 93, 3793.

4) (a) Labinger, J. A.; Hart, D. W.; Seibert, W. E.; III; Schwartz, J. J. Am. Chem. Soc. **1975**, 97, 3851. (b) Nakamura, A.; Otsuka, S. ibid. **1973**, 95, 7262.

5) McDermott, J. X.; White, J. F.; Whitesides, G. M. J. Am. Chem. Soc. **1976**, 98, 6521.

6) Bower, B. K.; Tennet, H. G. J. Am. Chem. Soc. **1972**, 94, 2521.

7) See, for example: Parshall, G. W. "Homogeneous Catalysis"; Wiley: New York, 1980; Chapter 3-5.

8) (a) Although cocerted olefin insertion/elimination may best describes this reaction for a variety of organometallic systems, other pathways are possible. For example, Sweany and Halpern have shown that the reaction with a radical pathway involving initial hydrogen abstraction by the olefin.[8b]
(b) Sweany, R. L.; Halpern, J. J. Am. Chem. Soc. **1977**, 99, 8335.

9) Klazinga, A. H.; Teuben, J. H. J. Organomet. Chem. **1980**, 194, 309.

10) Frederics, S.; Thomas, J. L. J. Am. Chem. Soc. **1978,** 100, 350.

11) Antinolo, A.; Gomez-sal, P.; Llardya, J. M. Otero, A.; Royo, P.; Carrera, S. M.; Blanco, S. G. J. Chem. Soc., Dalton Trans. **1987,** 975.

12) (a) Karplus, M. J. Chem. Phys. **1959,** 30, 11. (b) Karplus, M. J. Am. Chem. Soc. **1963,** 85, 2870. (c) Pople, J. A.; Bothner-By, A. A. J. Chem. Phys. **1965,** 42, 1339.

13) Nesmeyanov, A. N.; Gusev, A. I.; Pasynskii, A. A.; Anisimov, K. N.; Kolobora, N. E.; Struchkov, Yu. T. J. Chem. Soc., Chem. Commun. **1969,** 277.

14) Nesmeyanov, A. N.; Gusev, A. I.; Pasynskii, A. A.; Anisimov, K. N.; Kolobora, N. E.; Struchkov, Yu. T. J. Chem. Soc., Chem. Commun. **1969,** 739.

15) Guggenberger, L. J.; Meakin, P.; Tebbe, F. N. J. Am. Chem. Soc. **1974,** 96, 5420.

16) Johnson, C. K. ORTEP-II, Report ORNL-5138; Oak Ridge National Laboratory: Oak Ridge, TN, 1974.

17) Klazinga, A. H.; Teuben, J. H. J. Organomet. Chem. **1978,** 157, 413.

18) Stewart, J. M. X-ray 76, Report TR-446; University of Maryland: College Park, MD, 1976.

Summary and Conclusions

1.   A series of titanium-diene complexes of type $TiCp^*X(diene)$ $(Cp^*=C_5Me_5$, $X=Cl$, Br, I) were first prepared according to our own method.   NMR studies together with X-ray analyses of these complexes revealed the novel prone and supine conformations of the s-cis-coordinated diene ligands.   All of these complexes adopt metallacyclo-3-pentene structure, but have enhanced η^4-diene coordination character as compared with Zr- and Hf-diene complexes.

Low-valent titanium-diene species generated by abstraction of halide ligand in $TiCp^*X(diene)$ on treating with RMgX or Mg metal show superb catalysis for highly selective linear dimerization of 1,3-dienes.   For example, isoprene was catalyticaly converted to tail-to-head bonded dimer, 2,6-dimethyl-1,3,6-octatriene, with high selectivity (99%).   Low-valent titanium species generated in situ by the reaction of $TiCp^*Cl_3$ with 3 equivalents of RMgX has higher catalytic activity for linear dimerization of isoprene.   Formation of a novel head-to-head bonded dimer, 3,6-dimethyl-1,3,6-octatriene, was observed in case of less bulky $TiCpCl_3/3RMgX$ system.

2.   The crystal structures of a series of titanium-allyl complexes have been determined by the X-ray diffraction method.   The coordination geometry of a non-substituted allyltitanium compound was determined using $TiCpCp^*(allyl)$ (1) with mixed ancillary ligands since $TiCp_2(allyl)$ (2) includes crystal disorder.   To clarify the effect of substituent(s) on allyl group, structure analyses of $TiCp_2(1,3-dimethylallyl)$ (3) and $TiCp_2(2-methylallyl)$ (4) were also demonstrated.   The allyl groups in all of these

complexes coordinate to the metal in symmetric η^3-fashion. The complex **1** exhibits the shortest Ti-allyl bonds. The longest Ti-C(1)/C(3) bonds are seen in the complex **3**, while the complex **2** shows the longest Ti-C(2) bond.

3.   Novel heterobimetallic complexes of type $YbCp^*_2(\mu-R)AlR_2$-(THF) were first prepared by the reaction of $YbCp^*_2$(THF) with AlR_3. The X-ray analysis of triethylaluminum complex revealed the unique mono-alkyl bridged structure. This complex shows good catalysis for polymerization of ethylene with relatively narrow polydispersity. AB type block copolymerization of ethylene with MMA was first realized by using this complex, i.e. after polymerization of ethylene, poly(MMA) was introduced to the polyethylene living end by repeated addition of MMA.

4.   The lanthanide(II) complexes of type $LnCp^*_2(donor)_x$ (Ln=Yb, Sm; x=1, 2) were found to be quite effective catalyst for syndiotactic polymerization of MMA. The polymerization proceeds in a living fashion. These catalyst systems involve following remarkable features, i.e. 1) highly syndiotactic (rr=91.2%) poly(MMA) were formed at low temperature in quantitative yield, 2) polydispersity of the resulted polymers are exceedingly narrow (M_w/M_n<1.10), 3) polymerization occurs very rapidly in a living fashion leading to high molecular weight poly(MMA) with narrow polydispersity. Any other catalyst systems which satisfies the whole items 1)-3) has not yet reported.

5.   Hydridoniobium(ethylene) complex was found to readily react with various 1-alkynes such as propyne, 1-butyne, and phenyl-acetylene under mild conditions to afford air-sensitive pale-yellow crystals of $NbCp_2(Et)(alkyne)$ in high yields. Resulting complexes prefer the exo-geometry as confirmed by NMR studies in

sharp contrast to the endo-preference of the hydrido(olefin) complexes of niobocene. Bulky alkynes such as 3,3-dimethyl-1-butyne, trimethylsilylacetylene, and diphenylacetylene behaves in a different manner and gave rise to the formation of hydrido-niobocene complexes of type $NbCp_2(H)(alkyne)$ with exo-geometry as confirmed by the X-ray analyses of 3,3-dimethyl-1-butyne and trimethylsilylacetylene complexes. The reaction of $NbCp_2(H)$-(ethylene) with inner alkyne, 2-butyne, affords the ethyl(alkyne) complex, $NbCp_2(Et)(2-butyne)$. The NMR studies and X-ray analysis of this complex revealed the existence of an agostic interaction between $Nb-CH_2$ and Nb.

List of Publications

1. Structural Features in Electron-Deficient (η-Pentamethyl-cyclopentadienyl)titanium-Diene Complexes and Their Catalysis in the Selective Oligomerization of Conjugated Dienes,

Yamamoto, H.; Yasuda, H.; Tatsumi, K.; Lee, K.; Nakamura, A.; Chien, J.; Kai, Y.; Kasai, N.

<u>Organometallics</u>   **1989**, <u>8</u>, 105.

2. Diene Complexes of Pentamethylcyclopentadienyltitanium Chloride. Synthesis and First X-ray Structure of Titanium-Diene Complexes,

Chien, J.; Kai, Y.; Kasai, N.; Yamamoto, H.; Yasuda, H.; Nakamura, A.

<u>Chem</u>. <u>Lett</u>. **1987**, 1545.

3. Synthesis and X-ray Structure Analysis of Novel Ethyl-Bridged Ytterbium-Triethylaluminum Complex: $(\eta\text{-}C_5Me_5)_2Yb\cdot Al(C_2H_5)_3(THF)$,

Yamamoto, H.; Yasuda, H.; Yokota, K.; Nakamura, A.; Kai, Y.; Kasai, N.

<u>Chem</u>. <u>Lett</u>. **1988**, 1963.

4. Steric Effect of Allyl Substituent on the Molecular Structures of Titanium-Allyl Complexes,

Chien, J.; Kai, Y.; Kasai, N.; Yamamoto, H.; Yasuda, H.; Nakamura, A.

submitted for publication.

5. Living and Highly Syndiotactic Polymerization of Methyl Methacrylate Catalyzed by Organolanthanide(III) and Organolanthanide(II) Complexes,

Yasuda, H.; Yamamoto, H.; Yokota, K.; Miyake, S.; Nakamura, A.

submitted for publication.

6. Molecular Structure and Chemical Behavior of Alkyne Complexes of Cp_2MH and Cp_2MR (M=Nb, Ta),

Yasuda, H.; Arai, T.; Yamamoto, H.; Nakamura, A.; Chien, J.; Kai, Y.; Kasai, N.

submitted for publication.

Related Papers

1. Facile Reduction of Organometallic Halides with Bis(pentamethylcyclopentadienyl)ytterbium and the X-Ray Structure of $(C_5Me_5)_2YbCl(THF)$,

Yasuda, H.; Yamamoto, H.; Yokota, K.; Nakamura, A.

Chem. Lett. **1989**, 1309.

2. Template Synthesis of Substituted Cyclopentanones by Zirconocene/Olefin/CO systems,

Akita, M.; Yasuda, H.; Yamamoto, H.; Nakamura, A.

Polyhedron **1990**, in press.

3. Tumor Inhibition by Organometallics. Activity of Titanocene Derivatives and Some Niobium and Tantalum Compounds,

Yasuda, H.; Yasuhara, T.; Yamamoto, H.; Takei, K.; Nakamura, A.

Chem. Express **1988**, 3, 375.